

https://dspace.org/

Characterization of cell elongation and chromosome segregation determinants in mycobacteria

Mdlalose, Noluthando Magugu

2020
https://hdl.handle.net/10539/31950

Downloaded from a DSpace repository. https://dspace.org/

CHARACTERIZATION OF CELL ELONGATION AND CHROMOSOME SEGREGATION DETERMINANTS IN MYCOBACTERIA

Noluthando Magugu Mdlalose (1606903)



A dissertation submitted to the Faculty of Health Science, University of the Witwatersrand, Johannesburg, in fulfillment of the requirements for the degree of Master of Science in Medicine.

2020

Declaration

I, Noluthando Magugu Mdlalose declare that this compiled Dissertation, is my own and unaided work. It is being submitted for the Degree of Master in Medicine in the University of the Witwatersrand, Johannesburg. It has not been submitted before any degree or examination at this or any other University.

_____ _____

(Noluthando Magugu Mdlalose) Date

Dedication

THIS WORK IS DEDICATED TO MY CLOSE FAMILY AND FRIENDS WHO HAVE ALWAYS SUPPORTED ME THROUGH MY STUDIES.

Presentation arising from this research

Conference:	Molecular Biosciences Research Thrust (MBRT)
Presentation:	Poster
Venue and year:	University of the Witwatersrand, 2019

Abstract

Tuberculosis (TB) continues to lay a heavy burden on public health systems worldwide and is one of the leading causes of death from a single infectious agent, namely *Mycobacterium tuberculosis* (*Mtb*). The burden of TB is not only represented by the current active disease cases, which are associated with a high mortality rate but also the ongoing threat of latent TB infection, which further exacerbates the epidemic. The emergence of multi-drug resistant strains created an urgent need for the identification and investigation of more effective therapeutics with less toxicity that can potentially reduce the treatment period and eventually eliminate this disease. In this context, the mycobacterial cell wall, which is a complex multi-layered envelope, assembled at the cell poles, represents an ideal area for the discovery of new drugs. The biosynthesis of this macromolecule is coordinated by the enzymatic addition of chemically diverse cell wall layers. The enzymes which regulate the cytosolic layers of peptidoglycan (PG), arabinogalactan (AR) and mycolic acid (MA) synthesis are localized at cell growth and division sites. These enzymes have to be carefully regulated to maintain cell wall homeostasis and any disturbances will affect cell survival, thus making the process of cell wall assembly vulnerable for drug development. The mycobacterial PG layer has been identified as being a crucial component of cell wall integrity. The remodeling of PG is facilitated by several enzymes including penicillin-binding proteins (PBPs), which carry out their function through interacting with partnering proteins. This study was focused on identifying the interacting partners of Wag31/DivIVA, an important cell division protein that is localized at the poles and facilitates the recruitment of other cell division proteins. Interacting partnering proteins were identified through a mycobacterial protein complementation assay (M-PFC). The screen identified five novel different interaction partners. Three of these possibly contribute to chromosome segregation (RecR) and cellular processes including cell division (UvrABC transporter and Cys proteins). DivIVA proteins have been demonstrated to interact with a great variety of proteins in other species, from transmembrane to cytosolic proteins. This ability to interact is attributed to the highly conserved amphiphilic domains. These new partners provide additional information on how DivIVA coordinates cellular growth and also identifies new proteins that can serve as potentially important drug targets.

Acknowledgments

"*The name of the Lord is a strong tower; the righteous run to it and are safe"* **Proverbs 18:10**

Firstly, I acknowledge the Almighty Lord Jesus Christ "uMvelinqangi" I wouldn't be here today had it not been for His goodness and His kindness. It is not by my will but purely His grace and Mercy.

Next I would like to acknowledge my ancestor's, ngibonga abangasekho ekhaya oNyanda wePhahla, oDikane, Sgombe Somgabashu. Ngyabonga Gogo "Eldah Gugile Mdlalose-Madlala", dadewethu "Slindile Felicia Mdlalose" noBaba wami "Phumlani Allan Mdlalose", ningamaDlozi amahle empilweni yami.

"Ngabe niyangibona yini lapho nikhona? Ngabe niyaziqhenya yini ngami? Nizishaya isifuba ngami? "

I, would like to extend my words of gratitude to my supervisor Prof. Bavesh Kana for your patience, the technical assistance and solicitous discussions about this project, I learned a lot from him.

My mother, Busisiwe Beatrice Mdlalose, thank you for your tireless prayers and support, for your words of affirmation, for always encouraging me to do my best even when I was losing hope. To my siblings, Musawenkosi, Siyamukela, and Phumelele Mdlalose thank you for believing in me, thank you for sacrificing for me, you have in many ways shown me that there are people who are willing to go an extra mile to ensure a lighter journey. This journey was much smoother because of your presence and support. My family at large thanks for sharing my joys and sorrows and thank you for the support.

To the colleagues at (Centre for Biomedical TB Research) CBTBR, thank you for providing a pleasant working environment. To Moagi, I am truly indebted to you for your tireless efforts of guidance and support from the time of my arrival at the CBTBR and the design for this dissertation work "Izandla zidlula ikhanda, Makwande".

Lastly, I would like to thank the financial sponsors, the National Research Foundation (NRF), the University of the Witwatersrand and the DST/NRF CBTBR.

Table of Contents

Declaration 2
Dedication 3
Presentation arising from this research 4
Abstract 5
Acknowledgments 6
Table of Contents ..... **Error! Bookmark not defined.**
List of figures: 11
List of tables: 13
Nomenclature 14
1. Introduction 16
1.1. Tuberculosis 16
1.2. TB Infection, transmission and treatment 17
1.3. The mycobacterial cell wall 19
1.4. PG crosslinking 22
1.5. PG biosynthesis 23
1.6. Cell growth and division in mycobacteria 26
1.6.1. Modes of growth in rod-shape bacteria 28
1.6. Chromosome segregation and bacterial cell division 29
1.7. DivIVA 31
1.7.1. Structure and function of DivIVA 31
1.7.2. Structural diversity in DivIVA peptides 32
1.7.3. DivIVA as a drug target for TB drug development 33
1.8. Hypothesis and research motivation 34
1.10. Aims and Objectives 34
1.10.1. Aim 34
1.10.2. Specific objectives 35
2. Materials and methods 36
2.1. Bio-informatics and database tools used 36
2.1.1. Database tools used to obtain DNA and protein sequences of interest 36

2.3. Bacterial strain and derivative growth conditions 40
2.3.1. Growth conditions for *E. coli* DH5□ and derivative strains 40
2.3.2. Growth conditions for *M. smegmatis* mc^{2}155 and derivative strains 40
2.4. DNA extractions 40
2.4.1. Chromosomal DNA extraction of *M. smegmatis* mc^{2}155 40
2.4.1.1. Small scale extraction of chromosomal DNA 40
2.4.1.2. Large scale extraction of chromosomal DNA 41
2.4.2. Plasmid DNA extraction of *E. coli* 41
2.4.2.1. Small scale extraction of plasmid DNA 41
2.4.2.2. Large scale extraction of plasmid DNA 42
2.5. DNA clean-up and removal of contaminating proteins 43
2.5.1. Sodium acetate precipitation 43
2.6. DNA manipulation 43
2.6.1. DNA amplification 43
2.6.1.1. PCR primer designing 43
2.6.1.2. Polymerase chain reaction (PCR) 44
2.6.1.2.1. Fusion High-Fidelity DNA polymerase reaction 44
2.6.1.2.2. Roche Faststart Taq DNA polymerase reaction 44
2.6.2. Restriction digestions 44
2.6.3. Agarose gel electrophoresis 45
2.6.4. Purification of DNA fragments 45
2.6.5. DNA phosphorylation and dephosphorylation 46
2.6.6. DNA ligation 46
2.6.7. DNA sequencing 47
2.7. Bacterial transformations 47
2.7.1. Chemically competent *E. coli* DH5□ cells preparation 47
2.7.2. Chemically competent *E.coli* DH5□ cells transformation 47
2.7.3. Electro-competent mc^{2}155 and derivative strain preparation 48
2.7.4. Electroporation of plasmids into *M. smegmatis* 48
2.7.5. Recombinant strain genotypic confirmation 48
2.8. Genomic DNA library construction 49

2.8.1. Restriction digestion of genomic DNA 49
2.8.2. Electro-competent *E. coli* DH5 cell preparation 49
2.8.3. Transformation of electro-competent DH5 50
2.9. Identification of MSMEG_4217 interacting partners 50
2.9.1. Assaying for MSMEG-4217 putative interacting partners 50
2.9.2. Putative interacting partners identification and sequencing 53
2.9.3. Quantitative analysis for M-PFC assay to assess protein-protein association between MSMEG_4217 and identified putative protein partners using Alamar Blue (AB) assay 54
2.10. Fluorescence microscopy 55
2.10.1. Localization of proteins of interest 55
2.10.2. The FM4/64 and the DAPI stains for membrane and DNA staining respectively 56
2.11. Microscopy analysis 56
2.12. Statistical analysis 57
2.13. Ethical considerations 57
3. Results 57
3.1 Bio-informatics analysis to determine the structure and protein interaction domains of DivIVA from mycobacteria 57
3.2 Protein interactions 61
3.2.1. Wild-type mc_2155 genomic DNA library construction and generation 61
3.2.2. Cloning of MSMEG_4217 into the bait vector pUAB400 63
3.2.3. Screening for interacting partners using the M-PFC assay and Trim resistance 65
3.2.4. Screening for MSMEG_4217 putative interacting partners 66
3.2.5. Identification of the MSMEG_4217 putative interactive protein partners 67
3.3. Assessing protein-protein interaction 76
3.3.1. Confirmation of the efficacy of the M-PFC assay by assessing protein-protein interaction of the two PG hydrolases, RipA and RpfB 76
3.3.2. Confirmation of the MSMEG_4217 interacting protein partners (Alamar Blue assay) 77
3.4. Bioinformatics analysis and cellular localization of chromosome segregation and cell division enzymes in wild-type *M. smegmatis* cells 81
3.4.1. Bioinformatics analysis of functional domains necessary for interaction in the partnering protein (MSMEG_5632) 81

3.4.2. Subcellular localization of MSMEG_5632 in wild-type *M. smegmatis* cells 82
3.4.2.1. Construction of the pTweety_MSMEG_5632_mRFP plasmid 82
3.4.2.2. Localization of MSMEG_5632 in wild-type *M. smegmatis* single cells 85
3.4.3. Bioinformatics analysis of functional domains necessary for interaction in the partnering protein (MSMEG_1577) 87
3.4.3.1. Construction of a MSMEG_1577 reporter in wild-type *M. smegmatis* single cells. 87
3.4.3.2. Localization of MSMEG_1577 in wild-type *M. smegmatis* cells 89
4. Discussion 91
4.1. Future prospects 95
4.2. Limitations 95
4.3. Concluding remarks 95
5. Appendices 96
Appendix E: Ethics waiver 102
..... 103
6. Reference list 104

List of figures:

Figure 1.1: Global estimation of TB incidence rates 17
Figure 1.2: Diagrammatic representation of the mycobacterial cell wall 20
Figure 1.3: Schematic representation of peptidoglycan structure and the different PG cross-linkages 23
Figure 1.4: Scematic representation of the peptidoglycan biosynthesis pathway 24
Figure 1.5: Schematic representation of PG hydrolytic and biosnthetic enzymes 25
Figure 1.6: Model of mycobacterial polar growth, cell elongation and cell division 27
Figure 1.7: Characteristic bacterial growth and division models 28
Figure 1.8: Schematic representation of the mycobacterial divisome and elongosome machinery 30
Figure 1.9: Predicted tertiary structure of M. smegmatis DivIVA and schematic representation of the domain organization 32
Figure 1.10: Aminopyrimidine-sulfuonamides (APYS) potent anti-tubercular compunds 33
Figure 2.1: Scematic diagram demonstrating the M-PFC assay principle 50
Figure 2.2: The M-PFC assay strategy followed to identify putative interacting partners for MSMEG_4217 53
Figure 2.3: The Alamar Blue assay was used as a quantitative measure of protein-protein interaction intensity 54
Figure 3.1.1 a: Tertiary structure and schematic representation of the domain organization of the B. subtilis and M. smegmatis DivIVA proteins 57
Figure 3.1.1 b: A superimposition structure of N-terminal M. smegmatis DivIVA (blue) and N-terminal B. subtilis DivIVA (coral) 58
Figure 3.1.2: Comparison of the B. subtilis DivIVA conserved domains with other DivIVA Firmicutes abd Actinomycetes homologs 59
Figure 3.2.1: Genomic DNA restriction digest of wild-type M. smegmatis mc2155 61
Figure 3.2.2: Construction and restriction profiling of pUAB400_DivIVA 63
Figure 3.2.3: The M-PFC assay Trim resistance for mc:: RipA + RpfB strain 64
Figure 3.2.4: The M-PFC assay screening for the identification of MSMEG_4217 interacting partners 65
Figure 3.3.1: Putative protein interacting partners screen 76
Figure 3.3.2: Quantification of protein-protein interaction using partial clones of MSMEG_4217 interacting protein partners 79
Figure3.4.1: Schematic representation of domain organization of MSMEG_5632 protein 80
Figure 3.4.2: Construction and restriction profiling of pTweety_mRFP_5632 82
Figure 3.4.3 : Subcellular localization patterns of MSMEG_mRFP_5632 in wild-type M. smegmatis 84
Figure 3.4.4: Schematic representation of domain organization of MSMEG_1577 protein 85
Figure 3.4.5: Construction and restriction profiling of pTweety_mRFP_1577 86

Figure 3.4.6: Subcellular localization patterns of MSMEG_mRFP_1577……88

Figure 4.1: A proposed model of DivIVA interacting partners function in mycobacterial physiology..... 92
Figure A1: Frementas molecular weight markers (III and IV)..... 97
Figure D1: Restriction profile of pUAB300..... 98
Figure D2: Restriction profile of pUAB400..... 99
Figure D3: Restriction profle of pTweety..... 99

List of tables:

Table 2.1.1. Database tools used to obtain DNA protein sequences of interest 36
Table 2.1.2. Bioinformatics and software tools used in this study to analyze genes and proteins of interest..... 36
Table 2.2.1. Plasmid created and/ or used in this study..... 38
Table 2.2.2. Bacterial strains created and/ or used in this study..... 39
Table 2.3. Parameters used for primer design..... 43
Table 3.1. MSMEG_4217 putative interacting protein partners obtained through M-PFC asay . 69
Table 3.2. MSMEG_4217 and the selective putative interacting protein partners..... 76
Table 3.3. Quantification of protein-protein interaction using between MSMEG_4217 and identified partial clones of ineracting partners..... 80
Table A1. Media supplements 96
Table A2. Solutions used for *E.coli* plasmid DNA extractions..... 96
Table A3. Solutions used for *M. smegmatis* DNA extractions..... 96
Table A4. Solutions used for DNA precipitation..... 97
Table A5. Solutions used for DNA electrophoresis..... 97
Table A6. Recipes for agarose gel elctroporesis..... 97
Table A7. Solutaions used for preparation of *E. coli* conpetent cells..... 97
Table A8. Solutions used for preparation of *M. smegmatis*competent cells..... 97
TableB1. Primers used for generation oof bait vector cloning into pUAB400 for proteininteraction study 98
Table B2. Primers used for the identification of putative interacting partners..... 98
Table B3. Primers used for the localization study 98

Nomenclature

Amp	Ampicillin
AG	Arabinogalactan
attB	$tRNA^{Gly}$ phage attachment site
BLAST	Basic local alignment search tool
bp	Base pairs
BSA	Bovine serum albumin
$CaCl_2$	Calcium chloride
CFUs	Colony forming units
CTAB	Cetyltrimethylammonium bromide
D-ala	D-alanine
DAPI	4',6-diamidino-2-phenylindole
D-glu	D-glutamine
DH5α	DH5 alpha cells (used for routine cloning)
DMSO	Dimethyl sulfoxide
DNA	Deoxyribonucleotide
E. coli	*Eschericia coli*
EDTA	Ethyldiaminetetraacetic acid
EtBr	Ethidium bromide
FhaB	Filamentous hemagglutinin
FM4/64	(N-(3-Triethylammoniumpropyl)-4-(-(6-(4- (Diethylamino) Phenyl) Hexatrienyl) Pyrimidinium Dibromide)
HIV	Human immunodeficiency virus
HCI	Hydrochloride
Hyg	Hygromycin
INH	Isoniazid
I-TASSER	Iterative threading aSSEmbly refinement
Kan	Kanamycin
LA	Luria-Bertani agar
LB	Luria-Bertani broth

Ldt	L,D- transpeptidase
LTBI	Latent TB infection
MA	Mycolic acid
mDHFR	murine dehydrofolate reductase
MDR-TB	Multi drug resistant TB
$MgCl_2$	Magnesium chloride
MIC	Minimum inhibitory concentration
M-PFC	Mycobacterial protein fragment complementation
mRFP	monomeric red fluorescent protein
Mtb	*Mycobacterium tuberculosis*
NaOH	Sodium hydroxide
NCBI	National center for biotechnology information
NEB	New england biolabs
OD	Optical density
PCR	Polymerase chain reaction
PG	Peptidoglycan
Pkn A/ B	Protein kinase A or B
PZA	Pyrazinamide
RNaseA	Ribonuclease A
Rif	Rifampicin
SEM	Scanning electron microscope
TAE	Tris-acetate-EDTA
TB	Tuberculosis
Trim	Trimethoprim
Tris	Trisamenomethane
UDP	Uridine diphosphate
WHO	World health organization

1. Introduction

1.1. Tuberculosis

Mycobacterium tuberculosis (*Mtb*) infection continues to lay a heavy burden on public health systems world-wide. The World Health Organization (WHO) estimated that nearly 10 million people fell ill with tuberculosis (TB) in 2018 (Figure 1.1) (WHO, 2019). There was an estimated 1.2 million TB deaths among HIV-negative people and an additional 251 000 deaths among HIV positive individuals. TB affects both men and women in all age groups but the highest burden is on men in the age range of $\geq$ 51 years, accounting for 57% of all TB cases in 2018 (WHO, 2019). Geographically, TB infection is prevalent in developing countries, with most of the estimated number of cases occurring in South-East Asia and Africa region, which account for 44% and 24% respectively. The Sub-Saharan African countries carry between 2000-2500 cases per 100 000 population per year (WHO, 2019). TB morbidity and mortality is further exacerbated by individuals with asymptomatic infection, termed latent TB infection (LTBI); these people are defined as carrying *Mtb* but have sub-clinical disease or no symptoms at all (Connell et al., 2011). TB is an airborne infectious pathogen caused by a bacterium, but environmental factors play a major role in driving the TB epidemic. The WHO 2015 TB report estimated that almost 2 billion people harbor LTBI as diagnosed by a delayed-type hypersensitivity reaction in response to subcutaneous challenge with purified protein derivative (PPD) (Boshoff & Barry, 2005; WHO, 2019). Individuals with LTBI pose a major concern as they carry a risk of progression to active TB disease (Chao & Rubin, 2010). Other threats against TB control include; co-infection with HIV and increasing emergence of multidrug-resistant (MDR) strains (Dheda et al., 2014).

Mtb was discovered by Robert Koch, who described the pathogen as a rod shaped acid-fast staining bacillus (Sakula, 1983; Dheda et al., 2014) with a unique multi-layered cell wall that is impermeable to a number of compounds. It has been hypothesized that this lack in permeability results in inherent tolerance of Mtb to antimicrobial agents. Drug-resistant TB continues to be a major public health burden with the annual emergence of approximately 1 million new cases of rifampicin-resistant TB (of which 78% had multidrug-resistant TB) (WHO, 2019). Drug resistance can occur when adherence to treatment is poor; firstly due to sub-lethal drug concentrations and failed bacterial killing and secondly very early induction of a combination of

many low-level-resistance mutations, which result in drug tolerance and eventual resistance (Dheda et al., 2014). These factors underpin the urgency for the development of effective control and preventative mechanisms to reduce TB infection. Vaccinating children with Calmette-Guérin (BCG) vaccine confers protection from severe forms of TB in children but does not protect adults from TB infection nor does it reduce the risk of progression from latent infection to active disease (WHO, 2019).

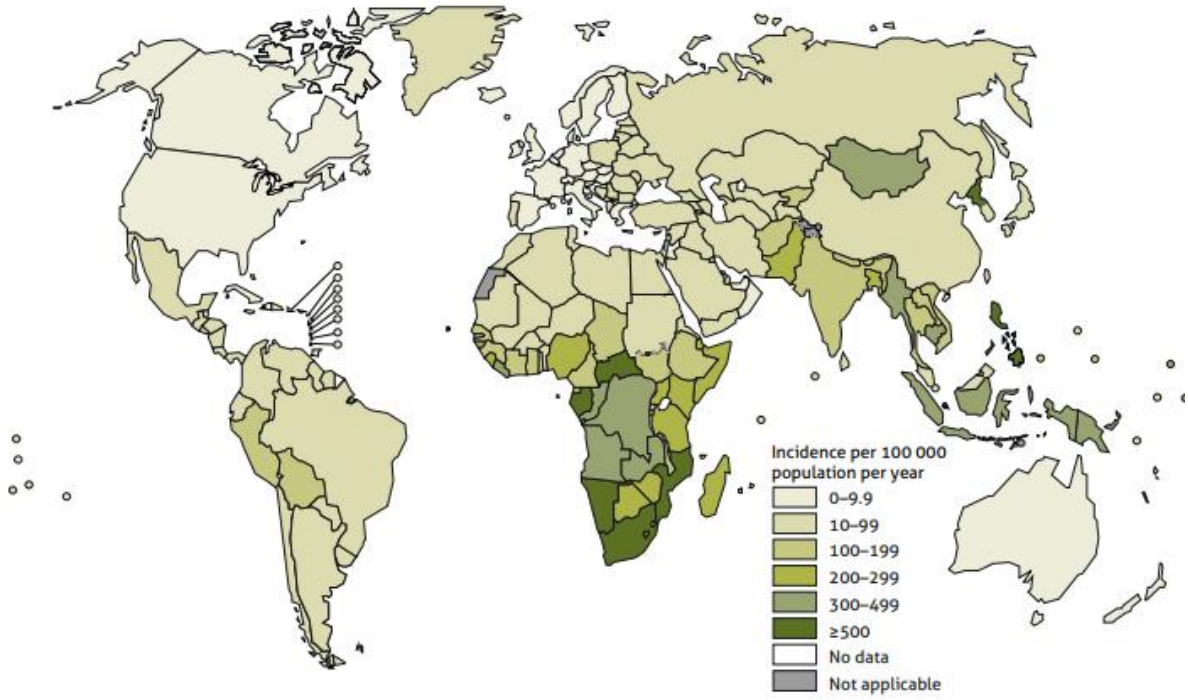


Figure 1.1: **Global estimation of TB incidence rates, 2018.** TB burden distribution of incident cases in developing countries predominantly in South-East Asia and the Sub-Saharan African region, image adapted from Global Tuberculosis Report 2018, WHO (2018).

1.2. TB Infection, transmission and treatment

There is one death due to TB in every 15 sec, confirming that *Mtb* is an incredibly successful human pathogen (Furin et al., 2019). Infection with *Mtb* bacilli can lead to two main events: an asymptomatic infection where there is persistence and or clearing of the pathogen, thus the disease does not progress or active TB disease with the individual presenting symptoms (Smith, 2003; Connell et al., 2011). Further than the classical model of distinct active and latent outcomes, the complex host dynamic microenvironment and the pathophysiology of the bacterium can give rise to a spectrum of TB disease. Most TB infections initiate through the

respiratory route of exposure, where aerosol droplets enter the alveolar passages and come in contact with the macrophages, the host's first line of defense (Smith, 2003). In the early stages of infection, dendritic cells also play an important role as antigen presenters, other important cells include monocytes and neutrophils (Marakalala et al., 2016). The bacteria are phagocytosed in a process initiated by bacterial contact with the macrophages, thus starting a cascade of events in the host lungs through the stimulation of pro-inflammatory responses in the form of cytokines and chemokines. This results in the additional recruitment of lymphocytes and monocytes which ultimately induce granuloma formation (Smith, 2003; Marakalala et al., 2016). The granuloma contains some compact immune cell aggregates and a ring of lymphocytes at the periphery all of which, enclose the infected *Mtb* macrophages. Granuloma structures vary in histological presentation from cellular, to caseous (necrotic), to completely fibrotic lesions (Kieser & Rubin, 2014; Marakalala et al., 2016). This is a critical point in the disease, as the formation of the granuloma is the host's attempt at controlling the infection. If the granuloma fails to eliminate the infection progression to active pulmonary TB disease results (Smith, 2003). This will lead to clinically observable active disease symptoms inlcuding persistent cough, coughing up of blood (phthisis) and wasting (weight loss, fatigue and fever) (Smith, 2003). Individuals who present with these symptoms but are not yet taking medication, put their household and other contacts at a risk of being infected (WHO, 2019).

TB is caused by bacteria, but environmental factors major greatly influence transmission. TB is often associated with the poor, who are predominantly malnourished, overworked, and lived in poor sanitation areas (Smith, 2003). Some key epidemiological determinants of TB in low-burden European countries are related to economic and socio-political factors and the diagnosis of active TB disease Current treatment of drug-sensitive, active TB requires the combinatorial administration of chemotherapeutics lasting for a period of six months. The first two months of treatment includes; a combination of Isoniazid (INH), Ethambutol (EMB), Pyrazinamide (PZA), and Rifampicin (RIF), followed by an additional four months treatment with two drugs (Rifampicin and Isoniazid) (WHO, 2015; Furin et al., 2019). Over the past 5 years, the treatment regimen has seen the introduction of two new drugs, Bedaquiline (BDQ) and Delamanid (DLM). These drugs are still going through multiple clinical trials with all forms of TB (Furin et al., 2019). Therapeutic advancements through the addition and or substitution of fluoroquinolones in the regimen did not present a treatment-shortening benefit over the known drug treatments.

However, administration of high dose rifampicin showed early promise for treatment shortening (Furin et al., 2019). Despite effort being invested in the development of new therapeutics, drug discovery still lags far behind the emergence of drug resistance, highlighting the need for the development of shorter treatment regimes. For this, new drug targets are needed and of interest, is the peptidoglycan (PG) layer in the cell wall and the enzymes responsible for its remodeling.

1.3. The mycobacterial cell wall

The mycobacterial cell wall is a complex, multi-layered structure that is required for cell growth and survival against stress (Kieser & Rubin, 2014). This structure is responsible for the maintenance of cell shape and protection against hostile environmental changes (Hett & Rubin, 2008). It consists of three distinct macromolecules; the mycolic acids (MA), arabinogalactan (AG) which are anchored by the PG layer (Figure 1.2) (Meniche et al., 2014). The high lipid density within the cell wall inhibits Gram staining, thus the mycobacteria are classified as acid-fast and can be detected by the Ziehl-Neelsen stain (Hett & Rubin, 2008; Kieser & Rubin, 2014). The mycobacterial cell wall is impermeable to a number of compounds and it has been hypothesized that this lack of permeability results in the inherent tolerance of *Mtb* to antimicrobial agents. As a result, the cell wall has become an attractive area for TB drug discovery as it is a rich source for anti-tuberculosis therapeutic development. This is further evidenced by the fact that many compounds used for TB chemotherapy target enzymes that synthesize distinctive layers of the cell wall (McNerney et al., 2000; Kieser & Rubin, 2014).

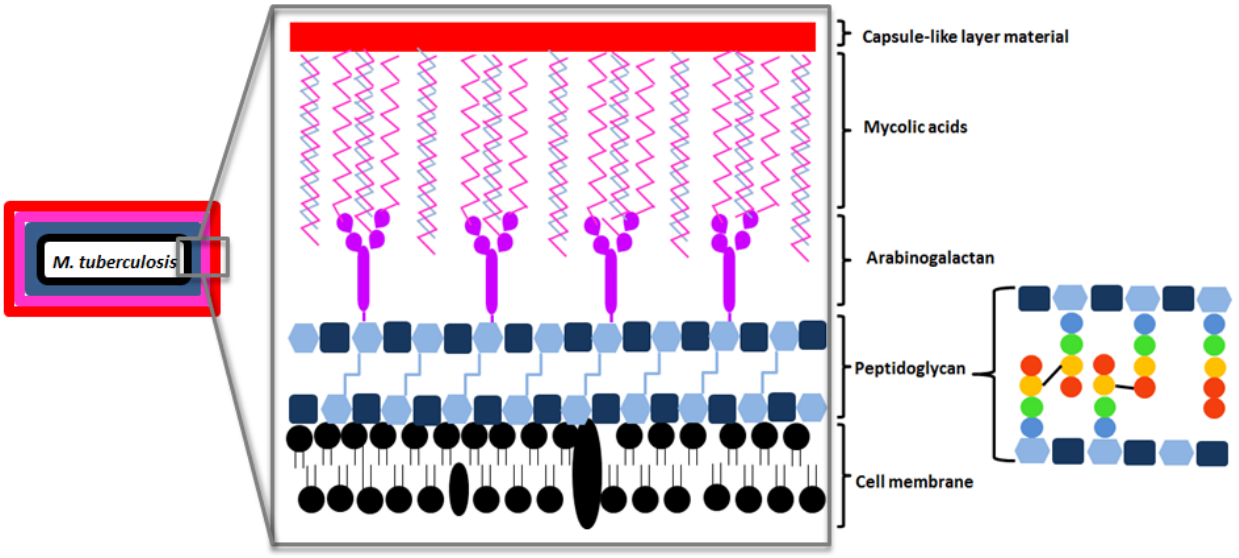


Figure 1.2: **Diagrammatic representation of the mycobacterial cell wall.** Different layers of the cell wall. The outer most layer is the mycobacterial capsule layer (red) made of capsule protein and polysaccharide. The MA in magenta is ligated to the AG in purple surrounding the (PG) layer in blue. The inner most layer is the phospholipid bilayer or cell membrane in black. The components of PG layer are shown; *N*-acetyl glucosamine navy square, *N*-acetyl muramic acid in light blue hexagon, L-alanine: blue circle, D-glutamine: green circle, *meso*-Diaminopimalate: yellow circle and D-alanine: red circle. Adapted from (Hett & Rubin, 2008; Kieser & Rubin, 2014).

This multi-layered macromolecule renders the growth of mycobacteria particularly complex in terms of synthesizing these different polymers (Kieser & Rubin, 2014). The outer most layer of mycobacterial wall is a non-covalently-linked capsule-like layer made up of proteins and polysaccharides, followed by a thick wax lipid coat of MAs which plays a crucial role that contributes to the impermeability of the cell wall (Hett & Rubin, 2008; Kieser & Rubin, 2014). MAs are long carbon chain composed of a short saturated meromycolate branch and two fatty acids (Ioerger et al., 2013). The arabinan from AG is ligated with the carbon chain of the MA. The galactan is composed of disaccharide unit repeats synthesized by galactofuranosyl transferases Gfl, Gfl1 and Gfl2 (Kieser & Rubin, 2014). Arabinan can be modified further by the addition of succinyl or unusual non-*N*-acetylated galactosamine (GalN) moieties; this modification has been known to greatly stimulate infection efficiency of pathogenic bacteria such as *Francisella tularensis* (Kieser & Rubin, 2014). The layer of arabinogalactan surrounds the PG layer (see figure 1.2). The PG or murein is a sophisticated material that is strong enough to provide scaffolding material to allow for bacterial shape maintenance and osmotic turgor

pressure protection during growth, yet flexible enough to allow cells to grow and elongate (Hett & Rubin, 2008). PG is composed of long polymers of the repeating disaccharide *N*-acetyl glucosamine and *N*-acetyl muramic acid (NAG-NAM) linked by β(1→4) glycosidic bonds. These residues are linked via peptide bridges; the peptide chain is often in this order: L-alanyl-D-*iso*-glutaminyl-*meso*-diaminopimelic acid (DAP) and D-ala-D-ala (Hett & Rubin, 2008; Kieser & Rubin, 2014). Compared to other rod-shaped bacteria such as *Eshcerichia coli* and *Bacillus subtilis*, mycobacterial PG layers are heavily crosslinked, more than 80% of this layer contains the non-traditional 3-3 peptide crosslink and less 4-3 crosslinks. The PG polymers encompasses modification; glycosylation of NAM residues and amidation of D-glutamine and *meso*-Diaminopimalate of the side chain (see figure 1.2) (Kieser & Rubin, 2014). The PG layer surrounds the inner plasma membrane layer, which anchors PG, AG and MA layers. The chemical composition of the PG, AG and MA structures and the pathways for their synthesis are well studied (Meniche et al., 2014). The MA, AG and PG are covalently linked together forming the MA-AG-PG complex. This complex is insoluble and is referred to as an essential core of the mycobacterial wall. with many Anti-TB therapeutics target the MA-AG-PG complex.

The synchronized synthesis and molecular linkages within the cell wall determine the growth and structure of mycobacterial cells (Meniche et al., 2014). The amount of pressure exerted by the microenvironment on bacterial cell, suggests that mycobacteria need to adapt in order to survive (Kieser & Rubin, 2014). Mycobacterial cell wall growth and division produces two daughter cells that possibly undergo extensive cell wall remodeling during infection. The mycobacteria has mastered the ability to withstand this highly stressful microenvironment encountered during infection (Dhar et al., 2013; Singh et al., 2013). In model rod-shaped bacteria, cell division has been studied extensively, but in the higher order bacteria including *M. smegmatis*, less is understood about the cell division requirements. In general, bacterial cell division requires the collaborative effort of many proteins in both space and time to facilitate the process of creating two daughter cells (Baranowski et al., 2019). However, it is still uncertain where the activity of the cell wall biosynthetic systems are spatially localized and how these systems must be coordinated in order for polar elongation to take place. In addition, there is still a gap in understanding the regulation of these enzymatic activities. Exploiting the activity of these enzymes and their protein interacting partners, by disrupting the coordination of cell wall

biosynthesis and biodegradation, should block or severely affect cell division. This can possibly lead to disturbance of the cell cycle and consequently result in bacterial killing.

1.4. PG crosslinking

Almost all known bacteria contain PG, excluding *Mycoplasma*, *Chlamydia* and the archaea species, where the membrane comprises of protein compounds i.e. psedomurein creating semirigid cell walls which replace PG (Pavelka, 2007; Hett & Rubin, 2008). The PG layer serves as a network and base for the attachment of the outer layers, thus introducing rigidity to the mycobacterial cell wall. Hence, the structure of PG is unique to bacteria and serves as a remarkable target for TB therapeutics. The biological significance of the difference in mycobacterial PG and PG common in other species is unknown. Most Gram-positive bacteria substitute lysine in the PG, but in actinomycetes and Gram-negative bacteria, DAP is commonly used. Mycobacterial PG consist of DAP-DAP and DAP-Ala peptide cross-inking, contrary to other common bacterial PG, which only consists of a dibasic residue (DAP-Ala peptide) for cross-linkage. This biological difference might provide increased rigidity to the PG to assist survival during stressful conditions (Hett & Rubin, 2008). The *N*-Glucoylmuramic acid NAM present in mycobacterial PG and the NAM present in other PG, could contribute to tightening the PG sacculus by providing further opportunity for hydrogen bonding, leading to the increase resistance to β-lactams and lysozyme (Hett & Rubin, 2008). PG is constantly remodeled and the important 3-3 crosslinking is maintained to promote resistance to the harsh conditions during chronic infection and antibiotic resistance (McNerney et al., 2000; Kieser & Rubin, 2014). Mycobacterial cell elongation occurs through the extension of the cell poles. This extension is mediated by the intercalation of new PG in the subpolar region of the cell (Kieser & Rubin, 2014). PG is highly conserved in mycobacterial species and the enzymes required for its biosynthesis need to be closely regulated ensuring viability (Kieser & Rubin, 2014).

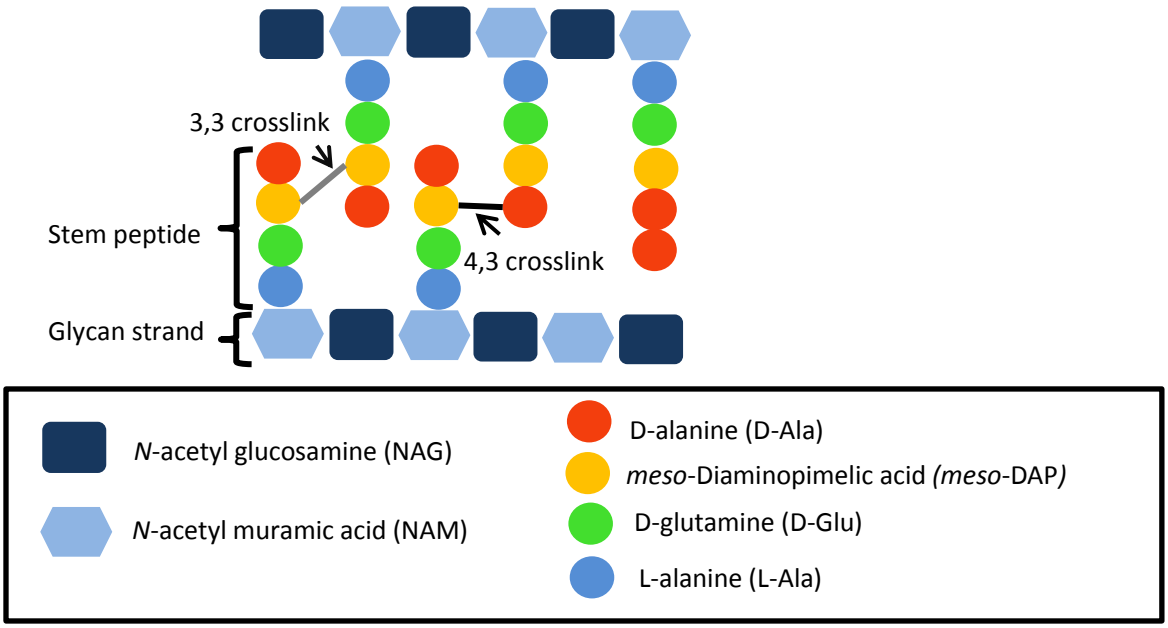


Figure 1.3: **Schematic representation of PG structure and the different PG cross-linkages**. The components of the PG layer are indicated: G: *N*-acetyl glucosamine navy square, M: *N*-acetyl muramic acid in light blue hexagon, L-alanine: blue circle, D-glutamine: green circle, *meso*-Diaminopimalate: yellow circle and D-alanine: red circle. The 4-3 crosslinks (black line) are formed by the linkage of the terminal D-ala and the *meso*-Diaminopimelic acid (*m*DAP) residues of alternating stem peptide, while the 3-3 crosslinks (grey line) are formed by the linkage between the alternating L-and D-centers of DAP residues of the PG stem peptide. Adapted from (Kieser & Rubin, 2014).

1.5. PG biosynthesis

The biosynthesis of PG layer is a multistep process mediated by an assortment of both periplasmic and cytoplasmic enzymes that function together to build, break down and remodel the PG layer (Hett & Rubin, 2008; Favini-Stabile et al., 2013). PG synthesis begins in the cytoplasm and the initial committed step involves the formation of fructose-6-phosphate from UDP-GLc*Nac*, through the catalysis of GlmSMU, followed by the synthesis of UDP-Mur*Nac* catalyzed by MurAB enzyme activity (Figure 1.4) (Hett & Rubin, 2008; Favini-Stabile et al., 2013). This is then followed by the sequential addition of amino acids catalyzed by the aminoligases (MurC, MurD, MurE and MurF). In the cell (inner) membrane, the phosphor-Mur*Nac*-peptide of UDP-Mur*Nac* which is part of the UDP-Mur*Nac* pentapeptide, is transferred to the decaprenyl-phosphate (cell wall subunit carrier) using the MurY, thus resulting in the formation of lipid I (Figure 1.4) (Hett & Rubin, 2008). Thereafter, lipid I is converted into lipid

II by MurG a peripheral membrane associated enzyme, through the addition of UDP-NAG. Lipid II is then translocated through the cell membrane into the periplasm by a cell wall subunit carrier Undecaprenol, with the aid of PG remodeling enzymes (FtsW/RodA) (Figure 1.4) (Barreteau et al., 2008). The final PG synthesis takes place in the periplasm, where the incorporation of newly formed lipid II subunits is attached to the existing PG sacullus (Barreteau et al., 2008; Hett & Rubin, 2008).

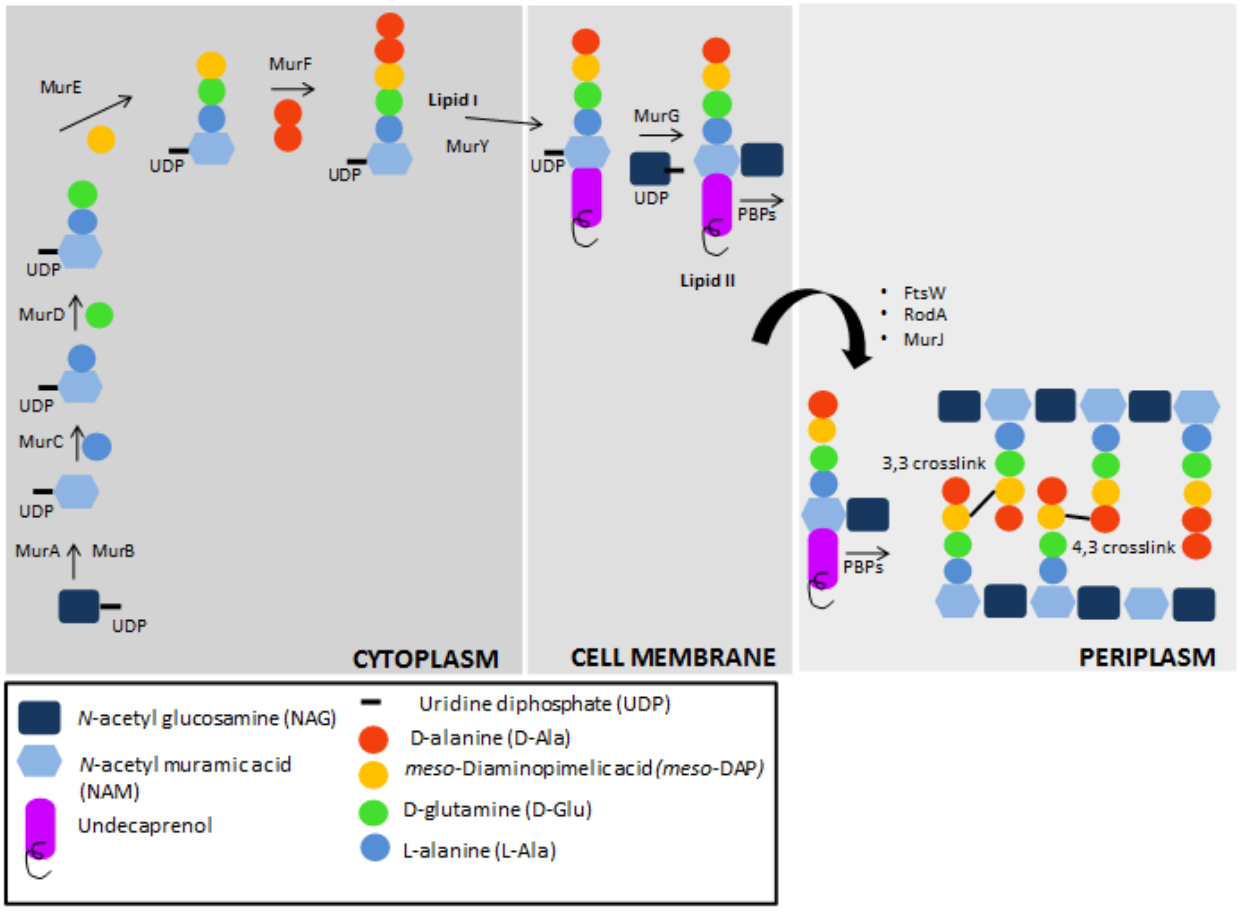


Figure 1.4: **Schematic representation of PG biosynthesis pathway.** In the cytoplasm NAG (navy square) is converted to NAG (light blue hexagon) by the action of MurA and B, this is followed by simultaneous addition of amino acids through the action of aminoligases (MurC to F) to create Lipid I. In the cell membrane, MurY and MurG catalyze the formation of Lipid I and Lipid II, respectively. Once the Lipid II has been created, it is then translocated and through the action of flippases (FtsW/RodA/MurJ), it is incorporated into the pre-existing PG through the action of PBPs. Figure adapted from (Barreteau et al., 2008; Hett & Rubin, 2008).

PG synthesis requires stringent regulation and the PG hydrolases and biosynthetic enzymes are crucial facilitators of this process. PG biosynthetic enzymes include; transglycosylase and transpeptidase and the hydrolytic enzymes include; amidases, muramidases, glucosaminidases, lytic transglycosylases, carboxypeptidases and endopeptidases (Hett & Rubin, 2008). The PG remodeling process is carefully controlled to meet the need for new subunits specifically during cell growth and division. The hydrolases are different in their function, to degrade PG at specific sites, peptidases break peptide bonds, amidases act on existing amide bonds, and glycosidases break glycosidic bonds (Figure 1.5) (Hett & Rubin, 2008). Some reactions show evidence that biosynthesis and hydrolytic enzymes have an antagonistic functional relationship, but recent studies have identified two classes of enzymes that physically interact and form complexes. These complexes act in a concerted fashion to break down bonds and generate gaps to allow new monomers to bind to the PG strand. An example of such a complex is the interaction between a resuscitation promotion factor B (RpfB) which functions as a (lytic transglycosylase) and the RipA (an endopeptidase), thus confirming that protein-protein interaction play a crucial role in regulating PG hydrolytic activity (Hett et al., 2007; Hett & Rubin, 2008).

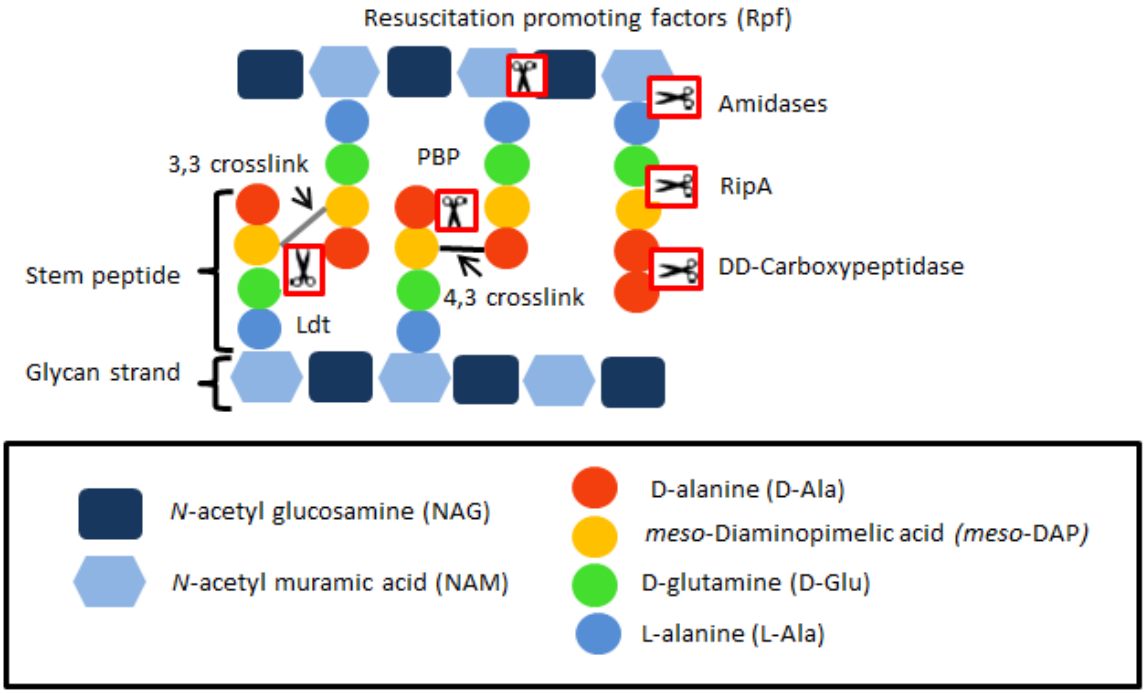


Figure 1.5: **Schematic representation of PG hydrolytic and biosynthetic enzymes.** The enzymes catalyzing the remodeling of PG layer; resuscitation promoting factors (Rpf) breaks the bond between the glycan strand, Amidases breaks the bonds between glycan strand and stem peptide,RipA (endopeptidase) breaks bonds between the *meso*-Diaminopimelic acid and carboxypeptidasees break the bond between D-alanine residue. Penicillin binding protein (PBP) breaks the 3,4 crosslinks and the 3,3 crosslink bond is broken by the L,D- transpeptidase (Ldt). Image adapted from (Barreteau et al., 2008)

1.6. Cell growth and division in mycobacteria

In mycobacteria, cell division need to be tightly regulated at the various levels to provide sufficient opportunity for phenotypic differences to develop between individual cells within a population (Kieser & Rubin, 2014). The unique ability of mycobacterial growth that produces daughter cell populations of varying sizes, growth rates and cell wall composition allows for a sophisticated heterogenic population. Bacterial cell proliferation process encompasses elongation of the cell where new cell wall material incorporation at both old and new poles at the sites of growth and division of the one cell forming two asymmetric daughter cells with equivalent genetic material to that of the mother cell (Hett & Rubin, 2008; Santi & McKinney, 2015; C. Baranowski et al., 2019). In *B. subtilis*, cell growth and division occur simultaneously, while in mycobacteria, division and elongation occur in spatially distinct regions and thus needs to be tightly regulated. Careful regulation ensures that division is completed before the growth at the

new pole commences, following the chronology; elongation, cytokinesis, septation and lastly physical separation (Kieser & Rubin, 2014; C. Baranowski et al., 2019). Numerous bacteria produce symmetrical progeny after cell division, with daughter cells of equal size. In mycobacteria (pole growers) the site of division simultaneously becomes the site of new pole elongation. In *B. subtilis*, the location of new cell wall synthesis along the side walls is directed by an actin protein called MreB. Mycobacteria have no such homolog but rather use DivIVA, also called Wag31, this protein nucleates new growth at the poles (Figure 1.6) (Hett & Rubin, 2008; C. Baranowski et al., 2019).

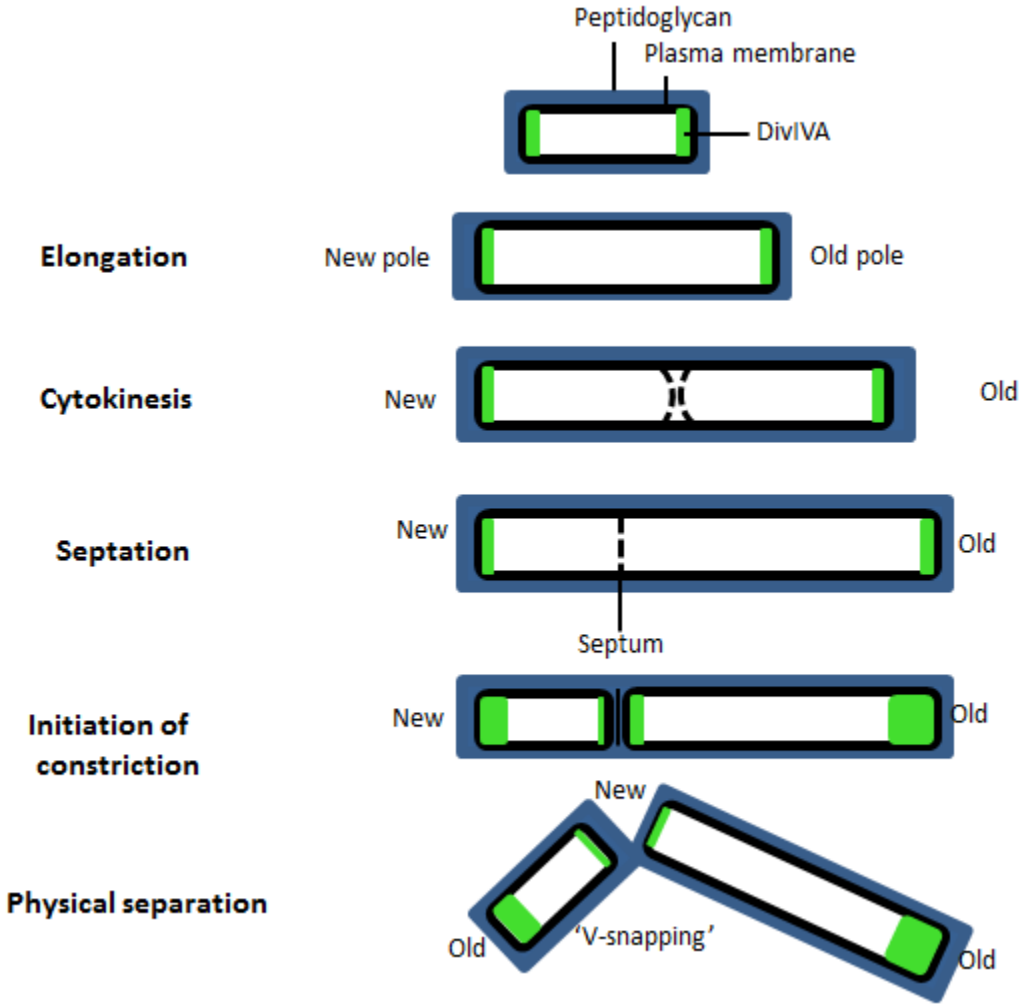


Figure 1.6: **Model of mycobacterial polar growth, cell elongation and cell division.** Mycobacteria cell growth extends by the of new cell wall material incorporation at the poles. Image adapted from (Kieser & Rubin, 2014).

1.6.1. Modes of growth in rod-shape bacteria

Cell division follows a simple process: segregation and replication of genetic material, division of cytoplasmic material then finally the production of new daughter cells. In mycobacteria, this process follows careful coordination and ensures proper localization and timely divisome assembly at midcell site after the final DNA separation step. In these localizations, PG hydrolases need to be carefully coordinated to prevent cell lysis and the timely synthesis of new PG meets the demand of the cell (Hett & Rubin, 2008; Santi & McKinney, 2015). Mycobacteria have developed a mechanism to maintain a fine balance between inert and nascent PG, the switch from nascent to inert is thought to be controlled at the septum, thus channeling all PG synthesizing enzymes to restrict PG synthesis at special areas (Figure 1.7) (Dhar et al., 2013; Baranowski et al., 2019).

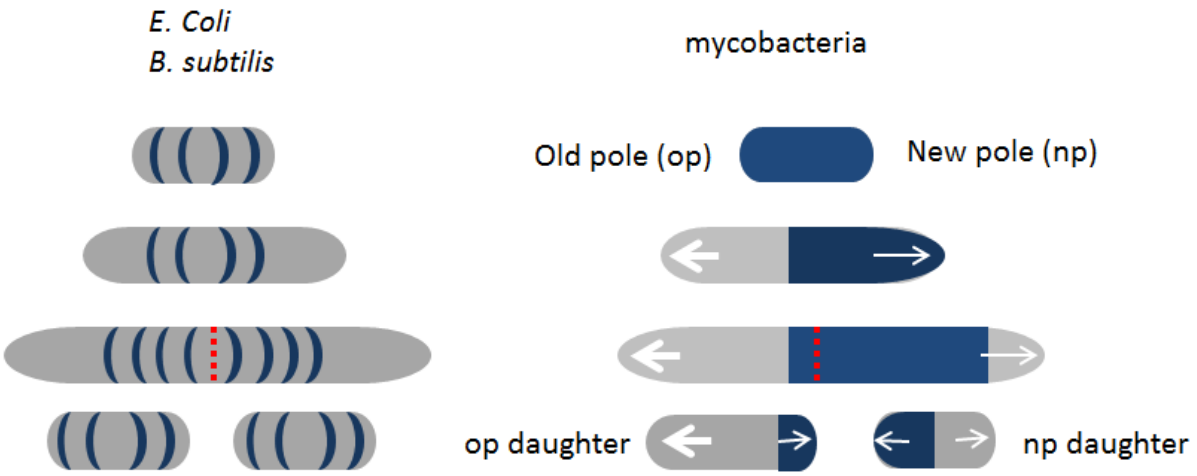


Figure 1.7: **Characteristic bacterial growth and division models.** Bacterial replication models of *E. coli B. subtilis* and mycobacteria. *E. coli* and *B. subtilis* grow by incorporating new cell wall along the lateral cell body (navy lines). Mycobacteria grow only at cell pole sites, at unequal levels (asymmetrically) of growth depending on the age of the pole. New cell wall incorporated at the growth regions (navy shaded regions). Arrows indicate polar region of new synthesis (the larger arrow indicates more growth dotted line shows the septum (red dotted line). Grey area is the new cell wall. Figure adapted from (C. Baranowski et al., 2019).

1.6. Chromosome segregation and bacterial cell division

The initiation of septation is facilitated by the self-activating GTPase, FtsZ, polymerizing into a ring-like structure called the Z-ring (Hett & Rubin, 2008; Kieser & Rubin 2014). The Z-ring functions for septation site determination approximately at mid-cell and providing the membrane constriction process with energy, in addition to providing a scaffold for PG remodeling enzymes (Dhar et al., 2013; Kieser & Rubin, 2014). This is simultaneously followed by the recruitment of divisome enzymes (FhaB, FtsW, FtsQ, CrgA and CwsA) and PG hydrolases (PonA1 and PonA2). The bridge formed between FtsZ and FtsQ is mediated by FhaB and ensures proper Z-ring formation, making FhaB a crucial interaction mediator. PBPB is recruited into the fold through the interaction of extracytoplasmic loop of FtsW (Figure 1.8), creating the FtsZ-FtsW-PBPB complex which joins the septum synthesis to cytoplasmic structural cues (i.e. Z-ring polymerization) (McNerney et al., 2000; Hett & Rubin, 2008). Following FtsZ, CrgA localizes to the divisome and also functions to recruit PBPB. CrgA interaction with CwsA assists the elongation and division process during cell proliferation by coordinating septum formation after elongation (Kieser & Rubin, 2014). Three PG synthases (PBPB, PBPA and PonA1) provide divisome stability and promote septum formation by synthesizing septal PG, PonA1 is the only known bifunctional PG, Synthase that localizes at the septum (Kieser & Rubin, 2014). PBPB interacts with an important late stage septation protein. This PBPB-DivIVA interaction is crucial for survival under oxidative stress. Similarly, DivIVA-CrgA interaction plays an important part in conveying messages between the division and elongation machineries (Figure 1.8) (McNerney et al., 2000; Baranowski et al., 2019). DivIVA localization determines the division site after the septum has been formed, as division proceeds there is an increase in DivIVA concentration, with more DivIVA deposited on the old pole compared to the newly formed pole (as seen in Figure 1.7) (Kieser & Rubin, 2014).

The process of chromosome segregation takes place simultaneously with replication, commencing just after the replication process has been initiated (Hett & Rubin, 2008). DNA partitioning and segregation is a fundamental process that facilitates the transfer of hereditary genomic material. ParA and ParB (partitioning proteins) proteins are involved in active segregation of chromosomes in mycobacteria (Bartosik et al., 2014). This partitioning system consists of A-type (ParA) and B-type (ParB) proteins. A-type proteins are ATPase's and allow

for segresome movement. The B-type proteins form nucleoprotein complexes by recognizing and binding to specific centromere-like sequences on the bacterial chromosome (Bartosik et al., 2014). ParB interacts with DNA and the ParA-ParB-DivIVA complex then pulls the replicating chromosome to the site of the growing pole, through the association of ParA with DivIVA. The concomitant interaction of the protein complex facilitates the accurate movement and positioning of genetic material to the daughter cells during cell division (Ginda et al., 2013; Bartosik et al., 2014). During segregation of mycobacterial chromosomes the ParB protein binds at the origin (OriC) of the chromosome, where it forms nucleoprotein complexes called the segresomes (Ginda et al., 2013). The movement of segresomes is ParA-dependent and is associated with the rapid extension of the new pole (Ginda et al., 2013). However, this mode of growth requires the segregation of DNA and the separation of cytoplasmic material in order to produce two daughter cells possessing similar genetic material and other cellular contents (Hett & Rubin, 2008). DivIVA orthologs have been reported to associate with cell wall synthesis proteins thus facilitating the process of cell division, chromosomal separation and growth (Meniche et al., 2014; Kieser & Rubin, 2014). DivIVA is spatially localized at the cell pole sites of negative curvature where polar growth occurs (Meniche et al., 2014). The interaction between DivIVA and other cell division and cell growth enzymes has been demonstrated (Meniche et al., 2014). However, it is still unclear as to how DivIVA is anchored and what other cell segregation proteins it interacts with to facilitate chromosomal segregation and cell wall synthesis. Exploiting the activity of the possible DivIVA anchoring partners by disrupting the coordination of DivIVA activity may yield new drug targets. This MSc focuses particularly in DivIVA protein family, which is discussed in further detail below.

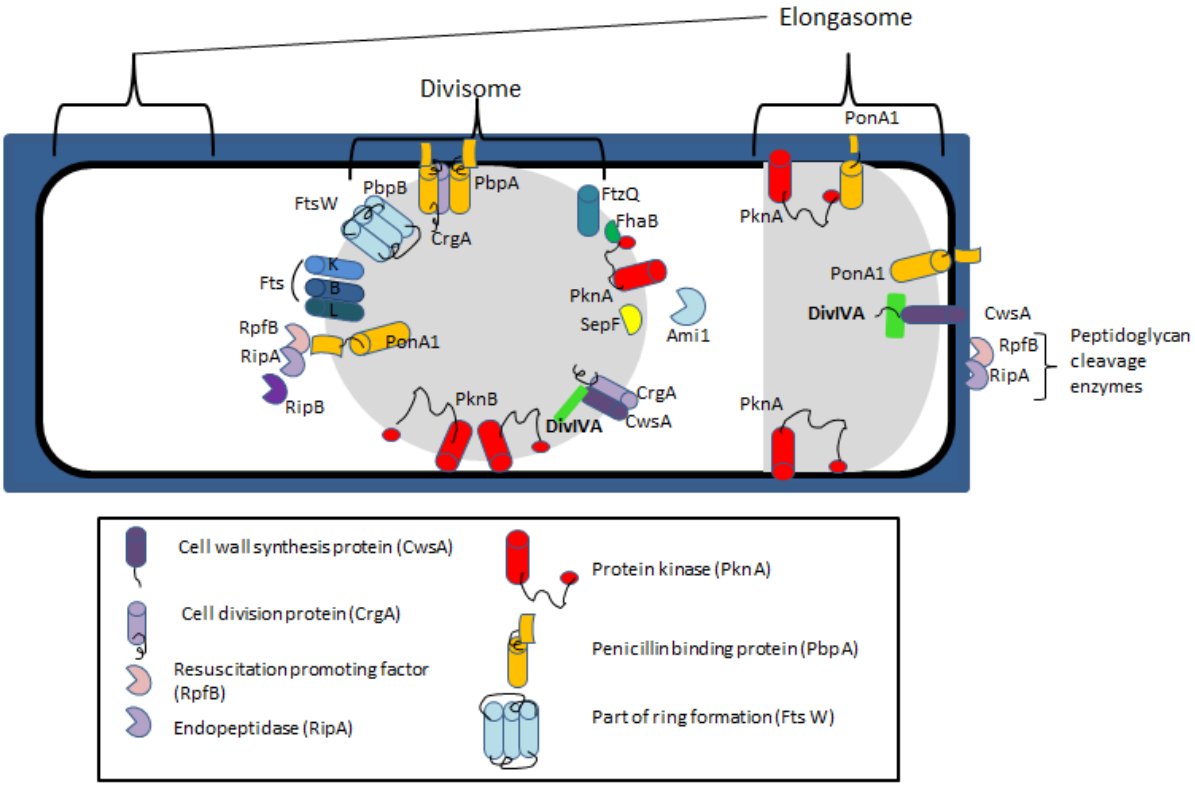


Figure 1.8: **Schematic representation of the mycobacterial divisome and elongasome machinery.** Mycobacterial partitioning and elongation proteins that facilitate cell division some interacting proteins have been shown but some have been identified through depiction. DivIVA shown in a light green rectangle Image adapted from (C. Baranowski et al., 2019).

1.7. DivIVA

1.7.1. Structure and function of DivIVA

The mycobacterial cell elongation protein, DivIVA, also called Wag31 or Ag84 (Antigen) is essential for survival in mycobacteria. It functions in cell pole localization directed by polar curvature (pole sensing protein) (Hett & Rubin, 2008; Kieser & Rubin, 2014). DivIVA is phosphorylated by protein kinases PknA/B (facilitate activation of proteins), these kinases control growth and PG biosynthesis in *Mtb* through phosphorylation of DivIVA and activation of the Mur enzyme (Jani et al., 2010; Turapov et al., 2018). DivIVA has the unique ability to associate with both division (septal PG synthase PBPB) and elongation (CwsA) proteins (Baranowski et al., 2019). Studies reported that this cytoplasmic protein interacts with mycolic acid synthesis enzymes (Kieser & Rubin, 2014; Baranowski et al., 2019). Primarily, DivIVA

localizes to the old pole and also localizes at the septum during late stages of division (Kieser & Rubin, 2014; Baranowski et al., 2019).

1.7.2. Structural diversity in DivIVA peptides

DivIVA protein is highly conserved in Gram-positive bacteria, with some structural diversity in the different species, leading to variants in functional capabilities. Mycobacterial DivIVA is made up of 260 residues (96 residues longer than *B. subtilis* DivIVA) containing two coiled coil domains, a N-terminal membrane (lipid) binding domain and a C-terminal (tetrameric) domain joined by a 100 residue linker region (Oliva et al., 2010; Choukate et al., 2019; Choukate et al., 2020). The mycobacterial DivIVA has the propensity to form trimers at the coiled coil rich intermediates with bending 'kinking' and branching assemblies (Choukate et al., 2019) It has been reported that DivIVA localization at the poles is due to geometric cues, such as negative curvature, sensing a mechanism for higher order assembling (Oliva et al., 2010; Choukate et al., 2020). In the linker that is housed between the two domain is a phosphorylation site, the active site that permits activation by protein kinases thus allowing regulation of DivIVA activity (see figure 1.9) (Oliva et al., 2010; Choukate et al., 2019). Due to its amphiphilic nature, DivIVA interacts with both cytoplasmic and transmembrane proteins. Examples include *B. subtilis* DivIVA interacting proteins that contribute to cellular processes such as cell division (MinJ), chromosome segregation (Sp0J), competence development (ComN and Maf) and protein secretion (SecA). Less is known about *M. smegmatis* DivIVA interacting protein partners and or anchoring partners (Halbedel & Lewis, 2019; Choukate et al., 2020). The variety of DivIVA interacting partners could be ascribed to the use of different interaction surfaces for the different binding partners (Halbedel & Lewis, 2019). The high connectivity of this protein with other important players in metabolism makes DivIVA an interesting target for anti-TB drug development.

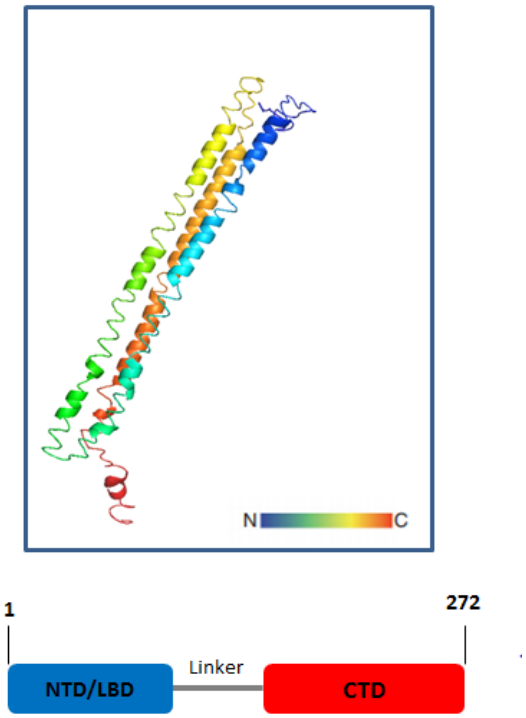


Figure 1.9: **Predicted tertiary structure of *M. smegmatis* DivIVA and schematic representation of the domain organization.** The schematic domain organization of DivIVA represented in a color spectrum beginning from blue to red (N to C-terminal), N-terminal domain (blue rectangle) and C-terminal domain (red rectangle). Image adapted from i-Tasser protein prediction software (http://zhanglab.ccmb.med.umich.edu/I-TASSER/) created August 2018.

1.7.3. DivIVA as a drug target for TB drug development

The mycobacterial DivIVA is an integral cell pole determinant and its regulatory activity is pivotal for polar growth. Hence, DivIVA has been identified as a target for anti-TB therapeutic agent aminopyrimidine sulfonamide, Figure 1.10 (Singh et al., 2016; Choukate et al., 2020). Further understanding of the biochemistry and mode of action of these novel therapeutic could identify new vulnerable targets in *Mtb*.

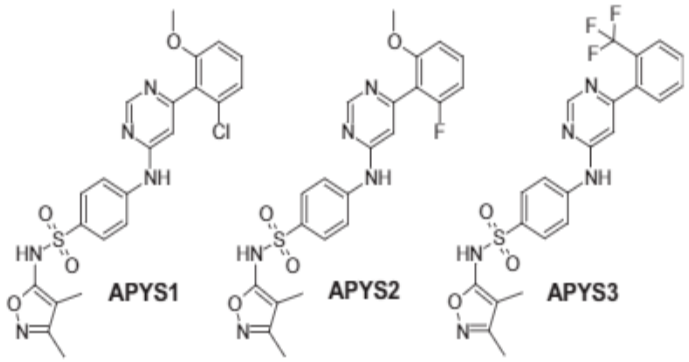


Figure 1.10: **Aminopyrimidine-sulfuonamides (*APYS*) potent anti-tubercular compounds**. Chemical structure of APYS potential DivIVA modulators, the structures were identified by phenotypic screening. Image adapted from (Singh et al., 2016).

1.8. Hypothesis and research motivation

Putative interacting partners of the *M. smegmatis* ParA and ParB homologues, which known cell pole determinants in mycobacteria, have been previously identified using microfluidic time-lapse fluorescence microscopy (Ginda et al., 2017). This technique was used to address the question of ParA and ParB dynamics in *M. smegmatis*, revealing the asymmetric action of segregation machinery driven by ParB complexes. The technique identified DivIVA as a ParA interacting partner. It was thus hypothesized that mycobacterial DivIVA plays a crucial role in cell growth, more specifically in cell elongation and division, through the close interaction with DNA segregation and cell wall synthesis enzymes. The focus of the current study is the identification of DivIVA anchoring partners, that is, those proteins that anchor DivIVA to the membrane. We hypothesize that DivIVA is anchored to the membrane through specific interaction, with as yet unidentified partnering proteins. This will be investigated as described below.

1.10. Aims and Objectives

1.10.1. Aim

The aim of the study is to identify interacting protein partners for DivIVA

1.10.2. Specific objectives

- To generate a protein interaction library for the identification of DivIVA interacting partners
- To study the domain organization of putative interacting partners.
- Cellular localization of putative interacting partners using fluorescence microscopy.

2. Materials and methods

2.1. Bio-informatics and database tools used

2.1.1. Database tools used to obtain DNA and protein sequences of interest

Table 2.1.1. **Database tools used to obtain DNA and protein sequences**

Database tools	Use in the study	Website address
Smegmalist	The Smegmalist database tool was used to investigate *M. smegmatis* mc²155 strain protein sequence and the genomic DNA of the genes of interest.	http://mycobrowser.epfl.ch/smegmalist.html
Tuberculist	The tuberculist was used to investigate the *Mtb* H37RV strain genomic DNA and protein sequences of interest.	http://tuberculist.epfl.ch
EcoCyc	The EcoCyc data base was used for the analysis of *E. coli* genomic DNA and protein sequence	http://www.ecocyc.org/ECOL/organism-summary

The bioinformatics and software tools used in this study for the identification and analysis of various genes and proteins of interest are listed below.

Table 2.1.2. **Bioinformatics and software tools used to analyze genes and proteins of interest.**

Bioinformatics and software tools	Use in the study	Website address
NCBI BLAST	The Basic Local Alignment Search Tool database was used for the comparison of protein sequences to locate similar regions of similarities between gene sequences of interest in *M. smegmatis* and related organisms.	http://blast.ncbi.nlm.nih.gov/Blast.cgi
pFam database	The Protein Family database was used for to identify and locate the position of functional domains in a protein sequence of interest	http://pfam.xfam.org/about
Clustal Omega	The Clustal Omega database was used to align multiple sequences of nucleotide or amino acid in order to	http://www.ebi.ac.uk/Tools/msa/clustalo/

	identify regions of similarity in protein sequence of interest and related organisms.	
STRING	The Search Tool for the Retrieval of Interacting genes/proteins (STRING) database was used for the prediction of protein-protein interactions between protein sequence of interest and unknown and known proteins in *M.smegmatis*	http://string-db.org/
I-TASSER	The Iterative Threading Assembly Refinement server is a tool was used for the identification of protein threading and function. This tool analyses the functional prediction of the identified putative interacting proteins.	http://zhanglab.ccmb.med.umich.edu/I-TASSER/
PyMOL	The PyMOL software is an open source molecular visualization system. This software was used to visualize and analyze the structure of the predicted protein of the identified putative interacting partners of interest.	https://www.pymol.org/
Fiji	The Fiji software is an data server image processing system. This software was used for to investigate the microscopic images that were captured using the fluorescence microscope, Zeiss Observer ZI inverted fluorescence microscope.	http://imagej.net/Fiji

2.2 Bacterial strains and plasmids generated/ used in the study

The plasmids and bacterial strains generated and/or used in this study are indicated in Table 2.2.1 and table 2.2.2 respectively.

Table 2.2.1. **Plasmids generated and/or used in this study**

Plasmids	Description	Source/Reference
pUAB300	*E. coli-Mycobacterium* episomal plasmid vector carrying the mDHFR fragments ([1], [2]). Hyg^R	Singh et al., 2006
pUAB400	*E. coli-Mycobacterium* integrating plasmid vector carrying the mDHFR fragment [3]. Kan^R	Singh et al., 2006
pUAB400+4217	Derivative of pUAB400 carrying the complete wild-type allele of MSMEG_4217. Kan^R	This study
pUAB300+RipA	Derivative of pUAB300 with inserted wild-type allele of *ripA*. Kan^R	CBTBR D. Ralefeta
pUAB400+RpfB	Derivative of pUAB400 with the wild-type allele of *rpfB*. Hyg^R	CBTBR D. Ralefeta
pTweety+mRFP	Complementation vector with the monomeric red fluorescent protein (mRFP). Kan^R	Pham et al., 2007
pTweety+mRFP+5632	Derivative of pTweety with the wild-type MSMEG_5632	This study

	full length allele with a C-terminal mRFP. Kan^R	
pTweety+mRFP+1577	Derivative of pTweety with the wild-type MSMEG_1577 full length allele with a C-terminally tagged monomeric red fluorescence protein. Kan^R	This study

Table 2.2.2. **Bacterial strains generated and/or used in this study**

Strain	Description	Source/ Reference
E.coli DH5α	*SupE44 ΔlacU169 hsdR17 recA1 gyrA96 thi-1 relA1*	Promega, Madison, WI
mc^2155	The *M. smegmatis* High frequency transformation strain ATCC 607	Snapper et al., 1990
mc^2155::RipARpfB	Derivative of mc^2155 with the integrated plasmids pUAB300+RipA and pUAB400+RpfB. $Kan^R Hyg^R$	CBTBR D. B.Ralefeta
mc^2155::4217	Derivative of *M. smegmatis* with the integrated plasmid pUAB400+MSMEG_4217. Kan^R	This study
mc^2155::pUAB400 pUAB300	Derivative of *M. smegmatis* with the integrated pUAB400 plasmid inserted at the *attB* site, and the episomal pUAB300 plasmid. $Kan^R Hyg^R$	CBTBR P. Mashilo
mc^2155::5632mRFP	Derivative of *M. smegmatis* with the integrated full-length allele of MSMEG_5632 with a C-terminal tagged mRFP. Created through electroporation of plasmid pTweetyMSMEG_5632_mRFP Kan^R	This study
mc^2155::1577mRFP	Derivative of mc^2155 with the integrated full-length allele of MSMEG_1577 with a C-terminal tagged mRFP. Constructed by electroporation of plasmid pTweetyMSMEG_1577_mRFP Kan^R	This study

Hyg^R: Hygromycin resistance. Kan^R: Kanamycin resistance, $Trim^R$: Trimethoprim resistance.

2.3. Bacterial strain and derivative growth conditions

2.3.1. Growth conditions for *E. coli* DH5α and derivative strains

E. coli DH5α and derivative strains were cultured in Luria-Bertani broth (LB) or on Luria-Bertani agar (LA) at 37 ˚C supplemented with appropriate antibiotics at the following concentrations: Ampicillin (Amp): 100 µg/ml or Streptomycin (Str): 50 µg/ml, Hygromycin (Hyg): 200 µg/ml, Kanamycin (Kan): 50 µg/ml and were grown overnight in liquid cultures at 37 ˚C with shaking at 250 rpm.

2.3.2. Growth conditions for *M. smegmatis* mc^{2}155 and derivative strains

M. smegmatis wild-type mc^{2}155 and derivative strains were cultured in Middlebrook 7H9 liquid media supplemented with 0.2% glucose, 0.5% glycerol, 0.085% NaCl, 0.05% Tween80 (herein referred as 7H9) and appropriate antibiotics at 37˚C or on Middlebrook 7H10 solid media supplemented with 0.2% glucose, 0.5% glycerol, 0.085% NaCl (herein referred as 7H10 agar). The concentrations of antibiotics used were as follows: Hyg: 50 µg/ml and Kan: 25 µg/ml. Middlebrook 7H9 cultures were grown at 37 ˚C with shaking at 250 rpm.

2.4. DNA extractions

2.4.1. Chromosomal DNA extraction of *M. smegmatis* mc^{2}155

2.4.1.1. Small scale extraction of chromosomal DNA

For the isolation of small-scale chromosomal DNA, the colony boil method was used for the extraction of wild-type mc^{2}155 *M. smegmatis* and derivative strains, where half a colony was scraped from solid media and subsequently resuspended in 50 µl of ds$H_2$0. Following this, 50 µl of chloroform was mixed into the suspension and then vortexed. The mixture was then incubated at 95 ˚C for 5 min, followed by centrifugation at 12 470 *X*g for 5 min and the supernatant was collected into a clean tube. For PCR, 5 µl of the aqueous layer was used as DNA template.

2.4.1.2. Large scale extraction of chromosomal DNA

For the isolation of bulk scale chromosomal DNA, the Cetyltrimethylammonium bromide (CTAB) was used for the extraction of wild-type mc^2155 *M. smegmatis* and derivative strains. The strains were cultured at 37 ˚C using the Middlebrook 7H10 agar for 2 days. Subsequently, cells were scraped off the plate and mixed in with 500 µl of TE buffer. The cells were then heat killed by incubating the suspension at 65 ˚C for 20 min. Thereafter, cells were incubated on ice for 10 min. Subsequently, 50 µl of lysozyme (10 mg/ml) was added to the mixture and followed by incubation period of an hour at 37 °C. Thereafter, 6 µl and 70 µl of a (10 mg/ml) concentration of proteinase K and 10% SDS, respectively, was added and incubated at 65 ˚C for 2 hours. This was followed by the addition of 100 µl of NaCl (5 M) and 80 µl CTAB/NaCl that was pre-warmed (10% N-cetyl-N,N,N-trimethylammonium bromide, 4.1% NaCl dissolved in dH_20). The mixture was subsequently incubated for 10 min at 65 ˚C. Following this, an equal volume of chloroform: Isoamyl alcohol (24:1 v/v) was added to the cells and mixed by a few inversions of the tubes, followed by centrifugation at 12 470 *Xg* for 10 min at room temperature. The top aqueous layer was transferred into a fresh Eppendorf tube and the precipitation of DNA was carried out by the addition of 600 µl of isopropanol, followed by centrifugation at 12 470 *Xg* for 30 min. Subsequently, the supernatant was poured off and 1 ml of ice-cold 70% ethanol was used to wash the pellet through centrifugation at 12 470 *Xg* for 5 min. The pellet was dehydrated using an Eppendorf Concentrator 5301 and resuspended in nuclease-free water to a final volume of 50 µl. This constituted as chromosomal DNA and was quantified using the NanoDrop ND-100 Spectrophotometer (NanoDrop technologies) and stored at 4 °C until further use.

2.4.2. Plasmid DNA extraction of *E. coli*

2.4.2.1. Small scale extraction of plasmid DNA

For the small-scale plasmid DNA extraction, the alkaline lysis mini-preparation method was used to extract plasmid DNA from *E. coli* DH5α and its derivative strains in order to isolate the plasmid of interest. The derivative strains were cultured in 2 ml of LB media supplemented with appropriate antibiotics and incubated at 37 °C. The cells were pelleted by centrifugation at 12470 *Xg* for 5 min and reconstituted in 80 µl of solution I (25 mM Tris-HCI, 10 mM EDTA, 50 mM Glucose; pH 8). Subsequently, 160 µl of solution II (0.2 M NaOH, 1% SDS) was added into the

mixed followed by a few inversions of the tubes and incubation for 5 min at room temperature. Thereafter, 120 µl of solution III (3 M potassium acetate, 11.5% acetic acid) was mixed in and incubated for a further 5 min on ice. Subsequently, the mixture was centrifuged for 10 min and the top aqueous layer was decanted into a clean tube. Thereafter, 3 µl of RNase A (10 mg/ml) was added into the supernatant and the suspension was incubated for a period of 15 min at 42 °C. The precipitation of plasmid DNA was carried out by the addition of 600 µl of isopropanol, followed by centrifugation at 12470 *Xg* for 30 min. The top aqueous layer was poured off and the pellet washed with 1 ml ice-cold 70% ethanol and dehydrated using an Eppendorf Concentrator 5301. The plasmid DNA pallet was reconstituted in nuclease free water to a final volume of 50 µl and quantified, and was stored at 4 °C for further use.

2.4.2.2. Large scale extraction of plasmid DNA

For the bulk preparation of plasmid DNA, the nucleobond DNA extraction kit (Macherey-Nagel) was used following manufacturer's instructions. The strains were cultured in 50-100 ml LB media supplemented with appropriate antibiotics at 37°C overnight. Cells were then pelleted by centrifugation at 4 500 *Xg* for 15 min at 4 °C. The supernatant was poured off and the pellet reconstituted in 4 ml of Buffer S1 (50 mM Tris-HCI, 10 mM EDTA, 100 µg/ml RNase; pH 8.0), followed by addition of 4 ml of Buffer S2 (200 mM NaOH, 1% SDS). The suspension was mixed by periodic inversion and incubation for 3 min at room temperature. Following this, 4 ml of Buffer S3 (2.8 M KAc; pH 5.1) was added into the suspension, mixed by inversion and incubated on ice for 5 min, followed by centrifugation at 1180 *Xg* for 30 min. Two and half ml of equilibrium buffer solution was passed through the nucleobond Ax100 column for the purpose of equilibration and this was followed by a 10 ml addition of Buffer N2 (100 mM Tris, 15% ethanol, 900 mM KCI, 0.15% Triton X-100, set to pH 6.3 with H_3PO_4). Subsequently, the clarified cell lysate was poured into the column. This was followed by 10 ml of Buffer N3 (100 mM Tris, 15% ethanol, 1.15 M KCI, set to pH 6.3 with H_3PO_4), which constituted the column wash step. Thereafter, 5 ml of Buffer N5 (100 mM Tris, 15% ethanol, 1 M KCI, adjusted to pH 8.5 with H_3PO_4) was used for elution of the plasmid DNA which was collected from the column in a clean tube. The precipitation of plasmid DNA was carried out by the addition of isopropanol to the collected suspension, which was then centrifuged at 12 470 *Xg* for 30 min. The

precipitated DNA was subsequently washed with 1 ml of ice-cold 70% ethanol, then followed by decanting the supernatant and drying the pellet using an Eppendorf Concentrator 5301.

2.5. DNA clean-up and removal of contaminating proteins

2.5.1. Sodium acetate precipitation

The isolated chromosomal and plasmid DNA was further purified using sodium-acetate precipitation to remove any salts, contaminating debris from protein and other impurities. In brief, sodium acetate (1/10 volume 3 M; pH 5.2) was added to the DNA suspension and (3 X volume) ice-cold 100% ethanol was also mixed into the suspension. The suspension was vigorously mixed, then followed by centrifugation at 12 470 *Xg* for 30 min. For the genomic DNA precipitation specifically, (1/10 volume, 3 M; pH 5.2) sodium acetate and (3 X volume) ice-cold 100% ethanol were mixed in with the DNA suspension and then incubated at -20 °C for 20 min. Subsequently, the suspension was pelleted by centrifugation at 12 470 *Xg* for 30 min. The supernatant was poured off and the pellet dried using an Epperndorf Concentrator 5301. Both the chromosomal and plasmid DNA pellets were reconstituted in nuclease-free water to a final volume of 50 µl. The DNA was quantified using the NanoDrop Spectrophotometer (NanoDrop technologies) and stored at 4 °C until further use.

2.6. DNA manipulation

2.6.1. DNA amplification

2.6.1.1. PCR primer designing

The online software Primer3 (http://bioinfo.ut.ee/primer3/) was used to design PCR parameters following the parameters shown in the table below:

Table 2.3. **Parameters followed for primer design**

	Size (bp)	Temperature (°C)	% GC
Minimum	18	55	30
Optimum	21	60	50
Maximum	24	65	70

2.6.1.2. Polymerase chain reaction (PCR)

2.6.1.2.1. Fusion High-Fidelity DNA polymerase reaction

The amplification of DNA fragments for cloning purposes was carried out using the Phusion High-Fidelity DNA polymerase (Thermo Scientific) following the manufacturer's instructions with minor changes. In brief, PCR reactions were made up to a final volume of 50 µl by adding the following constituents together; 5 µl X HF buffer, 8 µl of dNTPs to a final concentration of (0.2 mM each), 100 ng of DNA template, 2.5 µl of primers (1 mM each), 1 U of phusion DNA polymerase, 3% of dimethyl sulfoxide (DMSO) and nuclease free dH_2O to make up the final volume. The reactions were incubated in a thermo-cycler (Bio-Rad laboratories) following these cycling parameters; 3 min for the initial denaturation at 98 °C, 30 sec of 35 cycles for a second denaturation cycle at 98 °C, 30 sec of annealing at 65 °C, 1 min extension at 72 °C and 10 min final extension at 72 °C. The 1% agarose gel was used to visualize the PCR DNA products as outlined in section 2.6.3.

2.6.1.2.2. Roche Faststart Taq DNA polymerase reaction

To confirm clones using PCR, the Roche Faststart Taq DNA polymerase (Roche Applied Science) protocol was used following the manufacturer's instructions. In brief, PCR reactions were made up to a final volume of 50 µl by mixing together these following constituents: 5 µl of 10X Roche Faststart Taq DNA polymerase buffer, 10 µl 5X GC buffer, 2.5 µl of primers (1 mM each), 100 ng of DNA template, 1 U of Roche Faststart Taq DNA polymerase, 8 µl of dNTPs (0.2 mM each). The final volume of the reactions was topped up to 50 µl with nuclease free water. The reactions were incubated in a thermo-cycler (Bio-Rad laboratories) using the following cycling conditions: 3 min of initial denaturation at 95 °C, 35 cycles of 30 sec of secondary denaturation at 95 °C, 30 sec of annealing at 65 °C, 1 min of extension at 72 °C and 10 min of final extension at 72 °C. In order to visualize the PCR DNA products, a 1% agarose gel was used as indicated in section 2.6.3.

2.6.2. Restriction digestions

The restriction digest preparations were conducted using restriction enzymes purchased from Fermentas, New England Biolabs (NEB) and Roche Applied Science (Roche). The restriction

digests of plasmids and PCR products were performed following manufacturer's instructions. Briefly, restriction digestions were made up to a final volume of 20 µl per reaction with the addition of 1X recommended buffer, 1 µg of plasmid or PCR DNA was digested with 1 U of restriction enzyme and 2 µl of 100X BSA (Bovine serum albumin) when necessary, then topped up with nuclease-free water to recommended final volume. This was followed by incubation of the reaction at 37 °C for an hour, thereafter the reaction was heat inactivated at 65 °C for 10 min unless stated otherwise as per the manufacturer's instructions.

2.6.3. Agarose gel electrophoresis

Visualization of PCR products, isolated plasmid DNA and chromosomal DNA was carried out using agarose gel electrophoresis. The percentage of agarose gels used depended on the molecular weight of the sample to be visualized/ analyzed, low molecular weight samples were separated using 2% agarose gels and high molecular weight samples were separated using 0.8-1% agarose gels. The gel preparation was conducted as follows; 1X TAE buffer (1 mM EDTA and 0 mM Tris-acetate) with the combination with ethidium bromide to a final concentration of 0.5 µg/ml. To analyze the samples using electrophoresis, the agarose gel electrophoresis tanks (Bio-Rad laboratories) containing 1X TAE buffer were run at 80-90 V for duration of 45 min. In order to estimate size of the fragments, a molecular marker was run alongside the DNA samples being analyzed. Visualization of DNA on agarose gel was performed using the SYNGENE G-Box system.

2.6.4. Purification of DNA fragments

The purification of products of restriction digests or PCR products excised from an agarose gel was conducted using the NucleoSpin PCR clean-up and gel extraction kit (Macherey-Nagel) following manufacturer's directions with minor changes. In brief, the DNA sample was run on an agarose gel followed by the excision of the DNA fragment of interest and the fragment containing the excised DNA fragment was solubilized by mixing with binding buffer through incubation for 5-10 min at 50 °C. One volume of sample was mixed with 2 equivalent volumes of the PCR binding NTI buffer. Thereafter, the suspension was loaded into a NucleoSpin PCR clean-up column, which was placed into a collection tube. This was followed by the suspension being centrifuged at 11 000 *Xg* for 30 sec, for DNA binding. The flow-through was collected into

a tube and discarded, 700 µl of NT3 buffer was added into the column and further centrifuged at 11 000 Xg for 30 sec. The flow-through in the collection tube was discarded and the column dried by an additional centrifugation step for 1 min at 11 000 Xg. Thereafter, the DNA was eluted by the addition of 30 µl of elution buffer into a fresh Eppendorf tube with centrifugation at 11 000 Xg for 1 min. The DNA was stored at 4 °C for future use.

2.6.5. DNA phosphorylation and dephosphorylation

Linearized plasmid DNA was dephosphorylated to remove phosphate groups at the 5' end using Antarctic alkaline phosphatase (NEB). Briefly, 20 µl reactions were made by the addition of 2 µl of Antarctic Alkaline phosphate buffer (NEB), 1 µg of linearized plasmid DNA, 1 U of Alkaline Phosphatase and dH_2O to make up the final volume. The reactions were incubated for an hour at 37 °C followed by heat inactivation at 65 °C for 20 min.

2.6.6. DNA ligation

The ligation of PCR DNA fragments into plasmid DNA was conducted using T4 DNA ligase (NEB or Thermo Scientific) using the manufacturer's instructions with minor changes. Ligation reactions were made up to in a final volume of 20 µl per reaction, with the addition of 2 µl of T4 DNA ligase buffer, "X" amount (ng) of insert DNA (X- calculated using the formula indicated below) and made up to a final volume with dH_2O. To enhance the efficiency of the ligation reactions, the following molar (vector: insert) ratios were used for ligations; 1:1, 2:1 and 1:2. The reactions were incubated at room temperature for 20 min followed by heat inactivation at 65 °C for 10 min. Thereafter, the DNA ligation products were used to perform transformations using chemically competent *E. coli* DH5α cells, as explained in section 2.9.3. The following equation was used to calculate the amount of insert for each ligation (using 50 ng of vector as a starting concentration standard).

$$Amount\ of\ insert\ (ng) = \frac{Amount\ of\ vector\ (50\ ng) X\ Size\ of\ insert\ (bp)}{Size\ of\ vector\ (bp)}$$

2.6.7. DNA sequencing

To confirm that no mutations have been introduced into gene/region of interest during cloning of mycobacterial DNA, the DNA sequencing Facility of Stellenbosch University was used to perform DNA sequencing of all constructs. The BigDye Terminator v3.1 Cycle Sequencing kit (Applied Biosystems) was used for DNA sequencing and for the analysis of the sequencing data, the DNASTAR Software (DNASTAR) was used.

2.7. Bacterial transformations

2.7.1. Chemically competent *E. coli* DH5α cells preparation

To prepare the cells for cloning, the calcium chloride protocol was followed to produce chemically competent *E. coli* DH5α cells. A single colony of *E. coli* DH5α was picked to start a culture in 50 ml LB media and incubated overnight at 37 °C with shaking at 100 rpm. Following this, 1 ml of starter-culture was used as inoculum for a new culture, 100 ml LB incubated at 37 °C with shaking at 100 rpm for 3 hours. Thereafter, the cells were harvested by means of centrifugation at 1 180 *Xg* for 5 min at 4 °C. The supernatant was poured off and the cells reconstituted in 10 ml ice-cold $CaCl_2$ (0.1 M) and immediately incubated on ice for 20 min. The cells were centrifuged once more as detailed before and reconstituted in 5 ml of ice-cold $CaCl_2$ (0.1 M) and used immediately for transformations preparations with plasmids.

2.7.2. Chemically competent *E.coli* DH5α cells transformation

The chemically prepared competent *E. coli* DH5α cells 100 µl was aliquoted and mixed in with plasmid DNA. In brief, the cells were initially incubated on ice for 15 min and subsequently transformed using heat shock at 42 °C for 90 sec. Thereafter, the cells were resuspended with pre-warmed LB media and incubated at 37 °C for an hour with shaking at 100 rpm. Subsequently, the cells were plated on LA media that was supplemented with appropriate antibiotics. The LA plates were incubated overnight at 37 °C overnight. The following day, single colonies were picked and screened for positive clones following description in sections 2.4.2.1, 2.6.2 and 2.6.3.

2.7.3. Electro-competent mc^{2}155 and derivative strain preparation

Electro-competent *M. smegmatis* mc^{2}155 cells were picked and used to start a culture in 50 ml of Middlebrook 7H9 broth which was grown to an optical density $(OD)_{600nm}$ of 0.5-0.8. Subsequently, cells were harvested by means of centrifugation at 1189 *Xg* for 10 min at 4°C. The supernatant was poured off and the pellet washed with chilled 10% glycerol and harvested as before. The washing steps were carried out twice more and the cell suspension was reconstituted in a final volume of 2 ml using ice-cold glycerol. The cells were used for transformations with plasmids immediately.

2.7.4. Electroporation of plasmids into *M. smegmatis*

For electroporation of *M. smegmatis* cells or derivative strains, 300 µl of electro-competent cells was mixed with 1 µg of plasmid DNA and used for transformation. The cells and plasmid DNA suspension was transferred into an ice-cold 0.2 cm electroporation cuvette (Bio-Rad laboratories). The cells were first incubated on ice for 15 min and then pulsed using the Bo-Rad Gene Pulser XCell^{TM} (Bio-Rad laboratories) system following these parameters: voltage of 2500 V, time constant of 25 µF, resistance of 1000 Ω and distance of 0.2 cm. Immediately after electroporation, 800 µl of LB or 2xTY media was used to rescue the cells. Subsequently, the cells were poured into a clean tube and incubated at 37 °C overnight. Following incubation, the cells were centrifuged at 12 470 *Xg* and the pellet resuspended in fresh 500 µl Middlebrook 7H9 broth. The suspension was plated onto Middlebrook 7H10 agar supplemented with appropriate antibiotics and incubated at 37 °C for 3-5 days for selection.

2.7.5. Recombinant strain genotypic confirmation

The mc^{2}155 strains and their derivatives that were previously created had to be confirmed for the correct manipulation of genes using PCR: Briefly, after the selection on selective media, a single colony was isolated and small scale chromosomal DNA was performed following the by colony boil protocol as described in section 2.4.1.1. Subsequently, genotypic confirmation through PCR with FastStart Taq DNA polymerase (Roche) was carried out, using specific primers detailed in in Appendix B. All PCR reactions were conducted to a final volume of 25 µl, with the addition of 1X recommended PCR buffer provided by the manufacturer, 0.2 U FastStart Taq polymerase,

DNA template (5 µl), 4 µl dNTPs to a final concentration of 0.2 mM and 1X GC rich solution. The PCR cycling parameters were conducted following conditions described in section 2.6.1.1.

2.8. Genomic DNA library construction

2.8.1. Restriction digestion of genomic DNA

To isolate wild-type mc^2155 *M. smegmatis* genomic DNA, the CTAB method was followed as detailed in section 2.4.1.2 and the resulting DNA was subsequently viewed on a 1% agarose gel alongside a molecular weight marker to determine the quality of the extracted sample. Thereafter, the DNA quality was assessed using the NanoDrop ND-1000 Spectrophotometer (NanoDrop Technologies). A genomic library was created by conducting a 2-fold serial dilution series of a *Taq*I restriction enzyme digestion. Briefly, *Taq*I 20 U (NEB) was added to the first tube (containing a concentrated DNA digestion mix) and subsequently diluted in a 2-fold series with nuclease free dH_2O. The restriction enzyme was diluted in order to create partially digested genomic DNA of overlapping fragments. This was followed by assessment on 1% gel agarose using 5 µl of the reaction following the description in section 2.6.3 to isolate the partial digests in the 0.5-5.0 kbps fragment range. The selected partial digests were cleaned by sodium-acetate precipitation as detailed in section 2.5.1. The episomal prey vector (pUAB300) was linearized using *Cla*I 1U restriction enzyme (NEB) and ligation reactions were conducted following the following ratios: 1: 1, 1: 2, 1: 3 and 2: 1 (of vector:insert); as described in section 2.6.6. A cut and ligate negative control was also included.

2.8.2. Electro-competent *E. coli* DH5α cell preparation

E. coli DH5α single colony was isolated and used to create a starter culture in a 50 ml LB , which was incubated overnight at 37 °C with shaking at 250 rpm. Thereafter, 1 ml of the starter culture was subcultured into a 100 ml of LB media and incubated at 37 °C with shaking at 100 rpm for 3 hours. The cells were then incubated on ice for 10 min and harvested by centrifugation at 3081 *Xg* for 10 min at 4 °C. The supernatant was poured off and the cells reconstituted in 10 ml ice-cold 10% glycerol and immediately incubated on ice for 10 min. The cells were centrifuged twice more as detailed before and reconstituted in 4 ml of chilled 10% glycerol and used for transformations with plasmids and ligation reactions immediately.

2.8.3. Transformation of electro-competent DH5α

The transformation of electro-competent *E. coli* DH5α cells was conducted as follows: 25 µl of electro-competent cells was aliquoted and mixed together with the ligation reactions. The cells were firstly transferred into 0.1 cm electroporation cuvette (Bio-Rad) chilled on ice for 20 min before electroporation. Subsequently, the cells were pulsed using the Gene PulserX cell (Bio-Rad) following these parameters: voltage of 1800V, time Constance of 10 µF, resistance of 600 Ω and distance of 0.1 cm. Thereafter, the cells were rescued with pre-warmed 2xTY media immediately and incubated at 37 °C for 60 min with shaking at 200 rpm. Subsequently, the cells were plated on LA media that contained appropriate antibiotics. The LA plates were incubated at 37 °C overnight. Ten colonies were randomly selected and digestions were performed to assess insert presence (data not shown), following description in sections 2.4.2.1, 2.6.2 and 2.6.3. Thereafter, cells were scraped off collectively and the plasmid DNA was isolated using the Nucleobond Plasmid Purification Kit as detailed in section 2.4.1. This constituted the plasmid DNA of the genomic library which was stored at 4 °C for later use.

2.9. Identification of MSMEG_4217 interacting partners

2.9.1. Assaying for MSMEG-4217 putative interacting partners

The mycobacterial protein fragment complementation (M-PFC) system described by (Singh et al., 2006) was used to test the interaction between proteins of unknown functions. Briefly, the M-PFC works on a principle of separate murine dihydrofolate reductase (mDHFR which acts as a reporter) subunits, which can be reconstituted non-covalently, therefore resulting in a functional protein that confers resistance to a drug. The components are made up of a discontinuous subunit ([1], [2]) and an adenine binding subunit ([3]), which are often called the prey and the bait respectively. The resulting assembly of the putative proteins forms an enzyme which has the ability to hydrolyze trimethoprim (TRIM), enabling the identification of interacting partners on TRIM plates (see figure 2.1 below). The interacting proteins RpfB (resuscitation-promoting factor B) and RipA (Rpf- interacting protein A) are well studied partnering proteins and their protein interaction results in septal PG degradation, an important function in mycobacterial cell division (Hett et al., 2007, Hett et al., 2008). Given this demonstrated interaction in the literature, tehse two proteins served as an excellent positive control in this study. To identify the

MSMEG_4217 putative interacting partners, the library plasmid DNA was inserted into mc:: pUAB400 + MSMEG_4217 by electroporation using the protocol in section 2.8.4. Subsequently, 800 µl of pre-warmed 2xTY was added to the cells for rescue, followed by plating on Middlebrook 7H10 agar complemented with Kan (25 µg/ml) Hyg (50 µg/ml). After the 3-5 days incubation, cells were scraped off and reconstituted with fresh Middlebrook 7H9 and subsequently plated on Middlebrook 7H10 agar, supplemented with Kan (25 µg/ml) Hyg (50 µg/ml) and TRIM (7.5 µg/ml) and grown at 37 °C for 5-7 days. Positive growth was scored as positive interaction. The *ripA* and *rpfB* genes were independently cloned into bait and prey vectors (in another study at the CBTBR) and co-electroporated into mc^2155 following the protocol detailed in section 2.8.4. The resulting mc^2155 derivative strain mc:: pUAB300RipA + pUAB400RpfB served as a positive control. The plasmid only control was constructed by co-electroporation of the empty bait and prey vectors into mc^2155. The strain mc:: pUAB300 + pUAB400 served as a negative control.

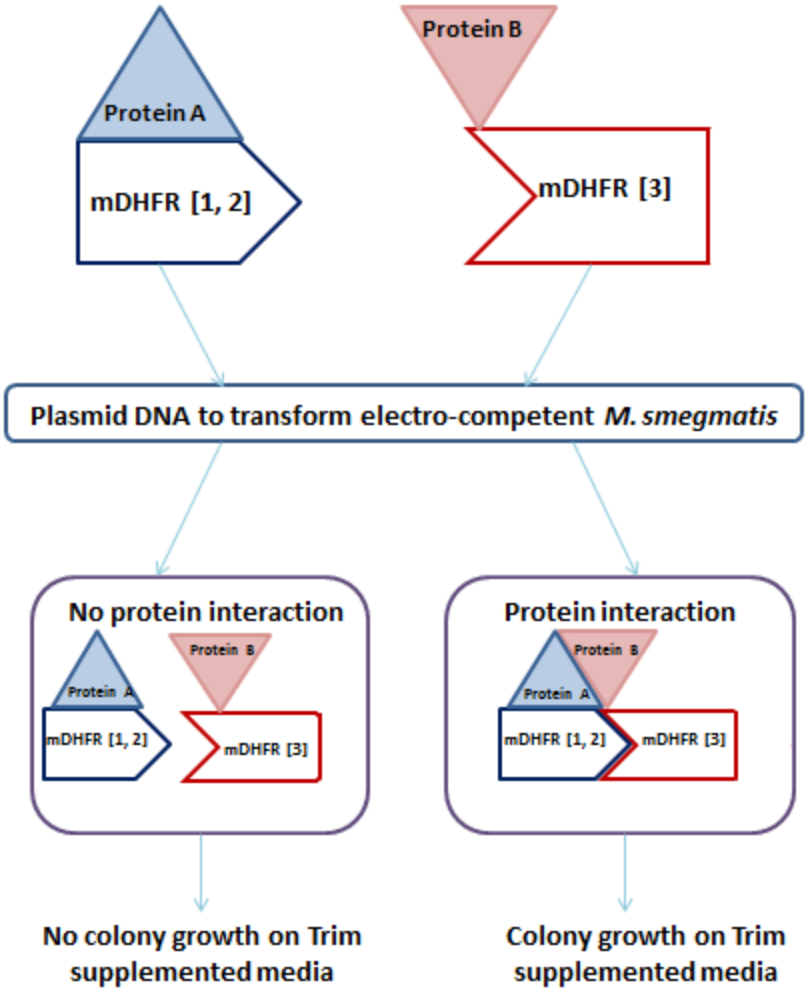


Figure 2.1: **Schematic diagram demonstrating the M-PFC assay principle.** Proteins (A and B) tagged with the mycobacterial dihydrofolate reductase dis-continuous fragments; (F1 and 2) and (F3) results in the reconstitution of a functional murine dihydrofolate reductase (mDHFR) and subsequently results in the resistance to antibiotic trimethoprim (trim) when grown on Middlebrook 7H10 agar supplemented with TRIM (7.5 µg/ml), Kan (25 µg/ml) and Hyg (50 µg/ml), thus depicting a positive interaction. In the event of there being no protein interaction between proteins (A and C), failure to reconstitute mDHFR, will result in no growth on Trim-supplemented plates. Image adapted from (Singh et al., 2006).

2.9.2. Putative interacting partners identification and sequencing

The isolation of small-scale chromosomal DNA of the putative interacting partners fragment cloned into the prey vector involved the colony boil method as detailed in section 2.4.1.1. The chromosomal DNA was used to transform chemically competent *E. coli* DH5α, following the protocol outlined in sections 2.8.2 and 2.8.3. The transformants were rescued with pre-warmed 2xTY and plated on LA for plating supplemented with appropriate antibiotics. The following day, the plasmid DNA was isolated using the small scale Alkaline Lysis miniprep protocol detailed in section 2.4.2.1. The resultant plasmid DNA sequencing was conducted in the DNA sequencing Facility of Stellenbosch University and the sequencing data analyzed by BLAST tool database (http://blast.ncbi.nlm.nih.gov/Blast.cgi). Figure 2.2 gives a diagrammatic outline representing the study design. The pFAM database tool was to identify functional domain in proteins of interest (http://pfam.xfam.org/about).

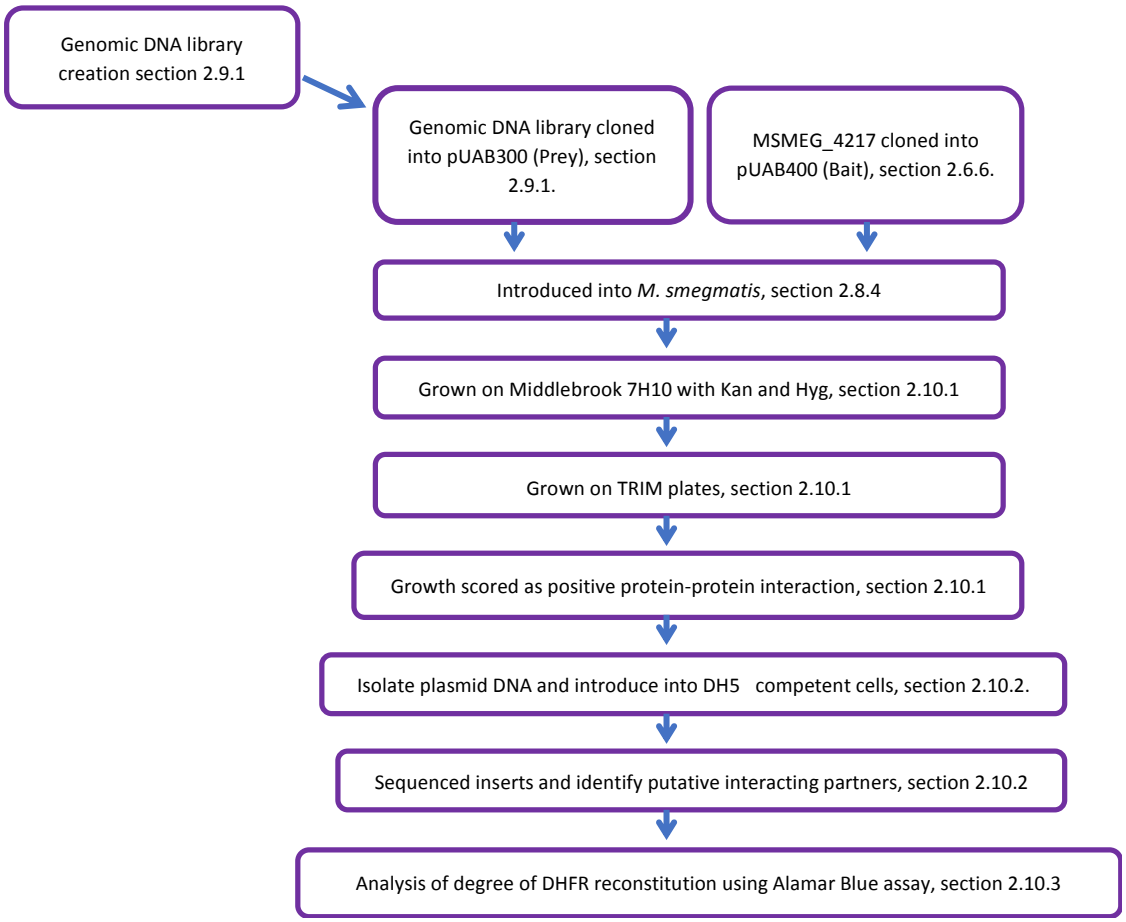


Figure 2.2: **The M-PFC assay strategy followed to identify putative interacting partners for MSMEG_4217.** The genomic DNA was created and cloned into the prey vector and transformed into wild-type mc^{2}155 *M. smegmatis* in combination with MSMEG_4217 cloned into the bait vector. Subsequently, colonies that emerged on Middlebrook 7H10 agar supplemented with Kan/Hyg plates were sub-cultured on Middlebrook 7H10 agar Kan/Hyg/TRIM and growth was scored as positive interacting proteins. Thereafter, plasmid DNA extracted from prey vector was screened for presence of inserts and sequenced. The resultant putative protein sequence was investigated further for the identification of the interacting partner using various bioinformatics tools.

2.9.3. Quantitative analysis for M-PFC assay to assess protein-protein association between MSMEG_4217 and identified putative protein partners using Alamar Blue (AB) assay

To confirm the identified putative interacting partners of MSMEG_4217, a quantitative assessment was used to investigate the degree of reconstitution of mDHFR between MSMEG_4217 and the identified protein fragments. The oxidation/reduction indicator Alamar Blue (AB) is widely used as a quantitative and sensitive assay to assess sensitivity of mycobacteria to anti-mycobacterial compounds. AB is reduced from a non-fluorescent blue to fluorescent pink color, which represents viability in the presence of drug and consequently can be used to measure the degree of reconstitution of mDHFR, which is a surrogate measure of interaction strength between two interacting proteins in this system (Singh et al., 2006). The *M. smegmatis* partial clones selected on Middlebrook 7H10 supplemented with Kan/Hyg/TRIM containing interacting partners were further assessed for the development of a pink color due to the reduction of AB. *M. smegmatis* clones containing interacting plasmids were cultured in Middlebrook 7H9 broth supplemented with Kan (25 μg/ml) and Hyg (50 μg/ml) using protocol as detailed in section 2.3.2. Subsequently, the cells were diluted in fresh Middlebrook 7H9 broth and $\approx 10^6$ of cells were plated on 96-well clear-bottom plates containing Middlebrook 7H9 broth. TRIM 2-fold serial dilutions were added to the microtiter plate. Control panels contained only Middlebrook 7H9 broth and dH_2O. Plates were incubated at 37 °C overnight. Thereafter, 15 μl of AB was added to each well on plates and incubated at 37 °C for 2-4 hrs. Fluorescence intensity was measured using a Cytofluor II microplate fluorometer (PerSeptive Biosystems) following these conditions: 530 nm excitation and 590 nm emission.

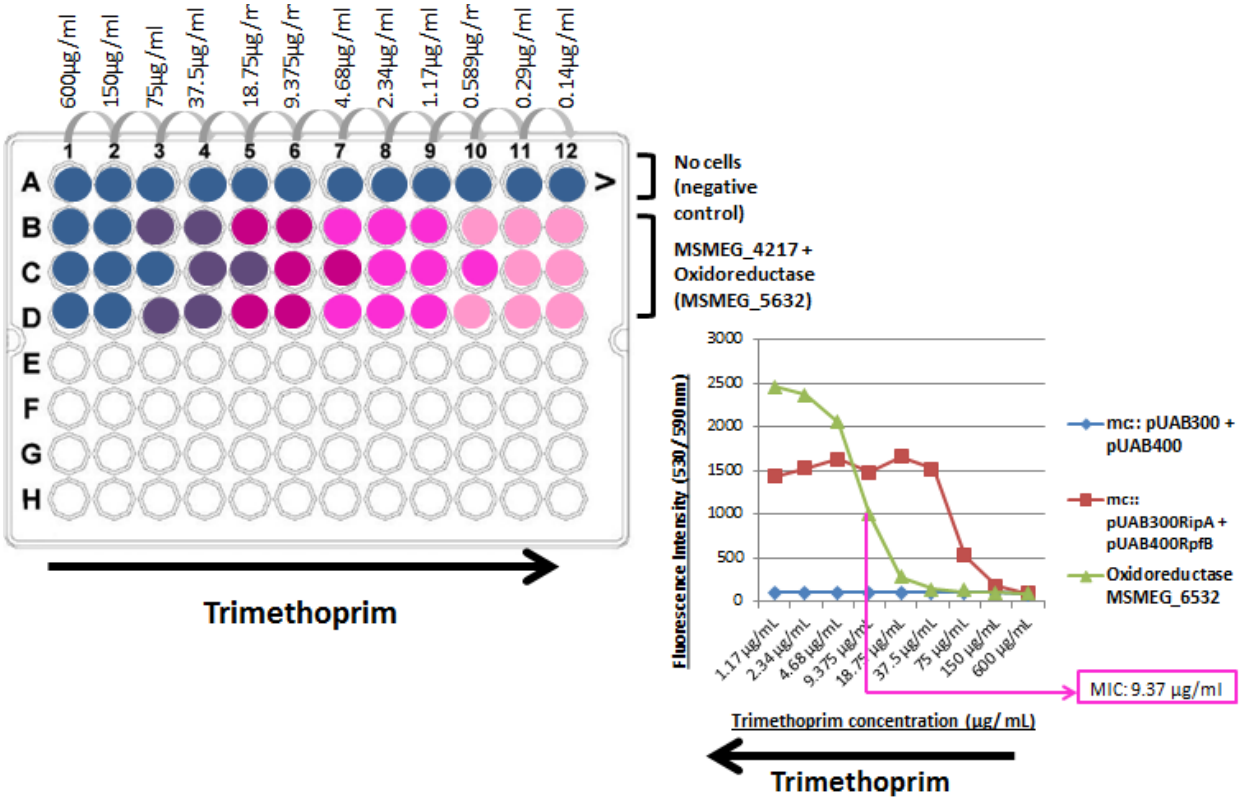


Figure 2.3: **The Alamar Blue assay was used as a quantitative measuring the degree of reconstitution of mDHFR between the DivIVA and the identified protein fragments..** The principle of this assay relies on the use of the colorimetric and fluorescent plate assay based on oxidation/ reduction indicator Alamar Blue (AB). The change from non-fluorescent blue to fluorescent pink color depicts the degree of reconstitution of mDHFR [F (1,2 and F(3)] driven by physically associating mycobacterial proteins. MIC – minimum inhibitory concentration.

2.10. Fluorescence microscopy

2.10.1. Localization of proteins of interest

The MSMEG_4217 identified putative interacting partners were assessed for localization of the protein of interest. Briefly, full length genes of interest were PCR synthesized using primers designed with the relevant open reading frame (ORF), to permit C-terminal fusion of the protein of interest with the monomeric red fluorescent protein (mRFP), following PCR parameters detailed in section 2.6.1.2.1. The synthesized PCR product was cloned into the plasmid pTweety_mRFP. The resultant construct was sequenced to ensure proper insertion of the full-length protein in-frame with the vector following the description in section 2.6.7. The construct

plasmid DNA was used to transform wild-type mc^2155 *M. smegmatis* cells or derivative strains using methods detailed in section 2.8.4. The derivative strains were cultured in Middlebrook 7H9 broth to log phase (OD_{600} =0.5-0.9), supplemented with appropriate antibiotics following the protocol described in section 2.3.2. Thereafter, the cells were harvested by centrifugation at 12 470 *Xg* for 1 min and washed twice with PBS (pH 7.4). Subsequently 5 µl was spotted and evenly spread on a glass slide with a 2% agarose pad, then covered immediately with a cover slip and air dried prior to viewing with the Zeiss 100x, 1.46 numerical aperture objective, mounted on Axio Observer ZI inverted fluorescent microscope. Aalysis of images was done using the ZEN lite software. Any image manipulations (brightness, contrast etc.) were applied to the entire image.

2.10.2. The FM4/64 and the DAPI stains for membrane and DNA staining respectively

The FM4/64 (Thermofischer) cell membrane stain and the DAPI (Sigma-Aldrich) bacterial DNA stain were used for the wild-type *M. smegmatis* and derivative strain staining as per the manufacturer's directions. This method involved culturing cells in 5ml Middlebrook 7H9 broth with the addition of appropriate antibiotics to an OD_{600nm}, followed by centrifugation at 12 470 *Xg*. The cells were then reconstituted in fresh Middlebrook 7H9 broth with the addition 5 µl of the FM4/46 stain and 2 µl of DAPI stain, the suspension was incubated at 37 °C for 20 min with shaking. Thereafter, the cells were visualized using the Zeiss Observer ZI inverted fluorescence microscope and the resultant images were then analyzed with the ZEN lite software (Zeiss) and the Fiji software (ImageJ). Any manipulations made on the image (brightness, contrast etc) were applied over the whole image.

2.11. Microscopy analysis

The Fiji software was used for the analysis of microscope images taken using the Zeiss Observer ZI inverted fluorescence microscope. All the statistical analyses were compiled using GaphPad Prism 6.

2.12. Statistical analysis

The GraphPad Prism 6 was used for statistical analysis of the mean and standard error's and P-values for all assays requiring statistical analyses. The P-values illustrate statistical difference illustrated as follows: P< 0.01: data is not significant, P< 0.0001 data is strongly significant.

2.13. Ethical considerations

The study conducted does not involve any human or animal participants therefore no consent and ethics forms were handed out and returned, but an ethics waver was applied for and granted. A copy of the ethics waiver is attached in the Appendix E.

3. Results

3.1 Bio-informatics analysis to determine the structure and protein interaction domains of DivIVA from mycobacteria

In mycobacteria, DivIVA self-assembles at the cell poles sites with a negatively curved membrane to form a scaffold required for recruiting cell wall biosynthesis enzymes. To examine DivIVA domains responsible for protein-protein interaction, the DivIVA protein of the well characterized *B. subtilis* counterpart was blasted against the *M. smegmatis* genome using the NCBI protein blast tool. The bioinformatics analyses revealed that the *B. subtilis* DivIVA protein is made of two domains; a highly conserved N-terminal domain and a C-terminal domain connected by a poorly conserved ~20 amino acid linker (Oliva et al., 2010; Halbedel & Lewis, 2019). The predicted tertiary structure of *M. smegmatis* DivIVA is larger with a total of 272 residues including an N-terminal membrane binding domain, a C-terminal involved in polar localization and a ~100 amino acid long linker between the two domains (Choukate et al., 2019; Choukate et al., 2020). The DivIVA membrane binding residue pair Phe17 and Arg18 are aberrant in *M. smegmatis* DivIVA and appear to be replaced by Lys21 and Arg22, which are conserved across other mycobacterial species (Figure 3.1.1 and Figure 3.1.2 A). From our analysis we observed a striking difference in the crystal structure of the lipid binding domain of mycobacterial DivIVA, suggesting that *M. smegmatis* DivIVA may use a different mode of lipid binding (and as a result membrane anchoring) than *B. subtilis* DivIVA (figure 3.1.1. b) (Choukate et al., 2019). To investigate for a possible anchor protein for DivIVA from *M.*

smegmatis a DivIVA, a genomic library was created. The DivIVA partnering proteins are studied in detail below (see figure 2.1 for the experiments conducted for analysis of the DivIVA partnering proteins).

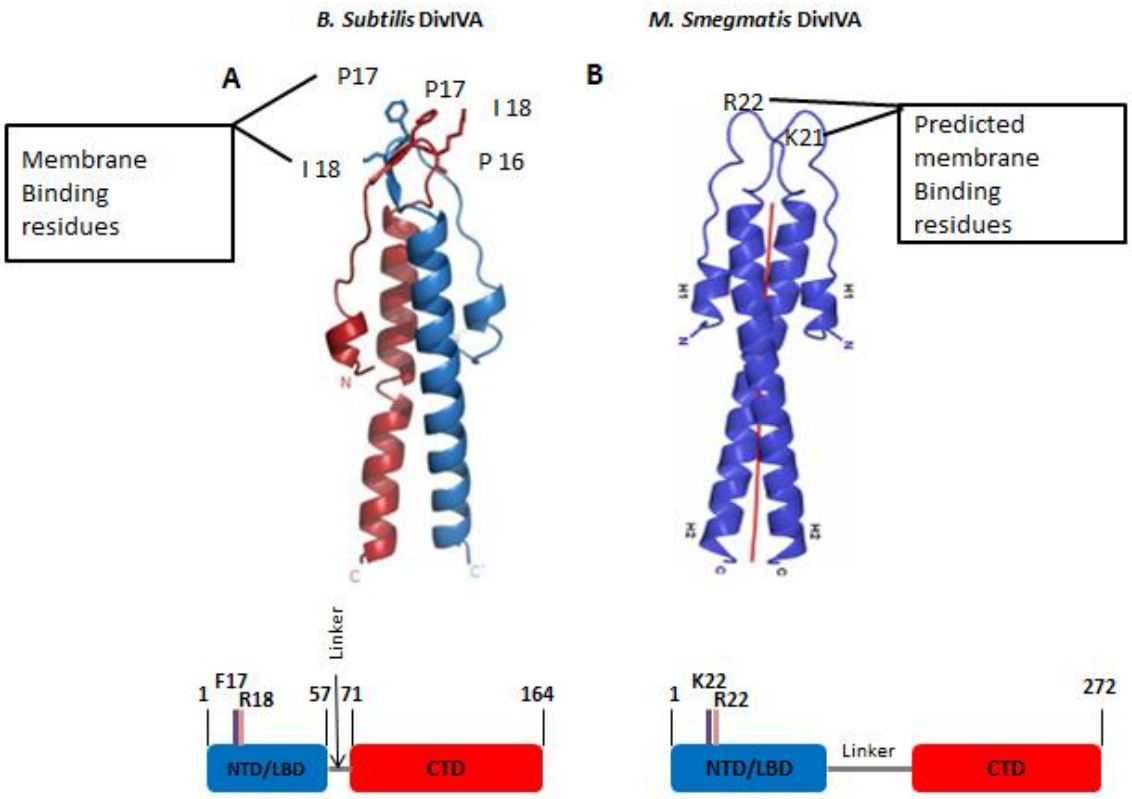


Figure 3.1.1 a: **Tertiary structure and schematic representation of the domain organization of the *B. subtilis* and *M. smegmatis* DivIVA proteins.** The illustration shows conserved motifs in DivIVA proteins (A) *Bacillus subtilis* DivIVA crystal structure forming a parallel coiled-coil dimer of the N-terminal domain are shown as ball and stick models exposing Arginine pair residues: P17 and I 18. (B) *Mycobacterium smegmatis* DivIVA N-terminal domain with predicted membrane binding residues indicated at K21 and R22. NTD/LBD: N-terminal domain/ Lipid Binding Domain (blue). CTD: C-terminal domain (red), images adapted from (Oliva et al., 2010; Choukate et al., 2019).

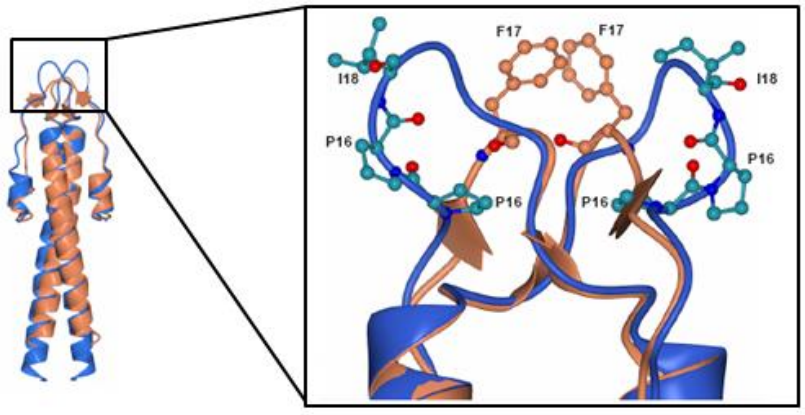


Figure 3.1.1 b: A **structural superimposition of N-terminal *M. smegmatis* DivIVA (blue) and N-terminal *B. subtilis* DivIVA (coral).** The crossed loop region in N-terminal DivIVA (blue) containing the sequences P_{16} P_{17} I_{18} indicating the different membrane binding residues (ball and stick, with carbon atoms shown in light blue, in red is oxygen atoms and nitrogen atoms in blue) the similar region in *B. subtilis* DivIVA (coral) containing the F17 residue (ball and stick, with carbon atoms in coral, oxygen in red and nitrogen in blue) are shown in the figure, image adapted from (Choukate et al., 2019).

A multiple sequence alignment of representative members of two subgroups, Firmicutes and Actinomyces, of the DivIVA protein family was created using the Clustal Omega (http://www.ebi.ac.uk/Tools/msa/clustalO/). To identify the conserved catalytic and divergent motifs in closely related bacteria (Firmicutes and Actinomyces), we compared sections of the N-terminal domain (NTD) and C-terminal domain (CTD) sequences of these commonly studied bacteria. The DivIVA protein sequence comparison revealed conserved amino acids ([F], [V] and [FL]), which are unique to the the N-termini domain and facilitate membrane binding and dimerization. These motifs occupy the same position in all species across both subgroups, highlighted in blue (Figure 3.1.2). The well-studied *B. subtilis* was used as a template to assess the structure of DivIVA from other bacteria. Whereas, the single amino acids ([M], [I], [K], [I] and [A]) are shared in the same order and spacing, they are only conserved within the Firmicutes subgroup, on Figure 3.1.2. In Actinomycetes, the motifs: ([M], [DV], [N], [E], [D], [D], [N] and [L]) are shared within the subgroup and occupy the same position (Figure 3.1.2). The *M. smegmatis* DivIVA protein contains a phosphorylation target site Thr73 (Figure 3.1.2) highlighted in yellow. All the bacteria in this subgroup were compared (using BLAST) against *M. smegmatis*, highlighted in purple. Residues colored in red represent the coiled-coil heptad repeats largely dominate across both subgroups (Halbedel & Lewis, 2019).

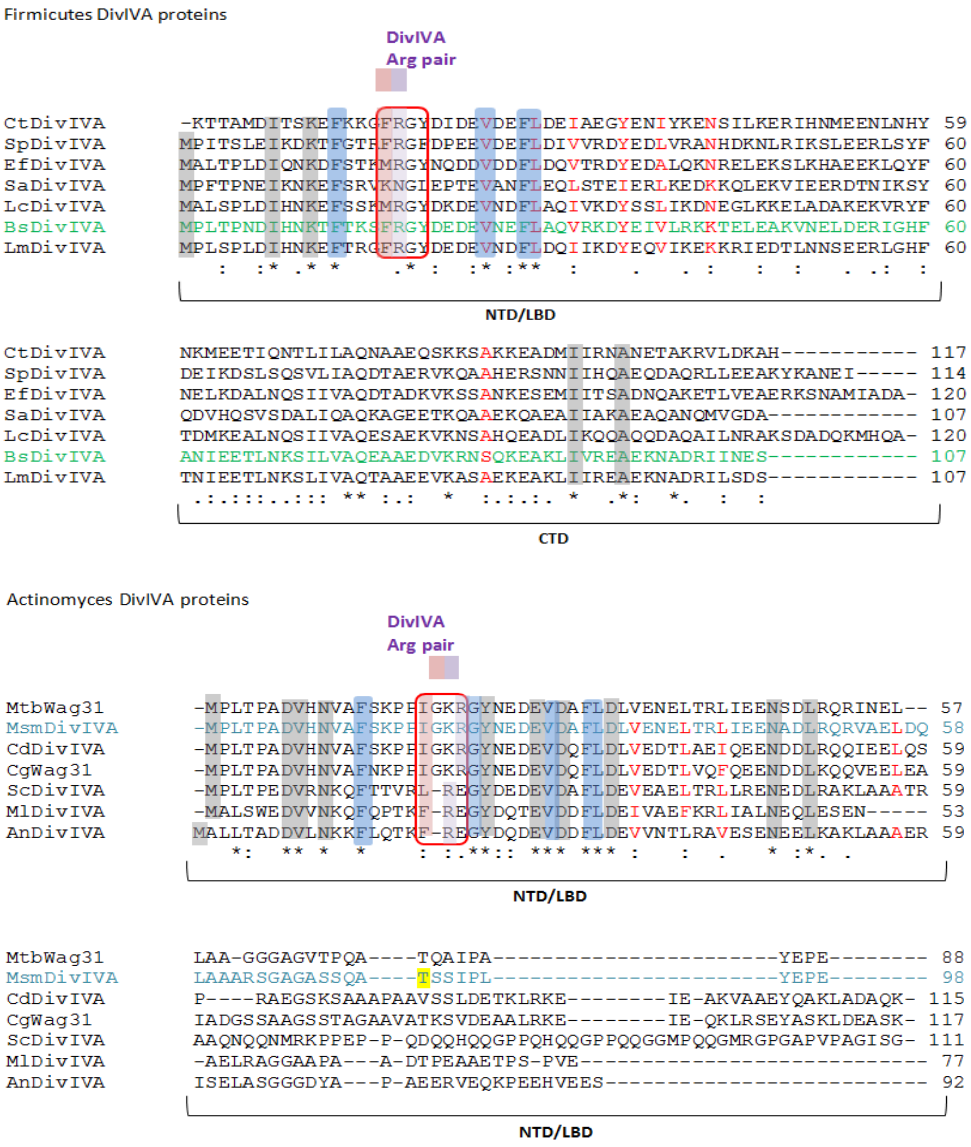


Figure 3.1.2: **Comparison of the *B. subtilis* DivIVA conserved domains with other DivIVA Firmicutes and Actinomycetes homologues.** Represented in the figure is the multiple alignment of two subgroups of the DivIVA protein family. Alignment of the Firmicutes: Ct (*Clostridium tetani*), Sp (*Streptococcus pneumoniae*), Ef (*Enterococcus faecalis*), Sa (*Staphylococcus aureus*), Lc (*Lactobacillus casei*), Bs (*Bacillus subtilis*), Lm (*Listeria monocytogenes*). Colored in light green is the *B. subtilis* DivIVA sequence (107- residues). Alignment of the Actinomycetes: Mt (*Mycobacterium tuberculosis*), Msm (*Mycobacterium smegmatis*), Cd (*Corynebacterium diptheriae*), Cg (*Corynebacterium glutanicum*), Sc (*Streptomyces coelicolor*), Ml (*Micrococcus luteus*) and An (*Actinomyces nasicola*). Amino acids conserved in all DivIVA protein are highlighted in blue, amino acid conserved in the same position within the subgroup are highlighted in grey, amino acids constituted the coiled coil heptad repeats are colored in red, the poorly conserved residues 16-19 are encircled with a red rectangle. Highlighted in yellow is the phosphorylation target site in *M. smegmatis*.

3.2 Protein interactions

This study aimed to identify putative interacting partners for *M. smegmatis* DivIVA designated MSMEG_4217, using the M-PFC assay which is used to assess the interaction between proteins of unknown functions (Singh et al., 2006). The motivation for identifying interacting protein partners of DivIVA was based on previous observation from (Ginda et al., 2013) demonstrating that ParA-DivIVA interaction has an essential role in the mycobacterial cell cycle, particularly in cell elongation and chromosome segregation through the close interaction with ParA and ParB proteins (herein referred as ParAB complex). In this regard, the approach for the study involved cloning of *M. smegmatis* DivIVA into the plasmid pUAB400 for the construction of a bait vector, thereafter the construction of a genomic DNA library of *M. smegmatis* followed in order to screen for putative interacting partners. Positive controls for the M-PFC assay was RpfB and RipA, a pair of mycobacterial proteins previously shown to interact (Hett et al., 2007).

3.2.1. Wild-type mc_2155 genomic DNA library construction and generation

To create a genomic DNA library to study protein interaction required mc^2155 *M. smegmatis* DNA of high quality. Briefly, the mc^2155 *M. smegmatis* strain was grown on Middlebrook 7H10 agar (see section 2.3.2.) and incubated at 37 °C for 2 days. Subsequently, bacterial cells were scraped off and a large-scale genomic DNA was extracted using the CTAB method detailed in section 2.4.1.2. The genome of mc^2155 and mycobacterial species is predominantly made of high G+C content, therefore a restriction enzyme targeting A+T recognition sites is best used to cut the genome less frequently, to generate a partial digest. Hence, *Taq*I from NEB (recognition site: T^CGA) was used in this study. High concentrations of the restriction enzyme (e.g. 20U) would digest the DNA to completion whereas the lower concentration of the DNA would create partial digests of the DNA. Using the enzyme of choice *Taq*I, a 2-fold serial dilution series of restriction digests was created following protocol detailed in section 2.9.1 and the reactions were incubated at 37 °C for 2 hrs. Thereafter, the digested DNA reactions were visualized on 1% agarose gel alongside an uncut DNA control resulting in a series of partially digested genomic DNA (figure 3.2.1). The high concentrated partially digested DNA fragments in the range 0.5 and 5.0 kbps was the desired fragment range for this study, shown in lane 3 and 4 corresponding to 10 U and 5 U of enzyme (shown in red dotted square in figure 3.2.1.). The selected partial

digests were pooled together and cleaned by sodium acetate precipitation described in section 2.5.1 and resuspended in nuclease free dH_2O.

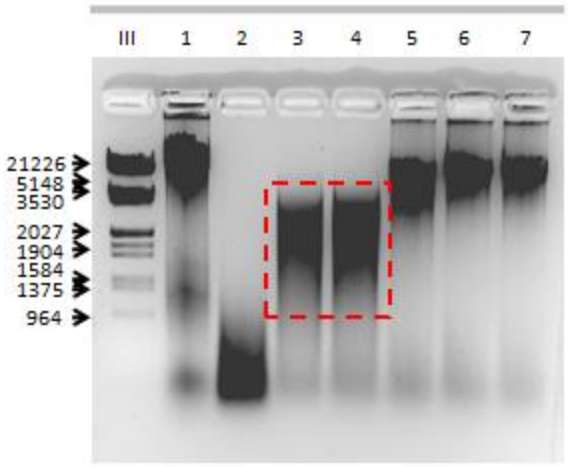


Figure 3.2.1: **Genomic DNA restriction digest of wild-type *M. smegmatis* mc^{2}155.** The *M. smegmatis* mc^{2}155 Genomic DNA library was created using *Taq*I restriction enzyme. A 1% agarose gel was run to assess the different units of enzyme used, marker III (Fermentas), lane (1) uncut mc^{2}155 genomic DNA, lane (2) 20 U, lane (3) 10 U, lane (4) 5 U, lane (5) 2.5 U, lane (6) 1.25 U lane (7) 0.625 U. Red box indicates the partial digests mc^{2}155 genomic DNA within the expected fragment range, approximately 0.5-5 kbps, the expected range for this study (labeled in base pairs).

The episomal vector, pUAB300 (prey vector), was linearized with restriction enzyme *Cla*I (NEB) following protocol described in section 2.6.2, for ligations with the prepared genomic DNA library. Ligation preparations were created following protocol detailed in section 2.6.6. The electro-competent *E. coli* DH5α cells were prepared with ice-cold 10% glycerol following the protocol in section 2.9.2 and the cells were transformed with the ligation reactions following the protocol in section 2.9.3. Thereafter the transformants were cultured on LA agar media supplemented with *Hyg* and incubated at 37 °C overnight. The transformation efficiency was calculated and estimated to be $2x10^5$ CFU/ml; a transformation efficiency within the range 10^4-10^5 is considered adequate (Van Die et al., 1983; Inoue et al., 1990). A few cells were picked (~10) and screened for the presence of inserts against an empty plasmid control (empty vector, pUAB300). Thereafter, all colonies were scraped off and a large-scale plasmid DNA extraction was carried out following the protocol in section 2.4.2.2.

3.2.2. Cloning of MSMEG_4217 into the bait vector pUAB400

The protein of interest MSMEG_4217 (DivIVA) was PCR synthesized as described in section 2.6.1.2 using the PCR primers listed in Appendix B. Followed by restriction digest of the pUAB400 integrating vector (bait vector) with the same restriction enzymes used for the insert to create compatible 'sticky-ends' ends. Thereafter, the prepared *E. coli* DH5α competent cells were transformed with the ligations. A single putative clone was screened using restriction profiling and sequenced to further confirm the genetic integrity of the plasmid (data not shown). The restriction profile of the construct pUAB400+DivIVA is shown in Figure 3.2.2.

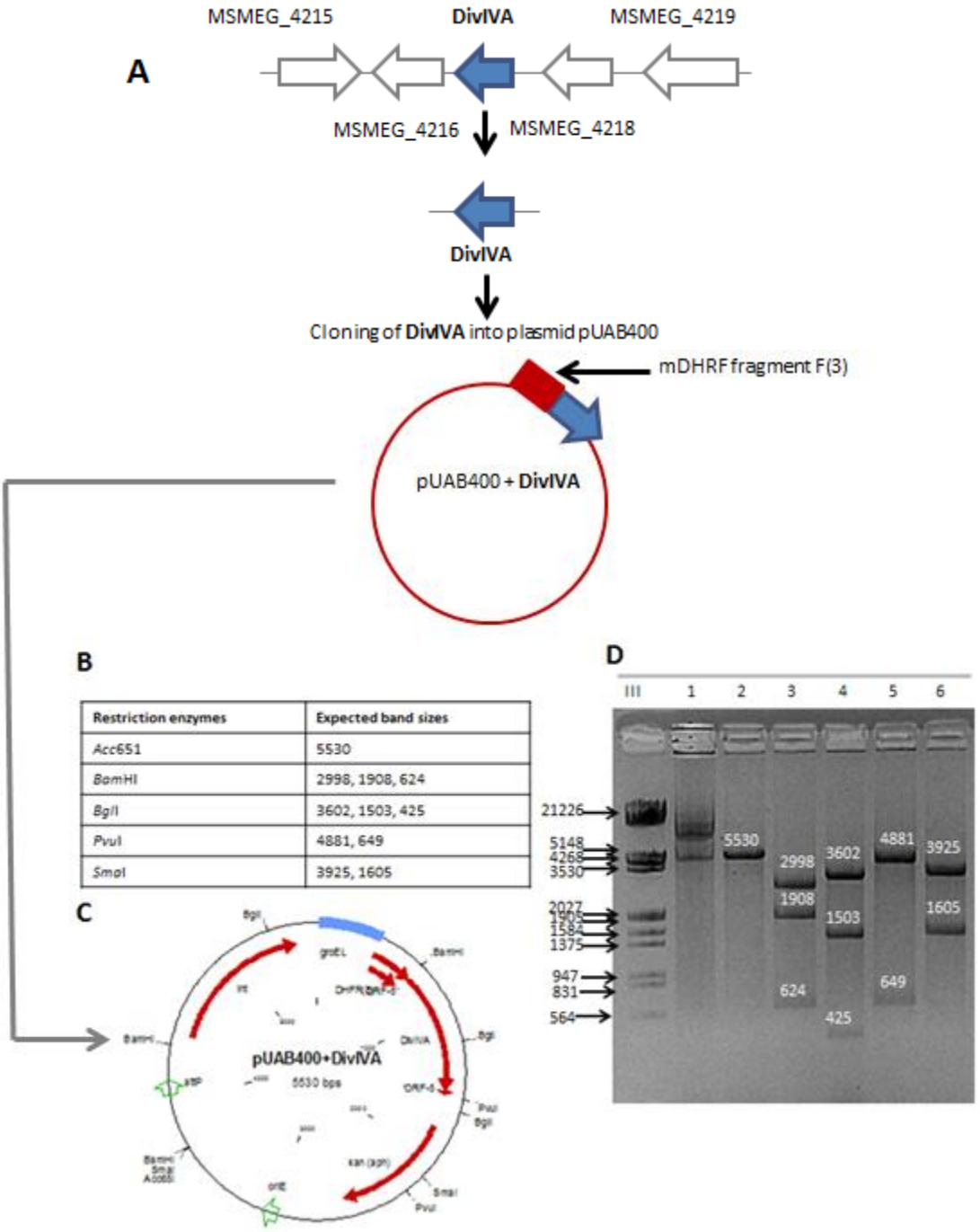


Figure 3.2.2: **Construction and restriction profiling of pUAB400_DivIVA.** (A) The mc^{2}155 genome map indicating the location of the *MSMEG_4217* gene and the cloning strategy for the insertion of *MSMEG_4217* gene. (B) Table indicating the restriction enzymes used for the analysis of pUAB400+MSMEG_4217 bait vector and the expected band sizes. (C) Plasmid map of pUAB400+MSMEG_4217. (D) Agarose gel indicating the DNA band sizes expected (labeled in base pairs). Lane 1: uncut, Lanes 2-6 represent *Acc*651, *Bam*HI, *Bgl*I, *Pvu*I and *Sma*I respectively. All of the expected sizes were observed.

3.2.3. Screening for interacting partners using the M-PFC assay and Trim resistance

To assess interacting partners using the M-PFC assay, the strain mc::pUAB300RipA + pUAB400RpfB was cultured on Middlebrook 7H10 agar supplemented with Kan (25 μg/ml) and Hyg (50 μg/ml) and different Trim concentrations (30, 15, 10 μg/ml). The cultures were grown over the period of 7 days with daily monitoring. No growth was observed after the 7-day incubation period (data not shown). This was concerning, as these were this strain represented the positive control. To address this, (considering all other factors i.e. growth media enrichment) the Trim concentration was further decreased to a concentration of 7.5 μg/ml and the experiment repeated using all other conditions that were similar. Growth was observed for the positive control on the 4th day of incubation and most importantly the negative control clone pUAB300 + pUAB400 produced no growth on Trim plates. The results for the strain mc::RipA + RpfB cultured with controls on a concentration of 7.5 μg/ml are reported in figure 3.2.3 and table 3.3.1. At this concentration, there was some background on the library plate but single colonies emerged on top of this background.

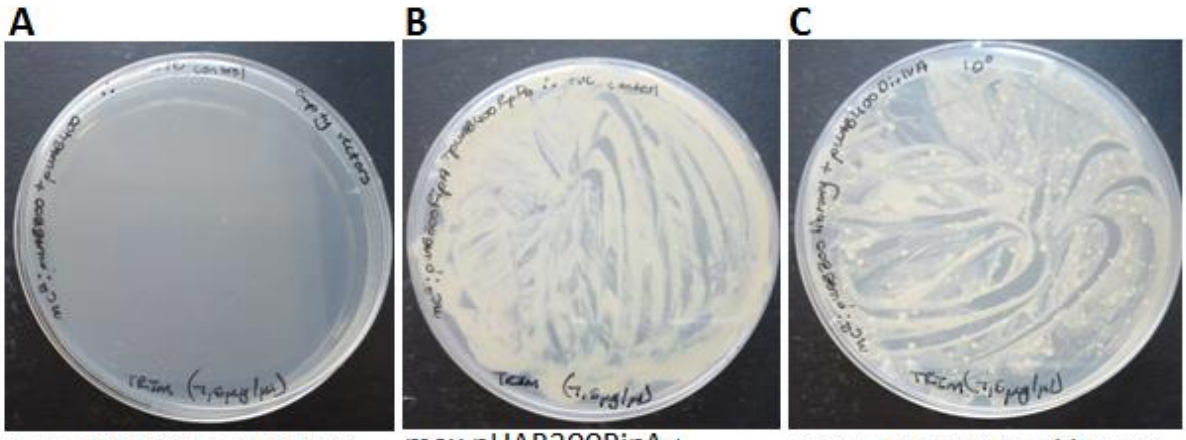


Figure 3.2.3: **The M-PFC assay Trim resistance for mc::RipA + RpfB strain.** The mc::RipA+ RpfB strain was cultured with the Trim concentration of 7.5 μg/ml allowed for growth. The test was conducted with the negative control mc::pUAB300+ pUAB400 (empty) vectors and the *Taq*I library+MSMEG_4217 incubated at 37°C over a period of 4 days.

3.2.4. Screening for MSMEG_4217 putative interacting partners

The prepared plasmid library DNA cloned into the prey vector pUAB300 was introduced into the mc::pUAB400+MSMEG_4217 strain by electroporation and the transformants were cultured on Middlebrook 7H10 agar supplemented with Kan (25 µg/ml) and Hyg (50 µg/ml) and grown at 37 °C for 5-7 days. Subsequently, the colonies were scraped off and re-suspended in Middlebrook 7H9 broth and then sub-cultured on Middlebrook 7H10 agar supplemented with Kan (25 µg/ml) Hyg (50 µg/ml) and Trim (7.5 µg/ml) grow at 37 °C over a period of 5-7 days and growth was scored as positive interaction. In the initial screen the concentration of the transformed cells was too high, therefore we opted for plating the transformed cells in a 2-fold dilution series to allow for a more even distribution of colonies, Figure 3.2.4.

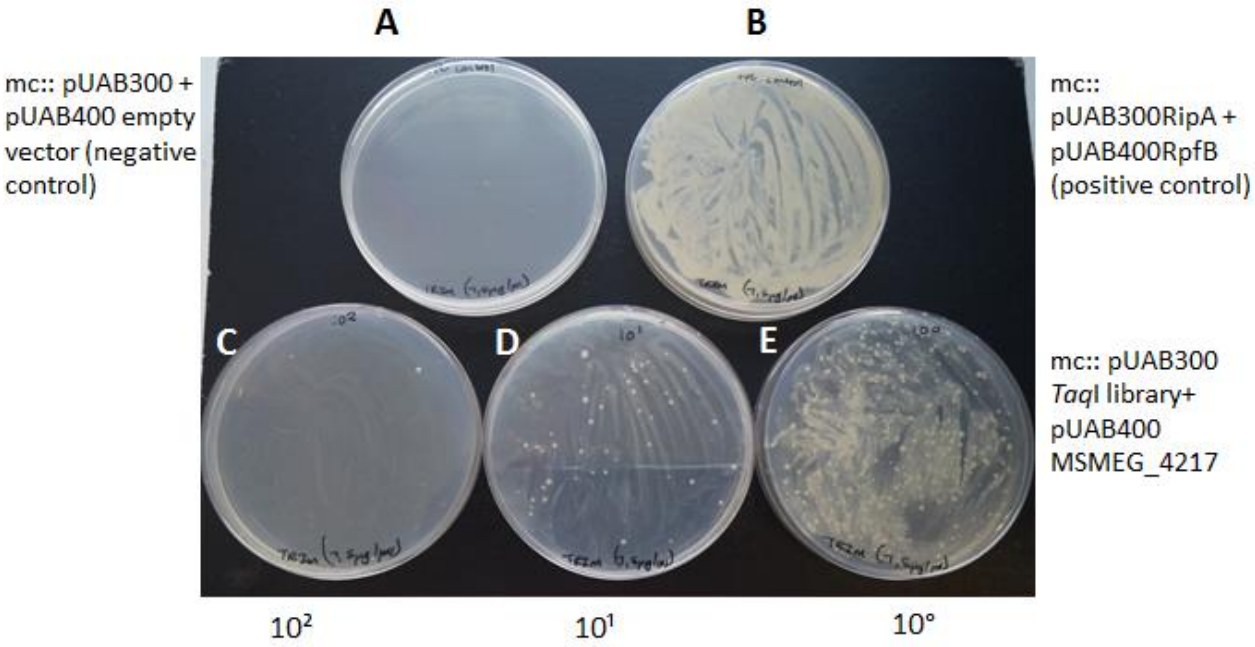


Figure 3.2.4: **The M-PFC assay screening for the identification of MSMEG_4217 interacting partners.** The results obtained for protein-protein interaction screen for MSMEG_4217 using the M-PFC assay. (A) Negative control empty vector (mc:: pUAB300 + pUAB400). (B) Positive control (mc:: pUAB300RipA + pUAB400RpfB). (C-D) Putative interacting partners for MSMEG_4217 were diluted (2-fold) in order to isolate single colonies, above cryptic background growth.

3.2.5. Identification of the MSMEG_4217 putative interactive protein partners

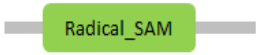
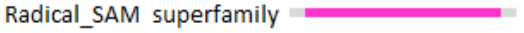
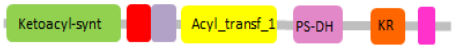
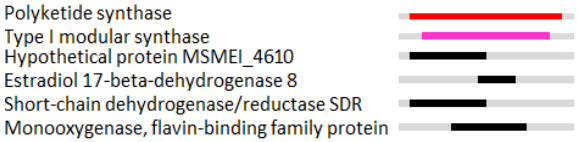
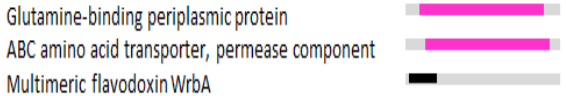
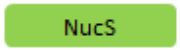
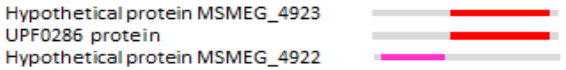
To identify the putative MSMEG_4217 interacting partners, the plasmid DNA of the positive clones (mentioned above) was isolated from *M. smegmatis*. Briefly, single clones were picked and cultured and small-scale plasmid DNA was extracted as described in section 2.4.2.1. The prepared *E.coli* DH5α cells were subsequently transformed with plasmid DNA and isolated again following the protocol in section 2.8.4. The plasmid DNA obtained at the end of the simultaneous culturing and transformations was not of good quality when assessed on 2% agarose gel prior to sequencing (data not shown). Hence, PCR primers were synthesized following the protocol detailed in section 2.6.1.1 to amplify the inserts in the prey vector. These primers were created using the carrier vector (prey vector) sequence flanking the cloning region where the fragment of interest would have been inserted. Thereafter, plasmid DNA extracted from *E. coli* DH5α cells was PCR amplified targeting the region of interest (identified protein fragment) following the protocol outlined in section 2.6.1.2.2. The recommended PCR primers for M-PFC system were used to identify protein sequences; the primers are listed in Appendix B. The PCR product was then sequenced to identify the insert.

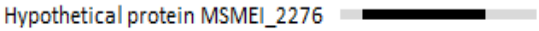
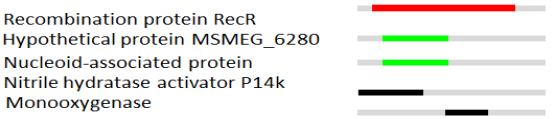
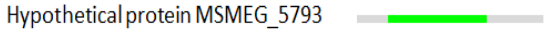
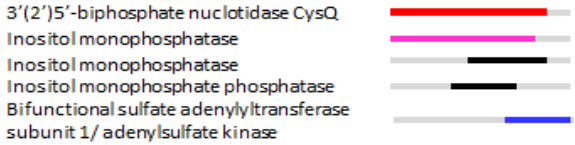
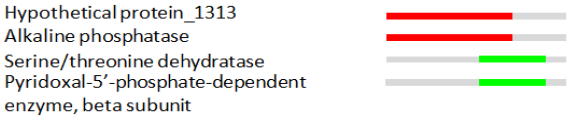
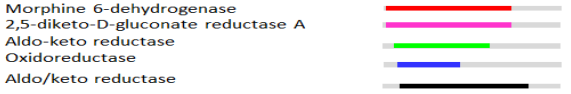
Sequencing data was obtained from the DNA sequencing Facility of Stellenbosch University and the nucleotide sequences were blasted using the Blastx (http://blast.ncbi.nlm.nih.gov/Blast.cgi) search tool to identify the insert by comparison of sequences between *M. smegmatis* and related organisms. A list of genes was generated after the nucleotide sequence was blasted and only the query sequence with high percentage similarity/ identity was considered for further analysis. To identify the correlating protein, the sequences obtained from the Blastx was analyzed using Blastn (http://blast.ncbi.nlm.nih.gov/Blast.cgi). A total of 35 putative interacting partners were identified for MSMEG_4217. The summary of the results is shown in table 3.1. This analyses revealed various possible interacting proteins for MSMEG_4217, some of which are transmembrane and cytosolic proteins. The screen also identified some known interacting partners that contribute to chromosome segregation (RecR) and also cellular processes including cell division (UvrABC transporter protein and Cys proteins). Some new proteins that were also discovered were the universal stress protein (having more than one hit) and some uncharacterized/ hypothetical proteins were also found to interact with MSMEG_4217.

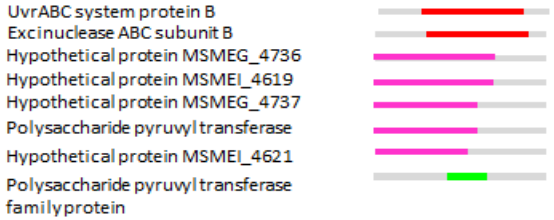
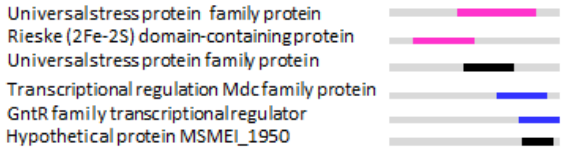
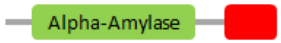
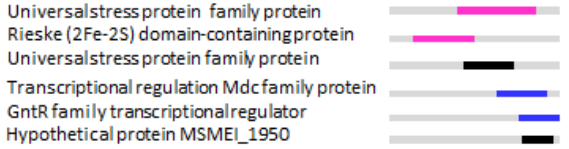
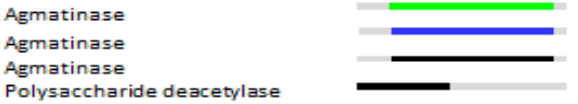
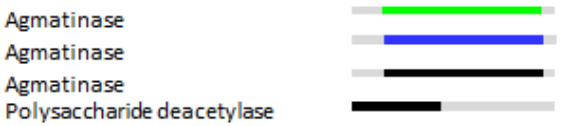
To study domain organization of the identified putative interacting partner, the sequences observed from Blastn were analyzed using pFam search tool (http://pfam.xfam.org/about) for the description on the domain organization for the proteins identified and the active binding sites which enable them to interact with MSMEG_4217. The domains found in the respective interacting partners are also contained within well characterized related species and enzymes involved in bacterial growth. The domains identified in the interacting partners include a glycosidase, glycosyltransferase and some proteins involved in transcription (Endonuclease NucS) machinery. The identified MSMEG_4217 protein fragments of the interacting partners and their conserved domains suggests that they might play a role during early stages of cell growth during chromosome segregation. MSMEG_4217 interaction with various partners within the cytosol and the membrane is most likely due to the amphiphilic nature of the protein, possessing different interaction surfaces for the binding partners (Halbedel & Lewis, 2019).

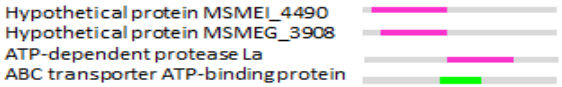
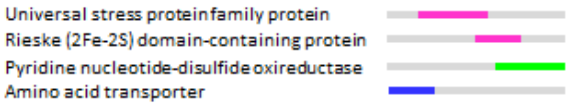
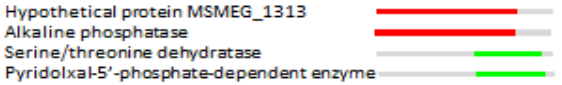
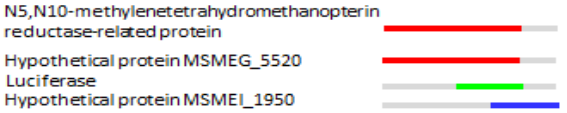
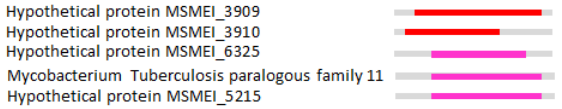
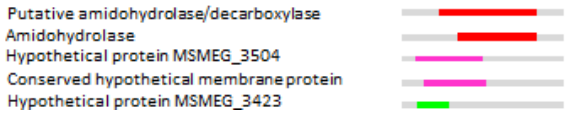
The library insert position within the full-length of the gene was located using Smart Blast server tool from NCBI. The Smart Blast in this regard was employed to search for the domain organization of the entire protein. Following this, the nucleotide sequence was translated using the Expasy translate tool (http://web.expasy.org/translate/). The resultant specific domains and similarities are tabulated in the table 3.1 below. The location of the fragments obtained within the full-length gene was identified and the NCBI-YP, MSMEI amd MSEG numbers are also represented from the Smart Blast server results The total query is shown as a grey bar, the summary of matches to known conserved domains are highlighted in a color spectrum ranging from red for best matches (covering >=200 bps of the reference species) to black (<50 bps of the reference species) matching the query sequence.

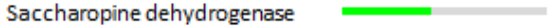
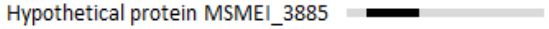
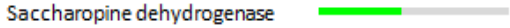
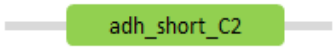
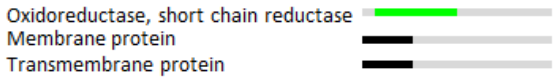
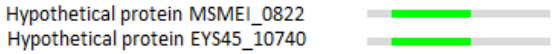
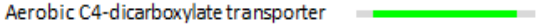
Table 3.1. **MSMEG_4217 putative interacting protein partners obtained through MPF-C assay.** The MSMEG_4217 identified interacting partners are shown. The NCBI-YP number, MSMEI number and MSMEG number of each protein partner including the conserved domain organization and the position of the interacting protein sequence that best matches the query sequence is given.

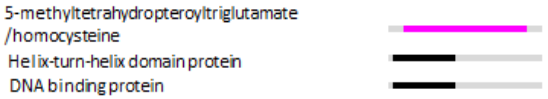
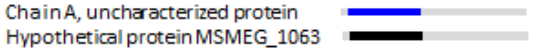
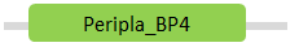
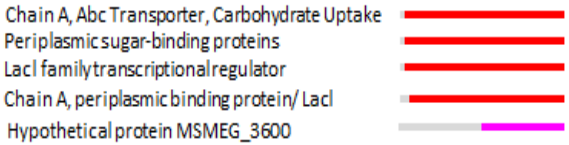
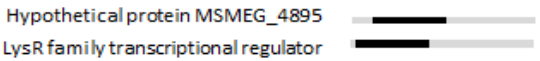
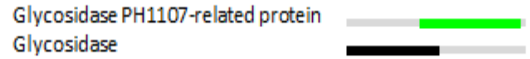
Protein	NCBI YP number MSMEI number MSMEG number	Conserved domain	Position of putative interacting partner within the full length protein sequence
Ribosomal RNA large subunit methyltransferase N	YP_886882.1		
Polyketide synthase	No data obtained		
Glutamine periplasmic protein/glutamine transporter permease	YP_890525		
Hypothetical protein/ Endonuclease NucS	YP_889178.1 MSMEG_4923		

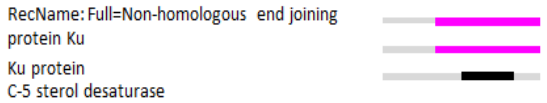
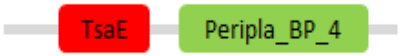
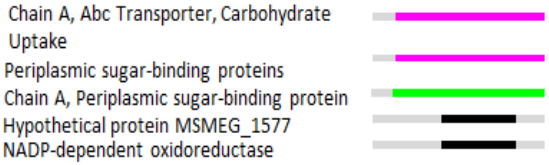
Hypothetical protein / protein HypE	MSMEI_2276		
RecR	YP_890498.1 MSMEG_6279		
Hypothetical protein	YP_890021 MSMEG_5793		
3’(2’)5’-biphosphate nuclotidase CysQ	YP_889228.1 MSMEG_4190		
Hypothetical protein/ Esterase-like activity of phytase	YP_885703.1 MSMEG_1313		
Morphine 6-dehydrogenase	YP_886747.1		

UvrABC system protein B	MSMEI_3727 MSMEG_3816		
Universal stress protein	YP_886001.1		
Alpha-amylase	YP_887879		
Arginase	No data obtained		
Arginase family	No data obtained		

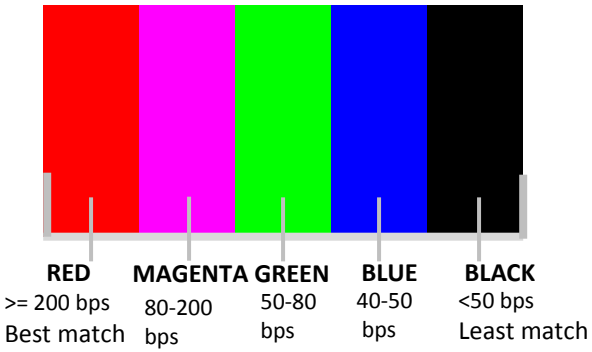
Hypothetical protein	MSMEI_4490		
Universal stress protein	YP_886001.1		
Hypothetical protein	YP_885703.1 MSMEG_1313		
N5, N10-methylenetetrahydromethanopterin reductase- related protein	YP_886360.1		
Hypothetical protein	MSMEG_3903 YP_888200.1		
Putative amidohydrase/ decarboxylase	No data obtained		

Saccharopine dehydrogenase	YP_890529.1		
Hypothetical protein	MSMEI_3885		
Saccharopine dehydrogenase	YP_890529.1		
Oxireductase, short dehydrogenase/ reductase	YP_889866.1 MSMEI_5482 MSMEG_5632		
Hypothetical protein	MSMEI_0822		
Aerobic C4-dicarboxylate transporter	YP_889548.1		

Shikimate 5-dehydrogenase	YP_889696.1		
Chain A, uncharacterized protein	No data obtained		
2OG-Fe (II) Oxygenase	No data obtained		
Chain A, Abc Transporter, Carbohydrate Uptake Transporter-2 (cut2) Family, Periplasmic Sugar-binding Protein	No data obtained		
Hypothetical protein	YP_889151.1 MSMEG_4895		
Glycosidase PH1107-related protein	No data obtained		

RecName: Full= Non-homologous end joining protein Ku	No data obtained		
Hypothetical protein chain A, Abc Transporter, Carbohydrate Uptake Transporter-2 (cut2) Family, Periplasmic Sugar-binding Protein	YP_885956.1 MSMEI_1539 MSMEG_1577		

Key:



3.3. Assessing protein-protein interaction

3.3.1. Confirmation of the efficacy of the M-PFC assay by assessing protein-protein interaction of the two PG hydrolases, RipA and RpfB

To confirm the identified protein interactions, the approach involved manipulation of the Trim concentration and further conformation through a quantitative assay for M-PFC. A few randomly selected interacting proteins were cultured as detailed in section 2.3.2 on Middlebrook 7H10 agar supplemented with Kan (25 μg/ml) Hyg (50 μg/ml) and a gradually increasing concentration by 5 μg/ml intervals of Trim from 7.5 to 50 μg/ml at 37 °C, over a period of 5-7 days. Colony growth was monitored daily, since the principle of the M-PFC assay dictates that the degree of reconstitution of mDHFR between two proteins is dependent on the emergence of a colony in the presence of drug. Hence, the greater the degree of reconstitution of mDHFR, the earlier the emergence of colonies. In contrast, the lesser the degree of reconstitution of mDHFR, the longer it takes for the colony to emerge on the media (Singh et al., 2006). For this, the strains were cultured over the course of 7 days with daily interval monitoring. After 7 days incubation, 30 μg/ml Trim concentration allowed for growth of the mc:: pUAB300RipA+ pUAB400RpfB (positive control) strain, evident by the resistance to the antibiotic trimethoprim. The results of mc:: pUAB300RipA+ pUAB400RpfB and a few randomly selected interacting proteins cultured on 30 μg/ml Trim are reported in Table 3.2 and figure 3.3.2.

Table 3.2: **MSMEG_4217 and the selective putative interacting protein partners**

Test strains	**Positive (+)/ Negative (-)**
(1) mc:: MSMEG_4217 + Saccharopine dehydrogenase	-
(2) mc:: MSMEG_4217 + Hypothetical protein MSMEI_3885	+
(3) mc:: MSMEG_4217 + Saccharopine dehydrogenase	-
(4) mc:: MSMEG_4217 + Saccharopine dehydrogenase	-
(5) mc:: MSMEG_4217 + Saccharopine dehydrogenase	-
(6) mc:: MSMEG_4217 + Oxidoreductase MSMEG_5632	+
(7) mc:: MSMEG_4217 + Hypothetical protein MSMEI_0822	-
(8) mc:: MSMEG_4217 + Aerobic C_4 –dicarboxylate transporter	+
(9) mc:: MSMEG_4217 + Shikimate 5-dehydrogenase	+
(10) mc:: MSMEG_4217 + 5-methyldropteroyltriglutamate	-
(11) mc:: MSMEG_4217 + MSMEG_1063	+

(12) mc:: MSMEG_4217 + OG-Fe (II) Oxygenase	-
(A) mc:: pUAB300 + pUAB400 negative control	-
(B) mc:: pUAB300RipA + pUAB400RpfB positive control	+

*The table shows results observed using randomly isolated interacting partners to assess the best TRIM concentration for the confirmation of the identified interacting partners and appropriate controls in M-PFC assay.

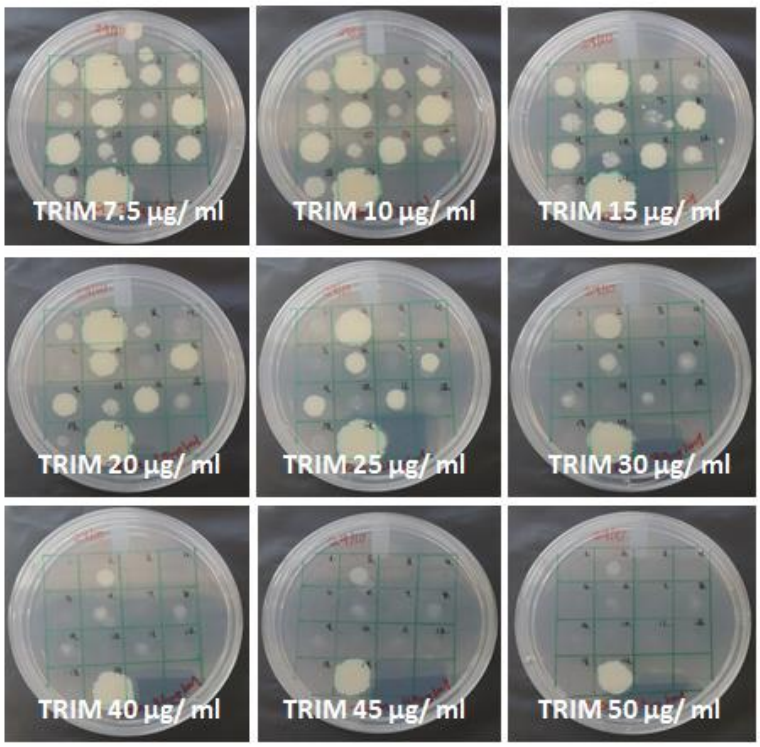


Figure 3.3.1: **Putative protein interacting partners screen.** Confirmation of interacting partners using different Trim concentrations. Randomly selected interacting partners cultured in Middlebrook 7H10 agar supplemented with Kan (25 µg/ml) Hyg (50 µg/ml) and Trim concentrations gradually increased in 5 µg/ml intervals (7.5 -50 µg/ml). Control strains included in the screen.

3.3.2. Confirmation of the MSMEG_4217 interacting protein partners (Alamar Blue assay)

The screen revealed interactions making use of the principle of the M-PFC assay based on the emergence of a colony dependent on time. Another assay was used to further quantify the degree of reconstitution of mDHFR and the protein-protein association in the identified interacting partners. This was done by monitoring growth in the presence of drug by the Alamar blue assay (Singh et al., 2006), following the protocol illustrated in section 2.10.3. Partial clones of the identified putative interacting partners were obtained and propagated on Middlebrook 7H9 broth supplemented with Kan (25 µg/ml) and Hyg (50 µg/ml) and the strains were grown as detailed in section 2.3.2. The strains were sub-cultured on 96 well plates and grown overnight, then Alamar Blue was added to the cultures and the fluorescence measured as detailed in section 2.10.3. The

Alamar Blue assay results of 6 selected interacting partial protein clones are shown in figure 3.3.2. *M. smegmatis* partial clones containing partners of MSMEG_4217 showed a varying range of the degree of reconstitution of mDHFR, this was observed by the development of pink color (color spectrum from purple, magenta to a very light pink appeared on the 96well plates). The mc:: RipA + RpfB (positive control) strain, was observed to survive the highest Trim concentration, (Hett et al., 2007; Hett & Rubin, 2008). The results indicate that RecR (MSMEG_6279) and the ABC Transporter / MSMEG_1577 have the greatest degree of reconstitution of mDHFR with MSMEG_4217. NucS (MSMEG_4923) and UvrABC protein B (MSMEG_3816) have the least degree of reconstitution of mDHFR. Results for the minimum inhibitory concentration (MIC) are listed in table 3.3.

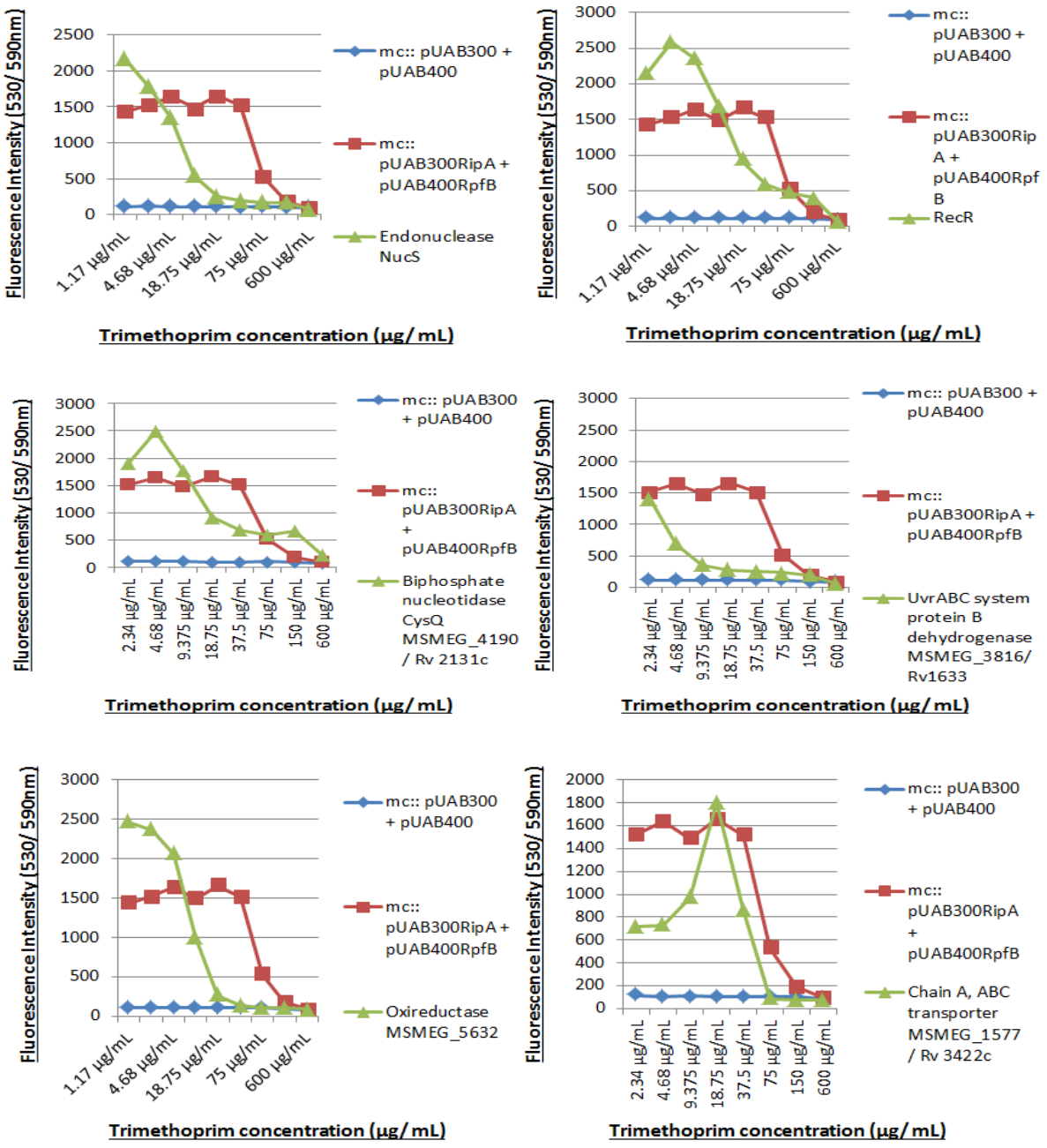


Figure 3.3.2: **Quantification of protein-protein interaction using partial clones of MSMEG_4217 identified interacting protein partners.** MSMEG_4217 and interacting protein partners fused to the complementary mDHFR fragments F[3] and F[1,2] respectively. This resulted in the reconstitution to a functional protein and conferring resistance to Trimethoprim and subsequent growth of the strain. Growth of the strain results in the reduction of Alamar Blue from non-fluorescent blue to fluorescent pink color, pink color scored as a positive interaction.

Table 3.3. **Quantification of protein-protein interaction between MSMEG_4217 and identified partial clones of interacting partners** MSMEG_4217 interacting partnering protein partial clone tested for protein association intensity, tested alongside control strains.

Test strains	**Trim MIC (µg/ ml)**
(1) mc:: MSMEG_4217 + Endonuclease NucS (MSMEG_4923)	9.37
(2) mc:: MSMEG_4217 + RecR (MSMEG_6279)	37.5
(3) mc:: MSMEG_4217 + Biphosphate nucleotidase CysQ (MSMEG_4190)	18.75
(4) mc:: MSMEG_4217 + UvrABC system protein B (MSMEG_3816)	9.37
(5) mc:: MSMEG_4217 + Oxidoreductase (MSMEG_5632)	18.75
(6) mc:: MSMEG_4217 + Abc Transporter (MSMEG_1577)	37.5
Negative control mc:: pUAB300 + pUAB400	-
Positive control mc:: pUAB300RipA + pUAB400RpfB	75

3.4. Bioinformatics analysis and cellular localization of chromosome segregation and cell division enzymes in wild-type *M. smegmatis* cells

3.4.1. Bioinformatics analysis of functional domains necessary for interaction in the partnering protein (MSMEG_5632)

The analyses thus far have confirmed protein interaction between MSMEG_4217 and the various identified interacting protein partners. Bioinformatics analysis was applied to acquire detailed information of several of the selected putative interacting partners. The selected interacting partners were examined for their domain organizations using pFam analysis (http://pfam.xfam.org/about) a protein database used for the identification of protein functional domains. The putative interacting partner MSMEG_5632 was selected for further analysis due to the prominent specific kinase abilility (discussed in detail below). This domain is contained within a well characterized PG remodeling enzyme of actively growing cells that work in association with other PG remodeling enzymes. The results revealed that MSMEG_5632 is a member of the short-chain dehydrogenase/reductase superfamily and has a molecular function of oxidoreductase activity (Lou et al., 2016). This protein has a highly conserved NAD(P)- binding domain (active site), which is responsible for the regeneration of NAD(P)H for biocatalytic synthesis. Some members of this family are classified as dual-specific kinases as they have the ability to phosphorylate and autophosphorylate a protein on the S/T and Y residues, which are of particular interest for this study (Nguyen et al., 2017). These types of kinases are ubiquitous in bacteria and are widely spread in Gram-positive bacteria, but most are not essential for bacterial viability (Pereira et al., 2011; Turapov et al., 2018). Interestingly, PknB has a similar characteristic domain important for catalytic activity (Turapov et al., 2018). In mycobacteria, DivIVA is phosphorylated or activated by PknB.

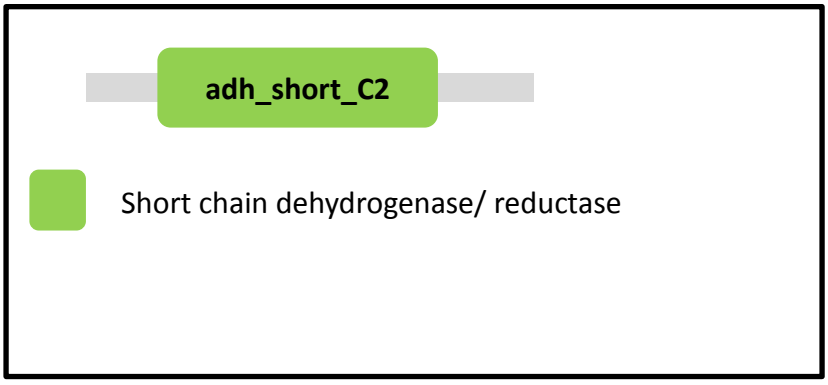


Figure3.4.1: **Schematic representation of domain organization of MSMEG_5632 protein.** The functional domain is represented in green showing the conserved short chain dehydrogenase/ reductase nucleotide binding and hydrolysis motif. http://pfam.xfam.org/ accessed on 20/08/2019.

M. smegmatis DivIVA has a phosphorylation target site that has to be activated in order to perform its function. Further detailed biochemistry is needed to determine the relationship between MSMEG_4217 and MSMEG_5632 interaction.

3.4.2. Subcellular localization of MSMEG_5632 in wild-type *M. smegmatis* cells

3.4.2.1. Construction of the pTweety_MSMEG_5632_mRFP plasmid

To further investigate the role of MSMEG_5632, the full length gene was cloned into the reporter plasmid pTweety_mRFP, thus creating a MSMEG_5632 C-terminally tagged mRFP derivative and the wild-type *M. smegmatis* mc^2155 cells were transformed with the plasmid DNA (Figure 3.4.2).This method was initially planned for all 6 selected interacting partners (Table 3.3), however, due to time constraints only MSMEG_5632 and MSMEG_1577 (discussed later) were taken further for investigation. Briefly, the MSMEG_5632 full length gene was PCR amplified with complementary restriction sites at each end and ligated into pTweety_mRFP to create an in-frame gene using the PCR primers listed in Appendix B. The pTweety_mRFP vector was linearized with complementing restriction enzymes. Ligations were performed using different ratios as detailed in section 2.6.6 and using *E.coli* DH5α cells were transformed with the ligation reactions. The clones were screened by picking a single colony and sub-culturing, followed by small-scale plasmid DNA extraction as described in section 2.4.2.1. The resulting

DNA was profiled with at least 5 restriction enzymes (Figure 3.4.2. B). The construct was sequenced to ensure no mutations were introduced during cloning (data not shown). The wild-type *M. smegmatis* mc^2155 cells were transformed with the construct creating mc::MMSEG_5632_pTweety_mRFP derivative strain.

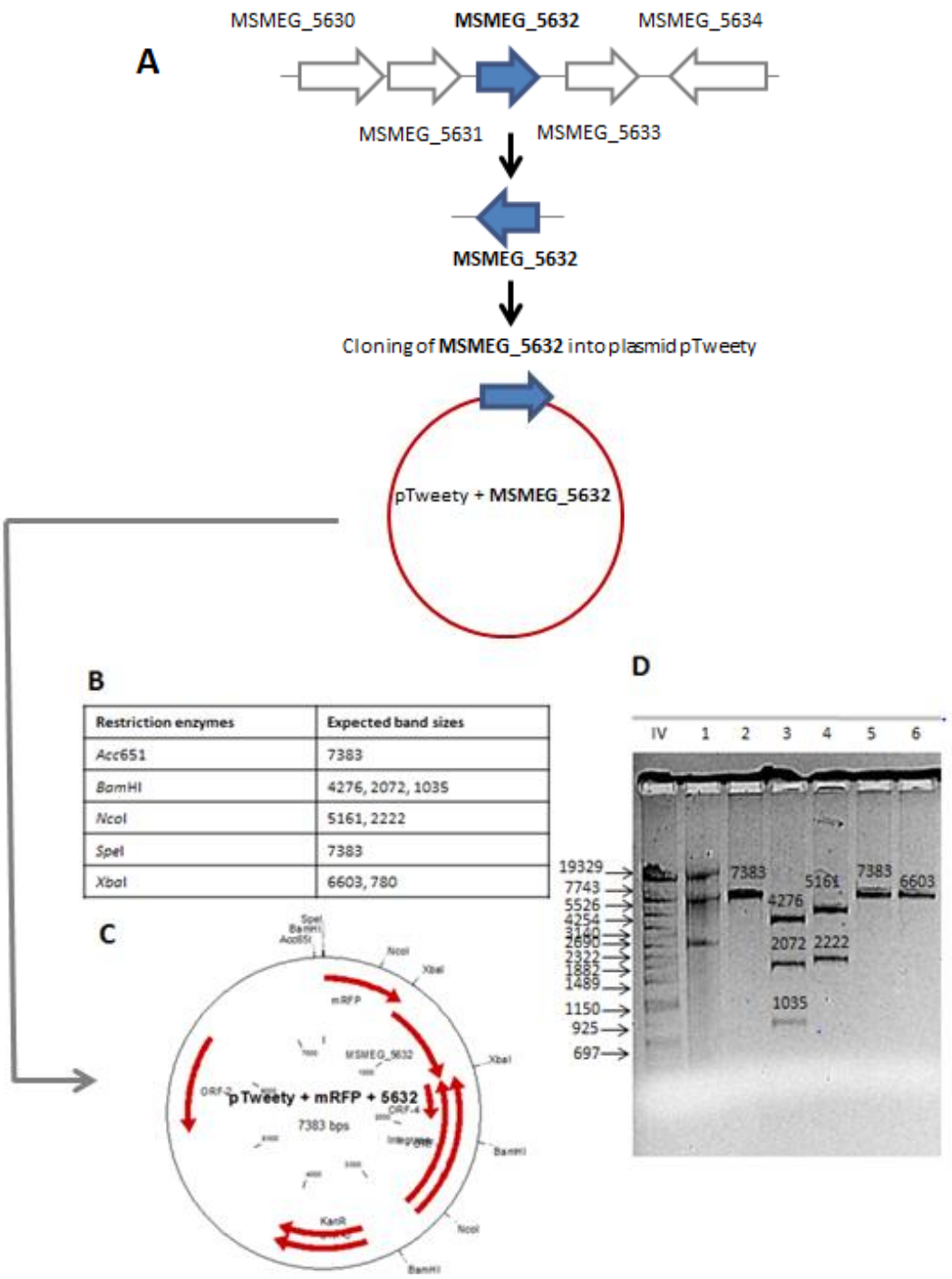


Figure 3.4.2: **Construction and restriction profiling of pTweety_mRFP_5632.** (A) The mc^{2}155 genome map indicating the location of the *MSMEG_6532* gene and the cloning strategy for the insertion of *MSMEG_6532* gene. (B) Table indicating the restriction enzymes used for the analysis of MSMEG_5632_pTweety_mRFP and the expected band sizes. (C) Plasmid map of MSMEG_5632_pTweety_mRFP. (D) Agarose gel indicating the DNA band sizes expected (labeled in base pairs). Lane 1, uncut; lanes 2-6, Acc651, *Bam*HI, *Nco*I, *Spe*I and *Xba*I.

3.4.2.2. Localization of MSMEG_5632 in wild-type *M. smegmatis* single cells

The subcellular localization patterns of MSMEG_5632 during cell growth and division in mc^2155 wild-type *M. smegmatis* cells were analyzed using the above-mentioned reporter strain. The analysis revealed localization patterns varying from sub-polar to mid-cell to bipolar. There are 5 distinct patterns that were observed: (i) Subpolar (ii) Bipolar and mid-cell (iii) Multiple mid-cell (iv) Subpolar and polar and (v) Punctate; shown in figure 3.4.3. The two most frequent patterns observed were subpolar and polar or the subpolar and mid-cell localization. These results suggest the involvement of MSMEG_5632 in different stages of cell growth. The last stage of cell division may be represented by a bipolar and midcell localization pattern, just before a cell divides into two cells. The bipolar and subpolar may represent new daughter cells before elongation takes place. The temporal and spatial localization of this protein predominantly in these sites suggests that it may play a role during late cell division.

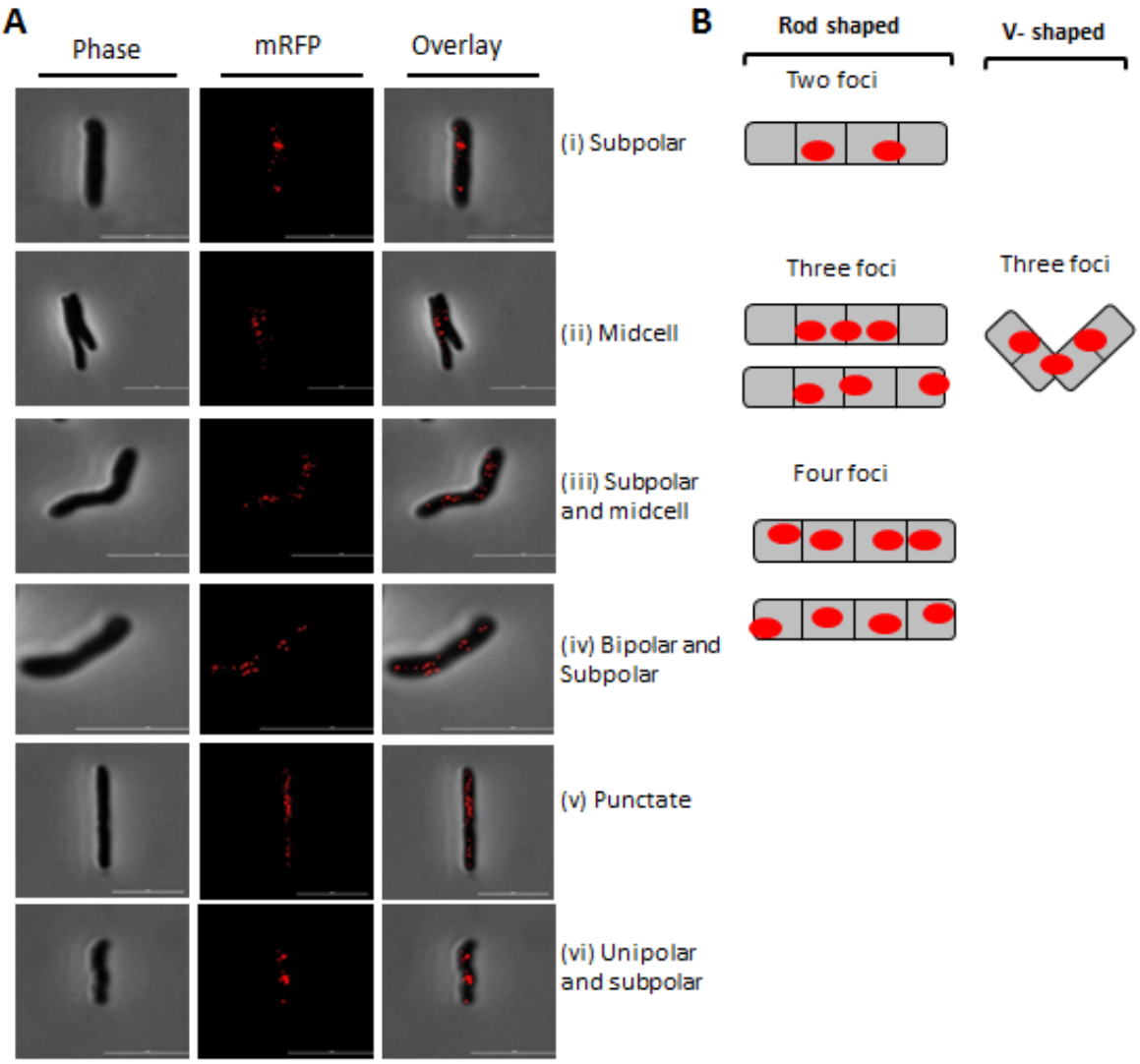


Figure 3.4.3 : **Subcellular localization patterns of MSMEG_mRFP_5632 in wild-type *M. smegmatis*.** (A) The different patterns of localization observed: i. Subpolar, ii. Midcell iii. Bipolar and midcell, iv. Subpolar and polar, v. Punctate, vi. Unipolar and subpolar (B) A schematic representation of the different localization patterns identified.

3.4.3. Bioinformatics analysis of functional domains necessary for interaction in the partnering protein (MSMEG_1577)

The MSMEG_1577 interacting partner nucleotide sequence was blasted and analyzed for domain orientation using pFam analysis (http://pfam.xfam.org/about). The results revealed that MSMEG_1577 is a member of a new family of protein kinases with a Ser/Thr/Tyr kinase activity, broadly conserved among bacteria. The domain organization in the hypothetical protein (uncharacterized protein) is composed the threonylcarbamoyltransferase complex ATPase subunit type 1 TsaE, a periplasmic binding region and sugar binding region of the Lacl family (figure 3.4.4). Some members of this family are classified as dual specific kinases, possessing the trait to phosphorylate and autophosphorylate a protein substrate on the S/T and Y residues (Nguyen et al., 2017). In addition, the MSMEG_4217 also comprises of an N-terminal phosphorylation target site domain (Thr73 residue) (Figure 3.1.2 B). The smartblast (http://blast.st-va.ncbi.nlm.nih.gov/blast/smartblast/) also revealed sequence identity to ML0377 a hypothetical protein with a highly conserved ATP/GTP-binding domain site motif.

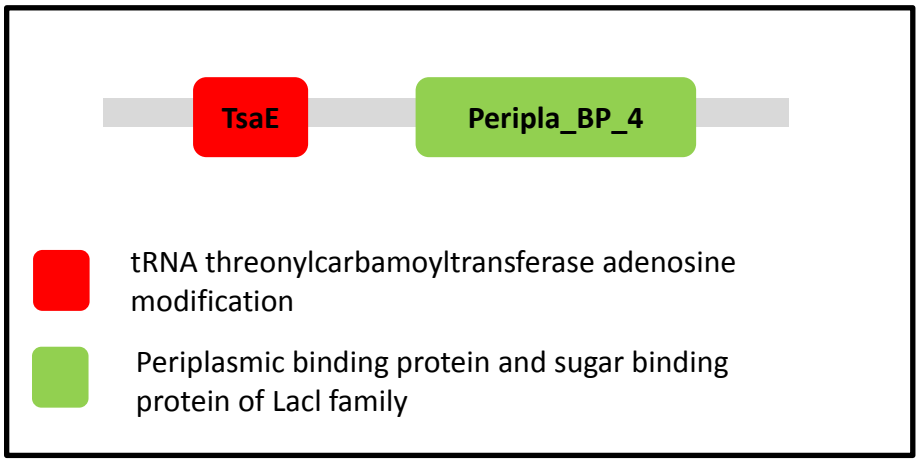


Figure 3.4.4: **Schematic representation of domain organization of MSMEG_1577 protein.** The functional domain is represented in green showing the conserved short chain dehydrogenase/ reductase nucleotide binding and hydrolysis motif. http://pfam.xfam.org/ accessed on 25/09/2019.

3.4.3.1. Construction of a MSMEG_1577 reporter in wild-type *M. smegmatis* single cells

For localization of MSMEG_1577, the putative interacting partner's full-length clone was integrated into reporter plasmid pTweety_mRFP as described previously. The construct was

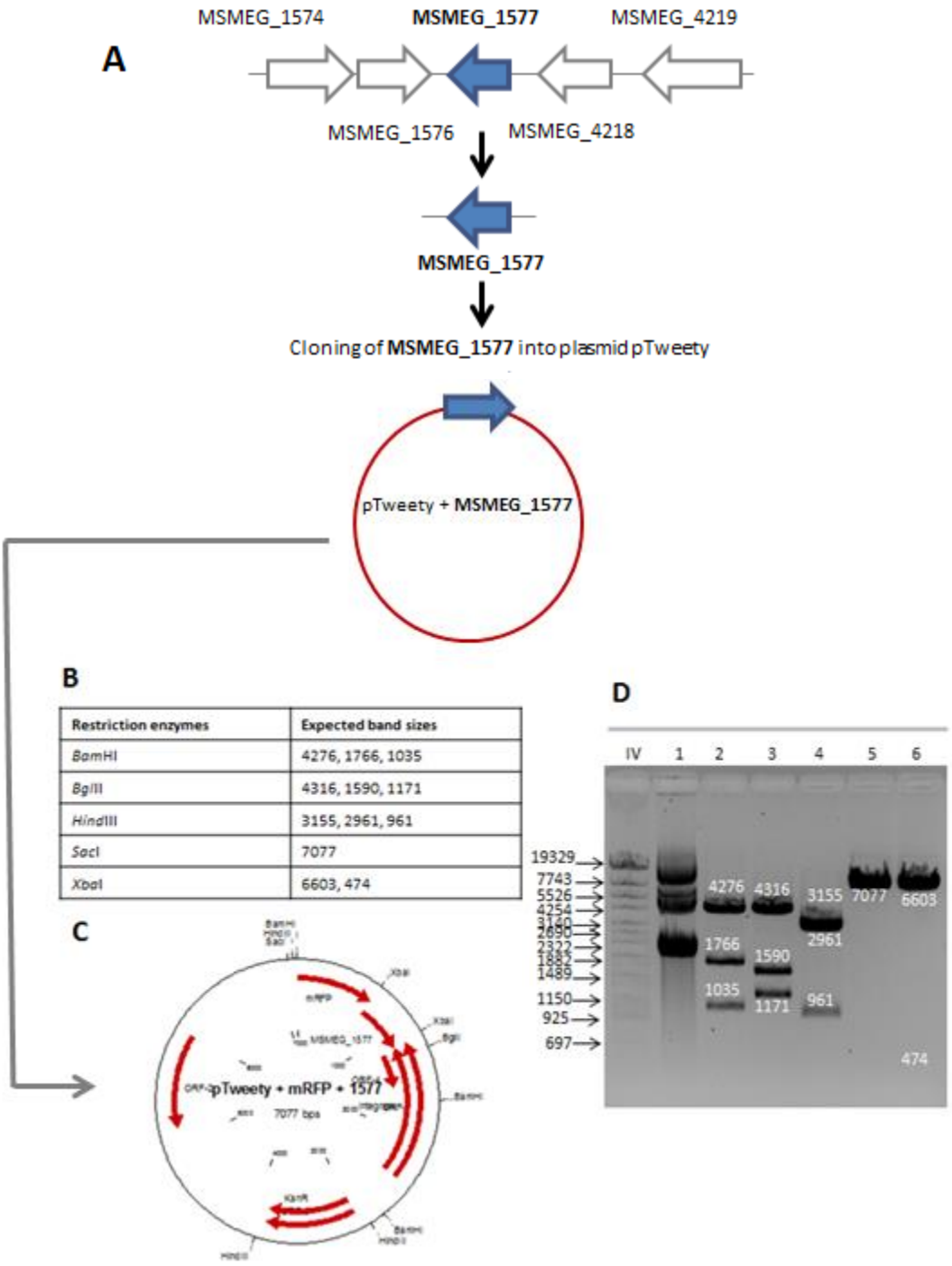


Figure 3.4.5: **Construction and restriction profiling of pTweety_mRFP_1577.** (A) The mc^{2}155 genome map indicating the location of the *MSMEG_1577* gene and the cloning strategy for the insertion of *MSMEG_1577* gene. (B) Table indicating the restriction enzymes used for the analysis of MSMEG_1577_pTweety_mRFP and the expected band sizes. (C) Plasmid map of MSMEG_1577_pTweety_mRFP. (D) Agarose gel indicating the DNA band sizes expected (labeled in base pairs). Lane 1: unit, Lanes 2-6: *Bam*HI, *Bgl*II, *Hind*III, *Sac*I, *Xba*I respectively.

sequenced to confirm gene integrity of the plasmid (data not shown) and also confirmation by restriction enzyme digestion was performed (Figure 3.4.5). The restriction digest with plasmid MSMEG_1577_pTweety_mRFP resulted in the expected banding patterns, therefore the plasmid was taken further to study the localization patterns in *M. smegmatis* cells through transformation creating a mc::MSMEG_1577_pTweety_mRFP derivative strain.

3.4.3.2. Localization of MSMEG_1577 in wild-type *M. smegmatis* cells

The subcellular localization patterns of MSMEG_1577 during cell growth and division was also analyzed in mc^2155 wild-type *M. smegmatis* cells using the above-mentioned approaches. The analysis revealed localization patterns varying from sub-polar to mid-cell to bipolar. Here, 4 distinct patterns were observed: (i) Bipolar and midcell (ii) Bipolar and subpolar (iii) Subpolar and mid-cell (iv) Punctate; shown in figure 3.4.6. The two most frequent patterns observed are the midcell and the Subpolar and midcell localization. The results presented also suggest the involvement of MSMEG_1577 in different stages of cell growth. This predominant septal localization pattern suggests the possibility of the protein interacting with divisome machinery or with proteins that work in concert at the midcell during cell division.

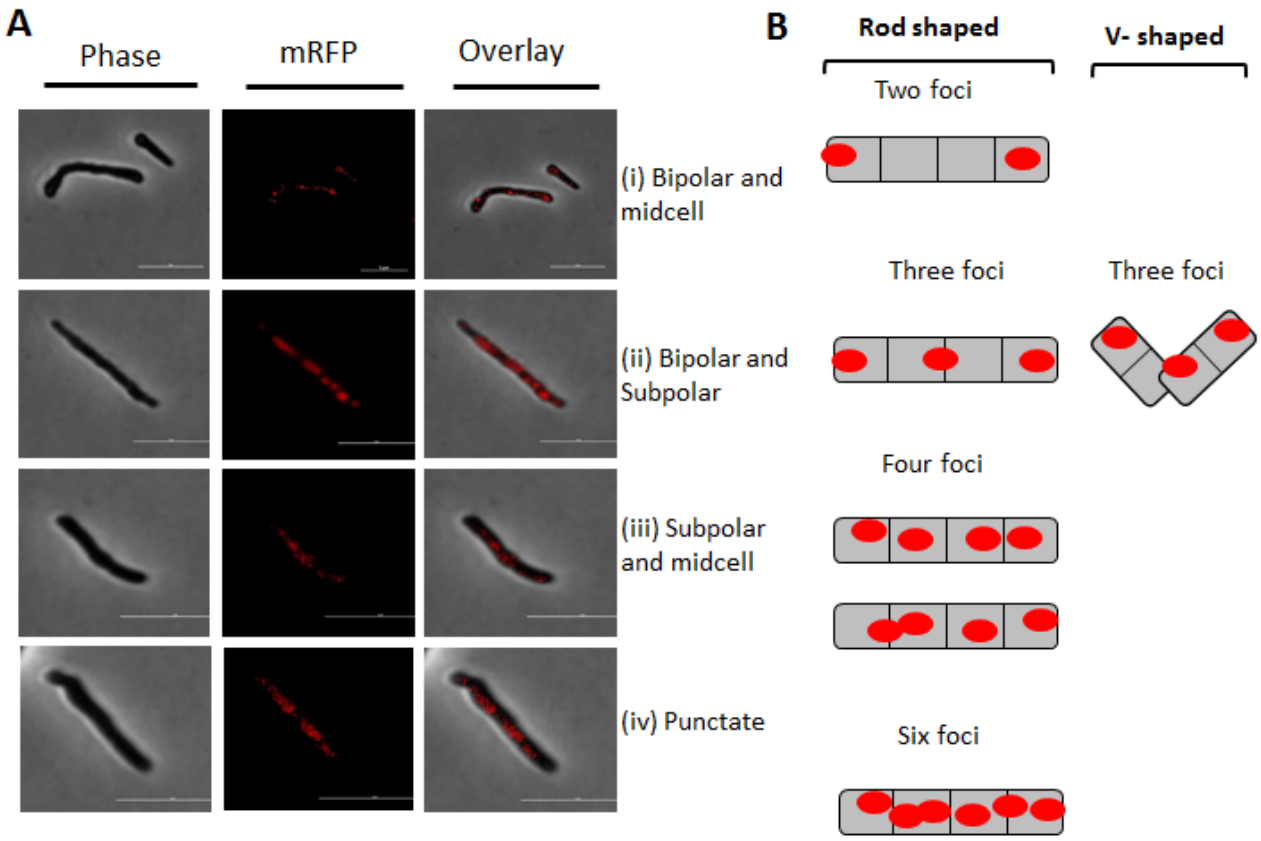


Figure 3.4.6 : **Subcellular localization patterns of MSMEG_mRFP_1577 in wild-type *M. smegmatis*.** (A) The different patterns of localization observed: i. Polar and midcell, ii. Bipolar and subpolar, iii. Subpolar and midcell, iv. Punctate (B) A schematic representation of the different localization patterns identified.

4. Discussion

TB claims over two million lives annually and the causative agent *Mtb* is a successful pathogen with an inherent ability to grow under stressful environments. One of its remarkable features is its ability to remain dormant within an individual for years and then reactivating to cause active TB (Hett & Rubin, 2008). There are several factors that influence this reactivation and these most likely relate to changes in host immune status (Chao & Rubin, 2010). The combined global pandemic of active and latent TB has driven research focused on identifying novel drug targets that can kill both replicating and non-replicating bacteria. Accordingly, understanding the processes of growth and cell division in this microorganism is crucial for the development of effective novel anti-TB drugs. There has been a growing interest in cell wall targeted research, focusing on essential components of the mycobacterial cell wall as potential drug targets (Kieser & Rubin, 2014). As mentioned earlier, the biosynthesis of PG relies on the coordinated activity of multiple proteins and enzymes which interact with each other to drive biosynthesis and remodeling of this polymer. Consequently, there are numerous potential targets for drug development, inhibition of which will provide important information in the vulnerability of these proposed drug targets (Hett & Rubin, 2008; Singh et al., 2016).

In other rod-shaped bacteria, an MreB actin-like protein is functionally responsible for the maintenance of cell shape. In mycobacteria, a tropomyosin-like protein called DivIVA is responsible for maintaining cell shape (Hett & Rubin, 2008). The cytosolic MreB guides the periplasmic PG synthesis enzymes and DNA partitioning through interaction with important proteins and enzymes that facilitate cell division (Hett & Rubin, 2008). DivIVA has been reported to interact with a partitioning protein complex to facilitate accurate movement and positioning of genetic material to the daughter cell during cell division (Bartosik et al., 2014). The ability of mycobacterial DivIVA to coordinate cell wall synthases is dependent on its phosphorylation state, which then coordinates the synthesis of PG and presumably the aging of the cell wall (Baranowski et al., 2019). In order to fill the knowledge gaps in the functionality of the mycobacterial DivIVA, the M-PFC assay was utilized to search for previously undescribed interacting partners for *M. smegmatis* DivIVA denoted MSMEG_4217. The method chosen for this investigation is based on the use of a well-established system to directly test the interaction

between two potential partners found within the natural mycobacterial environment and considering the requirement potential cytosolic cofactors (Veyron-Churlet & Locht, 2019).

Interaction between MSMEG_4217 and the identified putative partners

The M-PFC assay identified various putative interacting partners for *M. smegmatis* DivIVA revealing the possibility that this protein interacts with multiple other proteins during the process of growth. These results can be attributed to the complex structure of DivIVA, being amphiphilic and having the ability to associate with different binging partners with the use of multiple interacting surfaces (Oliva et al., 2010; Halbedel & Lewis, 2019). We found some interacting partners that were either membrane/periplasmically associated and cytosolic interacting protein partners that have been reported in other bacteria to play a role in PG biosynthesis. The screen identified three known interacting proteins involved in chromosome segregation (RecR) and cellular processes including cell division (UvrABC transporter and Cys proteins). Some new interactions arising from this study the such as an Oxidoreductase (predominantly a membrane associated protein) and NucS (an endonuclease) were also identified. These were not studied further due to time constraints.

RecR facilitates the function of DNA repair and may be associated with RecF and RecO (Gupta et al., 2015). The RecR has been reported to be involved in RecBC-independent recombinational DNA repair. RecR is also involved in DNA recombination. In *E. coli*, the recombination proteins are produced in the periplasm also and protein recruitment to this compartment is facilitated through translocation via the Sec proteins (Baumgarten et al., 2018). Interestingly, the mycobacterial RecR was assessed using the STRING (http://string-db.org/) the protein database that predicts protein-protein interactions between known and proteins of unknown function. This analysis revealed an interaction with UvrB, with a possible complex RecR-RecF-UvrB (data not shown). No interaction between the RecR protein has been reported. The translocation of membrane proteins across the Sec translocon does not necessarily involve direct interactions with the translocon proteins, rather interactions have been established within the Sec proteins per se, i.e. SecY and SecE, to create a complex that represents the core of the protein conducting channel (Baumgarten et al., 2018). The interaction between RecR and DivIVA suggests that during chromosome segregation, some form of DNA repair may be required.

The UvrABC complex proteins are known to be involved in a number of similar cellular functions. The UvrA protein functions as an exonuclease that facilitate the breaking of phosphodiesters bonds and cleaving the between 3' and 5' ends of nucleotides (Turapov et al., 2018). The complex firstly recognizes DNA abnormalities, then followed binding to the DNA strand, it carries out DNA repair processes. This is made possible through the ATP and DNA binding activity that is found within the protein subunits (Sung et al., 2009). The UvrB protein was identified to interact with DivIVA in this study, a component of the UvrABC complex that facilitates DNA binding. The UvrB protein has a conserved domain UB2H in the C-terminal (Eryilmaz et al., 2006; Truglio et al., 2006). The UvrB is the most studied of the Uvr proteins, with crystal structures that revealed ATP-bound forms additional to the C-termianl domain shown to have key roles in ATPase activity. Thus, these conserved interacting residues have been of interest in the processes of antibiotic design (Eryilmaz et al., 2006; Sung et al., 2009).

Another putative interacting partner is a member of a group of proteins called the Cys proteins. These have a range of functions within bacteria and predominantly function as ABC transporters. The well-studied CysA1 was identified in a screen and found to interact with the phosphorylated PknB, a major key role player in PG synthesis. CysA1 increased phosphorylation peptides within this group of proteins (Turapov et al., 2018). In our screen CysQ was identified to interact with DivIVA. This protein appears to have a nucleotidase activity, it functions to transport substances across the cellular membrane with the assistance of ATP binding and hydrolysis (Patel et al., 2002; Erickson et al., 2015). The role of putative interaction with DivIVA remains unknown.

NucS, another putative DivIVA interacting partner identified in this screen, is an endonuclease cleaving phosphodiester bonds in polynucleotides. It is found in *E.coli* and *S. aureus* alike and has been associated with spontaneous transition mutations and has a role in mutagenesis during bacterial growth (Ishino et al., 2018; Wiemels et al., 2017). NucS in this study was found to interact with DivIVA during the screening of interacting partners, when the protein was blasted, it was discovered that the gene had an association with the above-mentioned Sec proteins which play a crucial role in protein translocation during growth.

The interacting partners of *M. smegmatis* DivIVA is a subject not well understood as this protein itself is not exclusive in its localization, by localizing to different parts of the cell during different times of bacterial growth (Hett & Rubin, 2008; Turapov et al., 2018; Baranowski et al.,

2019). This temporal and spatial flexibility of mycobacterial DivIVA allows for different types of proteins and enzymes to have access for the purpose of interaction. This study has revealed a sophisticated variety of proteins that have been identified and as putative interacting partners of DivIVA. These results suggest that DivIVA carries out its activity through the interaction of many proteins, possibly at different stages of growth to regulate chromosome segregation, control cell division and orchestrate the remodeling of PG. This study has added new novel interacting protein partners in *M. smegmatis* DivIVA, that have not yet been studied, these are summarized in Figure 4.1.

A proposed model of DivIVA interacting partners

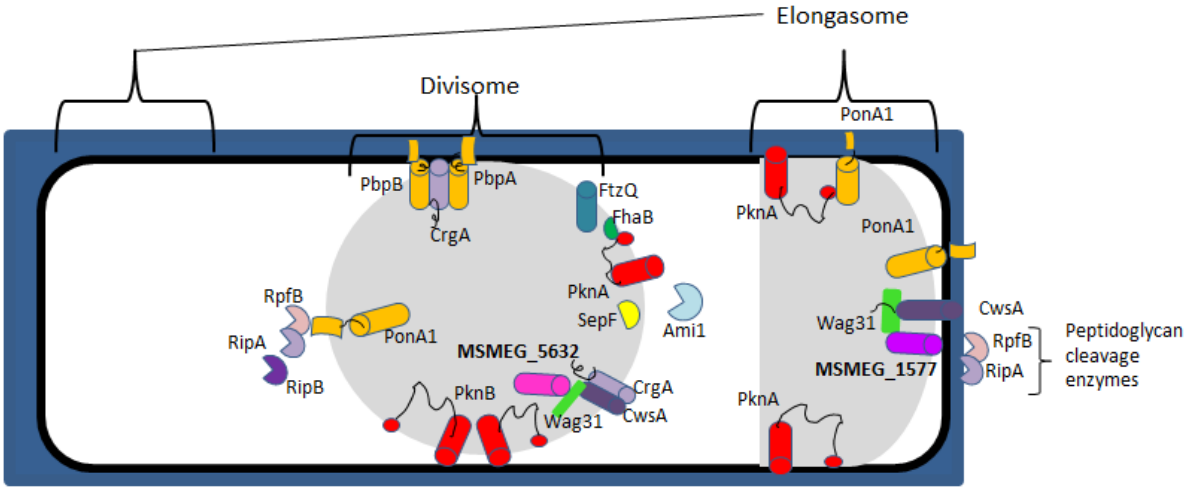


Figure 4.1: **A proposed model of DivIVA interacting partners function in mycobacterial physiology.** MSMEG_5632 and MSMEG_1577 form a protein complex with DivIVA (Wag31) independently. During cell growth, chromosome segregation and cell division, DivIVA activation is carefully regulated. Based on microscopic imaging analysis data, we observed that MSMEG_5632 is present at midcell and MSMEG_1577 is present at the pole and subpolar region. In addition, the model proposes that MSMEG_5632 is involved in DivIVA DNA binding during chromosome segregation. MSMEG_1577 is proposed to be involved in DivIVA localization to the poles during cell division through the interaction with MSMEG_1577. It should be noted that other patterns of localization were also observed for these proteins and as such, the model is a prediction that requires further validation.

4.1. Future prospects

Future work will encompass investigation of the functional roles of the interacting partners through full length gene cloning studies. Cellular co-localization of cell wall machinery (DivIVA) and the identified interacting partnering proteins in wild-type *M. smegmatis* cells, in order to interrogate the biochemical and biosynthetic consequences of the interaction to coordinate growth. This study has revealed spatial localization of the two putative interacting partners, MSMEG_5632 and MSMEG_1577 with DivIVA (Wag31). Further studies will involve assessing the function of DivIVA in the absence of these two interacting partners.

4.2. Limitations

The prediction of interacting partners of the mycobacterial DivIVA using the STRING analysis (http://string-db.org/) was one of the limiting factors in this study, due to the fact that modelling software is based on prediction algorithms. These require experimental validation.

4.3. Concluding remarks

Cell division is an extensively studied area in model rod-shaped bacteria *Escherichia coli* and *Bacillus subtilis* but not much is known about cell division in mycobacteria. The mycobacterial cell wall and the proteins involved in its remodeling remains an interesting area for TB drug development. Elucidating complexes involved in cell wall integrity during growth, and how they are regulated in both time and space to enable elongation of the cell, replication and segregation of the chromosome, together with destruction of the septum, is expected to yield new TB drug targets. This study identified novel interacting DivIVA partners that may be important for bacterial growth and provides new insight on investigation of the mycobacterial DivIVA protein as a putative drug target.

5. Appendices

Appendix A: Media and Solutions

Table A1. **Media supplements**

Media Supplement	Components
Luria- Bertani Broth (LB)	5 g yeast extract, 10 g tryptone, 10 g NaCl dissolved in 1L sdH_20.
Luria- Bertani Agar (LA)	5 g yeast extract, 10 g tryptone, 10 g NaCl and 1.5 g agar dissolved in 1L sdH_2O.
2xTY	10 g yeast extract, 16 g tryptone and 10 g NaCl dissolved in 1L sdH_2O.
Middlebrook 7H9	4.7 g Difco Middlebrook 7H9 powder and 2ml glycerol dissolved in 986 ml sdH_2O. Autoclave. 10 ml 100 X glucose salts and 2 ml Tween80.
Middlebrook 7H10	19 g Difco Middlebrook 7H10 powder and 5ml glycerol dissolved in 985 ml sdH_2O. Autoclave. 10 ml 100 X glucose salts.
Glucose salts (100X)	20 g glucose and 8.5 g NaCl dissolved in 100 ml sdH_2O.
Sucrose (75%)	75 g sucrose dissolved in 100 ml sdH_2O.
Tween80 (25%)	10 ml Tween80 dissolved in 40 ml sdH_2O.
X-gal (2)%	1 g X- gal dissolved in 50 ml deionized DMF.

Table A2. **Solutions used for *E. coli* plasmid DNA extractions**

Solution	Composition
Solution I	50 Mm glucose, 25 Mm Tris-HCl (pH 8) and 10 Mm EDTA dissolved in sdH_2O. Autoclave.
Solution II	1% SDS and 0.2 M NaOH dissolved in sdH_2O.
Solution III	3 M Potassium acetate and 11.5% acetic acid dissolved in sdH_2O.

Table A3. **Solutions used for *M. smegmatis* DNA extractions**

Solution	Composition
TE buffer	10 Mm Tris- HCI (pH 8) and 10 Mm EDTA dissolved in sdH_20. Autoclave.
CTAB/NaCl	4.1 % NaCl and 10 % N- acetyl –N, N, N –trimethyl ammonium bromide dissolved in sdH_20. Filter sterilize.

Table A4. **Solutions used for DNA precipitation**

Solutions	Composition
Chloroform: Isoamyl alcohol	24 ml chloroform and 1 ml isoamyl alcohol.
Sodium acetate	3 M Sodium acetate dissolved in sdH_20 (pH 5.3). Autoclave.

Table A5. **Solutions used for DNA electrophoresis**

Solution	Composition
Ethidium Bromide	10 mg/ml dissolved in sdH_2O.
TAE	50 X stock solution: 242 g Tris base 57.1 ml glacial acetic and 100 ml EDTA (pH 8) made up to 1L with sdH_2O.

Table A6. **Recipes for agarose gel electrophoresis**

Gel percentage (%)	Amount of agarose (g) in 50 ml TAE
0.8	0.4
1	0.5
2	1

Table A7. **Solutions used for preparation of *E. coli* competent cells.**

Solutions	Composition
$CaCl_2$ (1 M)	14.7 g $CaCl_2$ $2H_20$ dissolved in 100 ml sdH_20. Autoclave.
$MgCl_2$ (1 M)	20.3 g $MgCl_26H_20$ dissolved in 100 ml sdH_20. Autoclave.
TbfI	30 Mm potassium acetate, 100 Mm rubidium chloride, 10 Mm calcium chloride, 50 Mm manganese chloride and 15% v/v glycerol made up in sdH_2O. Adjusted to pH 5.8 with acetic acid.
TbfII	10 Mm rubidium chloride, 75 Mm calcium chloride, 10 Mm MOPS and 15% v/v glycerol made up in sdH_2O. Adjusted to pH 6.5 with diluted NAOH.

Table A8. **Solutions used for preparation of *M.smegmatis* competent cells.**

Solutions	Composition
Glycerol (10%)	10 ml glycerol to 90 ml sdH_20. Autoclave.

Appendix B: Primers

TableB1. **Primers used for generation of bait vector cloning into pUAB400 for protein interaction study.**

Primer pair	Primer sequence	Restriction site
MSMEG_4217 F	GTGCAGCTGATGCCGCTCACACCAGCG	*Pvu*II
MSMEG_4217 R	GTGAAGCTTTCAGTTGTTGCCGCGGTT	*Hind*III

Table B2. **Primers used for the identification of putative interacting partners**

Primer pair	Primer sequence	Restriction site
pUAB300 _F	CAGCTGCAGAATTCGAAGCTT	None
pUAB300_ R	ACGCTAGTTAACTACGTCGAC	

Table B3. **Primers used for the localization study.**

Primer pair	Primer sequence	Restriction site
MSMEG_5632 F	GTGTCTAGAATGCAGGTAGCCATCATC	*Xba*I
MSMEG_5632 R	GTGTCTAGATCACCGCGGAACCCAATC	*Xba*I
MSMEG_1577 F	GTGTCTAGAATGGGTGAGCGGGTGGAC	*Xba*I
MSMEG_1577 R	GTGTCTAGATCACGTCCGGCTCCAATG	*Xba*I

Appendix C: DNA molecular weight markers used in this study

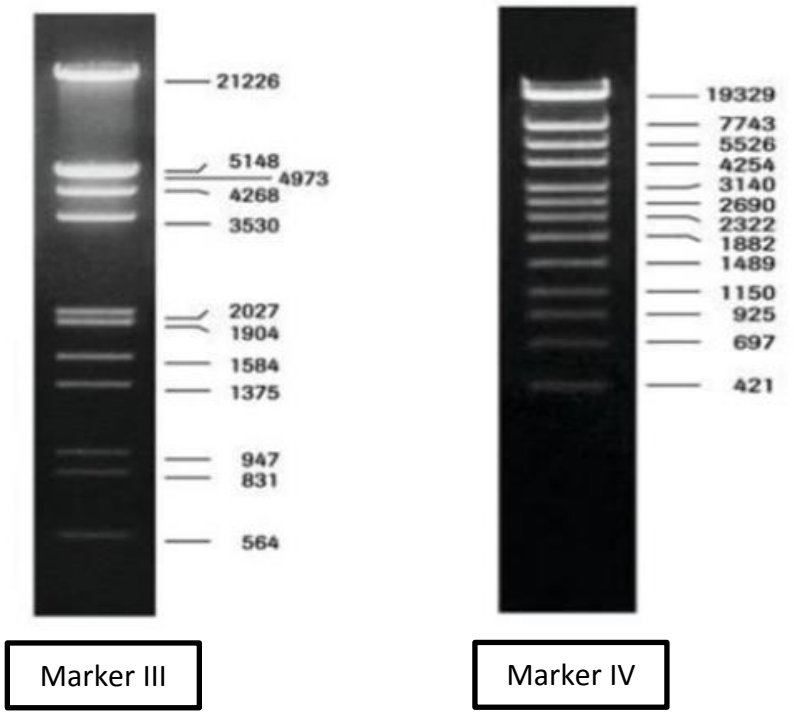


Figure A1: **Fermentas molecular weight markers (III and IV).**

Appendix D: Figures

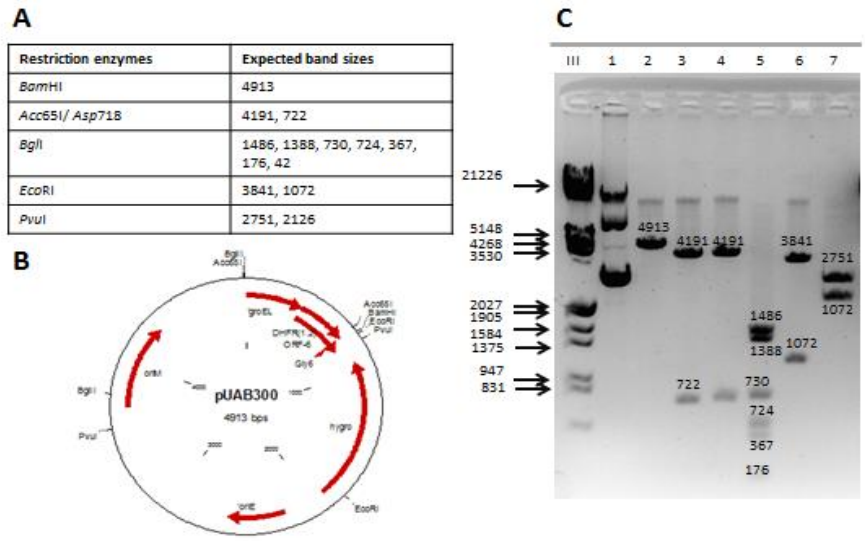


Figure D1: **Restriction profile of pUAB300.** (A) Table showing restriction enzymes used for profiling and the expected band fragment sizes. (B) Plasmid map of pUAB300 prey vector. (C) 1% agarose gel indicating expected DNA band sizes, marker III (fermentas), lane (1) uncut vector control, lane (2) *Bam*HI, lane (3) *Acc*65I, lane (4) *Asp*718, lane (5) *Bgl*I, lane (6) *Eco*RI, lane (7) *Pvu*I.

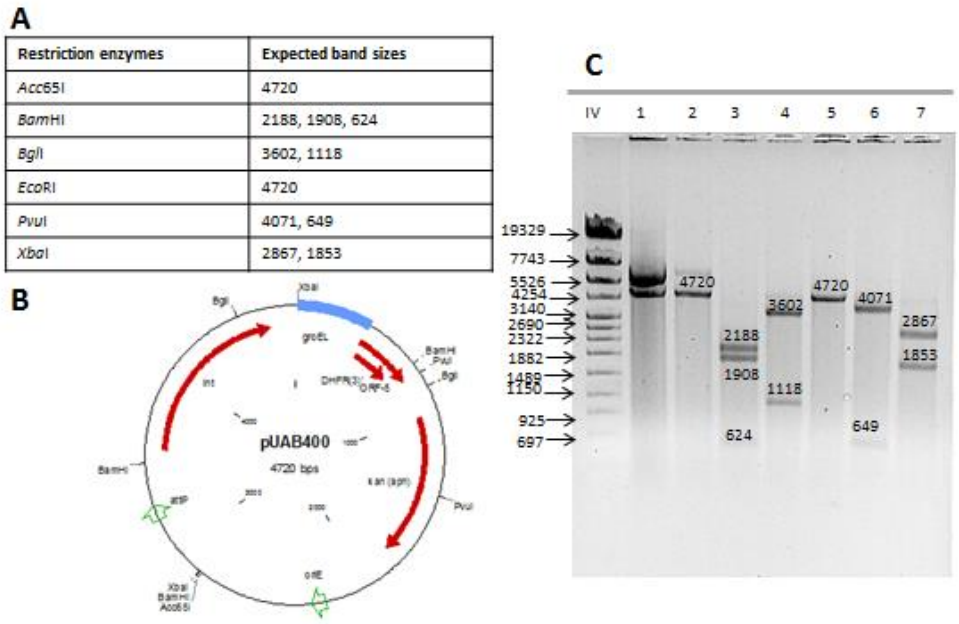


Figure D2: **Restriction profile of pUAB400.** (A) Table showing restriction enzymes used for profiling and the expected band fragment sizes. (B) Plasmid map of pUAB400 bait vector. (C) 1% agarose gel indicating expected DNA band sizes, marker IV (fermentas), lane (1) uncut vector control, lane (2) *Acc*65I, lane (3) *Bam*HI, lane (4) *Bgl*I, lane (5) *Ecol*RI, lane (6) *Pvu*I, lane (7) *Xba*I.

A

Restriction enzymes	Expected band sizes
*Aat*II	3733, 2870
*Hind*III	3155, 2487, 961
*Nco*I	5161, 1442
*Pst*I	4146, 2085, 372
*Spe*I	6603

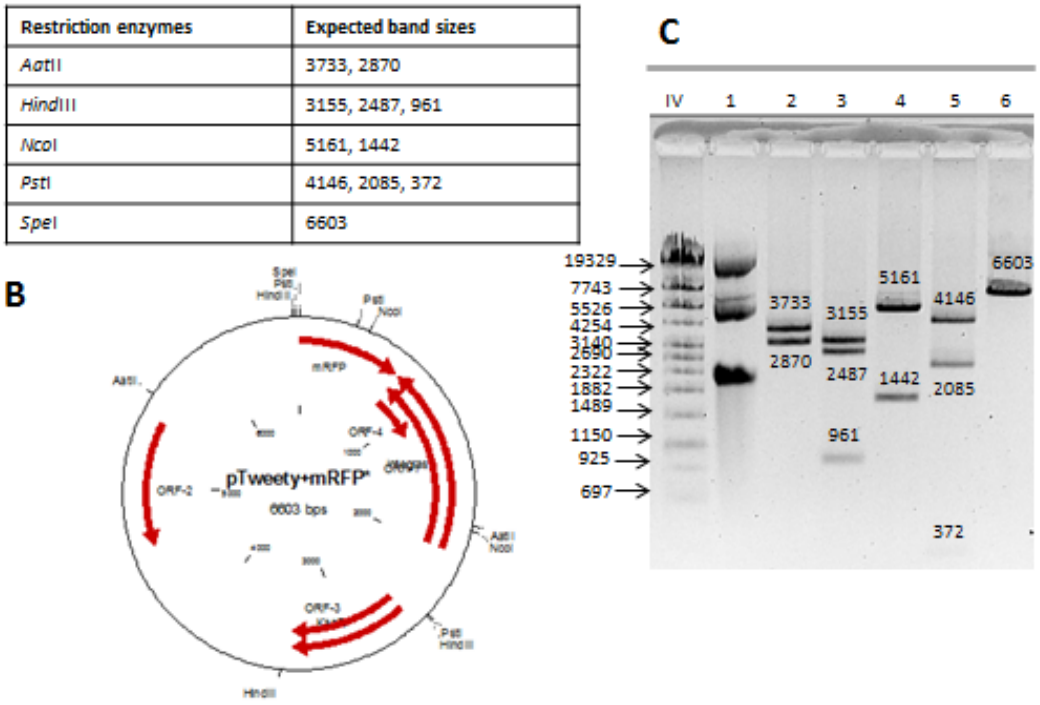


Figure D3: **Restriction profile of pTweety.** (A) Table showing restriction enzymes used for profiling and the expected band fragment sizes. (B) Plasmid map of pTweety reporter strain. (C) 1% agarose gel indicating expected DNA band sizes, marker IV (fermentas), lane (1) uncut vector control, lane (2) *Aat*II, lane (3) *Hind*III, lane (4) *Nco*I, lane (5) *Pst*I, lane (6) *Spe*I.

Appendix E: Ethics waiver

UNIVERSITY OF THE WITWATERSRAND, JOHANNESBURG

HUMAN RESEARCH ETHICS COMMITTEE (MEDICAL)

Office of the Deputy Vice-Chancellor (Research & Post Graduate Affairs)

TO: Ms N Mdlalose
School: Pathology
Department: CoE in Biomedical TB Research
National Health Laboratory Service

E-mail: Noluthando.Mdlalose@nhls.ac.za

CC: Supervisor: Professor B Kana <Bavesh.Kana@nhls.ac.za>
and <HREC-Medical.ResearchOffice@wits.ac.za>

FROM: Iain Burns
Human Research Ethics Committee (Medical)
Tel: 011 717 1252

E-mail: Iain.Burns@wits.ac.za

DATE: 19/11/2019

REF: *R14/49*

PROTOCOL NO: W-CBP-191119-01 (This is your ethics application study reference number. Please quote this reference number in all correspondence relating to this study)

PROJECT TITLE: *Characterization of cell elongation and chromosome segragation determinants in Mycobacteria*

Please find attached the Ethics Waiver Certificate for the above project. I hope it goes well and that an article in a recognized publication comes out of it. This will reflect well on your professional standing and contribute to the Government funding of the University.

MSWorks2000/Iain0007/ClearScanWaiver.wps

UNIVERSITY OF THE
WITWATERSRAND,
JOHANNESBURG

HUMAN RESEARCH ETHICS COMMITTEE (MEDICAL)

19/11/2019

Ref: W-CBP-191119-01

TO WHOM IT MAY CONCERN:

Waiver: This certifies that the following research does not require clearance from the Human Research Ethics Committee (Medical).

Investigator: Ms N Mdlalose
Student No. (if appropriate): 1114578
Staff No. (if appropriate):

Supervisor: Professor B Kana

School: Pathology
Department: CoE in Biomedical TB Research
National Health Laboratory Service

Project title: *Characterization of cell elongation and chromosome segragation determinants in Mycobacteria*

Reason: Laboratory study.
No human participants will be involved in the study.

Dr CB Penny
Chairperson: Human Research Ethics Committee (Medical)

Research Office Secretariat:
Physical address: Phillip Tobias Building, 3rd Floor, Office 302, Corner York Road and Princess of Wales Terrace, Parktown, Johannesburg 2193.
Postal address: Private Bag 3, Wits 2050
Tel Nos. +27 (0)11-717-1234/2656/2700/1252
Office E-mail: HREC-Medical.ResearchOffice@wits.ac.za.
Website:http://www.wits.ac.za/research/about-our-research/ethics-and-research-integrity/

6. Reference list

Baranowski et al., 2019a. The Dream of a Mycobacterium. In *Gram-Positive Pathogens, Third Edition*. American Society of Microbiology, pp. 1096–1106.

Baranowski, Rego, E.H. & Rubin, E.J., 2019b. The Dream of a Mycobacterium. In *Gram-Positive Pathogens, Third Edition*. American Society of Microbiology, pp. 1096–1106.

Barreteau, H. et al., 2008. Cytoplasmic steps of peptidoglycan biosynthesis. *FEMS Microbiology Reviews*, 32(2), pp.168–207.

Bartosik, A.A. et al., 2014. Transcriptional profiling of para and ParB mutants in actively dividing cells of an opportunistic human pathogen Pseudomonas aeruginosa. *PLoS ONE*, 9(1).

Baumgarten, T. et al., 2018. Optimizing recombinant protein production in the Escherichia coli periplasm alleviates stress. *Applied and Environmental Microbiology*, 84(12), pp.1–12.

Boshoff, H.I.M. & Barry, C.E., 2005. Tuberculosis - Metabolism and respiration in the absence of growth. *Nature Reviews Microbiology*, 3(1), pp.70–80.

Chao, M.C. & Rubin, E.J., 2010. Letting Sleeping dos Lie: Does Dormancy Play a Role in Tuberculosis? . *Annual Review of Microbiology*, 64(1), pp.293–311.

Choukate, K. et al., 2019. Crystal structure of the membrane anchoring domain of mycobacterial Wag31 : a dimer-of-dimer suggests how a Wag31 filament might self-assemble.

Choukate, K. et al., 2020. Higher order assembling of the mycobacterial polar growth factor DivIVA/Wag31. *Journal of Structural Biology*, p.107429.

Connell et al., 2011. Update on tuberculosis: TB in the early 21st century. *European Respiratory Review*, 20(120), pp.71–84.

Dhar, N. et al., 2013. Single-cell dynamics of the chromosome replication and cell division cycles in mycobacteria. *Nature Communications*, pp.1–10.

Dheda, K. et al., 2014. Global control of tuberculosis : from extensively drug-resistant to untreatable tuberculosis. *The Lancet Respiratory*, 2(4), pp.321–338.

Van Die, I.M., Bergmans, H.E.N. & Hoekstra, W.P.M., 1983. Transformation in Escherichia coli: Studies on the role of the heat shock in induction of competence. *Journal of General Microbiology*, 129(3), pp.663–670.

Erickson, A.I., Sarsam, R.D. & Fisher, A.J., 2015. Crystal Structures of Mycobacterium tuberculosis CysQ, with Substrate and Products Bound. *Biochemistry*, 54(45), pp.6830–6841.

Eryilmaz, J. et al., 2006. Structural insights into the cryptic DNA-dependent ATPase activity of UvrB. *Journal of Molecular Biology*, 357(1), pp.62–72.

Favini-Stabile, S. et al., 2013. MreB and MurG as scaffolds for the cytoplasmic steps of

peptidoglycan biosynthesis. *Environmental Microbiology*, 15(12), pp.3218–3228.

Furin et al., 2019. Tuberculosis. *The Lancet*, 393(10181), pp.1642–1656.

Ginda, K. et al., 2013. ParA of Mycobacterium smegmatis co-ordinates chromosome segregation with the cell cycle and interacts with the polar growth determinant DivIVA. *Molecular Microbiology*, 87(5), pp.998–1012.

Gupta, R., Shuman, S. & Glickman, M.S., 2015. RecF and RecR play critical roles in the homologous recombination and single-strand annealing pathways of mycobacteria. *Journal of Bacteriology*, 197(19), pp.3121–3132.

Halbedel, S. & Lewis, R.J., 2019. Structural basis for interaction of DivIVA/GpsB proteins with their ligands. *Molecular Microbiology*, 111(6), pp.1404–1415.

Hett, E.C. et al., 2007. A partner for the resuscitation-promoting factors of Mycobacterium tuberculosis. *Molecular Microbiology*, 66(3), pp.658–668.

Hett, E.C. & Rubin, E.J., 2008. Bacterial Growth and Cell Division: a Mycobacterial Perspective. *Microbiology and Molecular Biology Reviews*, 72(1), pp.126–156.

Inoue, H., Nojima, H. & Okayama, H., 1990. High efficiency transformation of Escherichia coli with plasmids. *Gene*, 96(1), pp.23–28.

Ioerger, T.R. et al., 2013. Identification of New Drug Targets and Resistance Mechanisms in Mycobacterium tuberculosis. , 8(9), pp.1–13.

Ishino, S. et al., 2018. Activation of the mismatch-specific endonuclease EndoMS / NucS by the replication clamp is required for high fidelity DNA replication. , 46(12), pp.6206–6217.

Jani, C. et al., 2010. Regulation of Polar Peptidoglycan Biosynthesis by Wag31 Phosphorylation in Mycobacteria. *BMC Microbiology*, 10(1), p.327.

Kieser, K.J. & Rubin, E.J., 2014. How sisters grow apart : mycobacterial growth and division. *Nature Reviews Microbiology*, 12(8), pp.550-562.

Lou, D. et al., 2016. The three-dimensional structure of Clostridium absonum 7α-hydroxysteroid dehydrogenase: New insights into the conserved arginines for NADP(H) recognition. *Scientific Reports*, pp.1–11.

Marakalala, M.J. et al., 2016. Inflammatory signaling in human tuberculosis granulomas is spatially organized. *Nature Medicine*, 22(5), pp.531–538.

McNerney, R. et al., 2000. Rapid screening of Mycobacterium tuberculosis for susceptibility to rifampicin and streptomycin. *International Journal of Tuberculosis and Lung Disease*, 4(1), pp.69–75.

Meniche, X. et al., 2014. Subpolar addition of new cell wall is directed by DivIVA in mycobacteria. *Proceedings of the National Academy of Sciences of the United States of America*, 111(31).

Nguyen, H.A. et al., 2017. Expanding the Kinome World: A New Protein Kinase Family Widely Conserved in Bacteria. *Journal of Molecular Biology*, 429(20), pp.3056–3074.

Oliva, M.A. et al., 2010. Features critical for membrane binding revealed by DivIVA crystal structure. *EMBO Journal*, 29(12), pp.1988–2001.

Patel, S. et al., 2002. Crystal structure of an enzyme displaying both inositol-polyphosphate-1-phosphatase and 3′-phosphoadenosine-5′-phosphate phosphatase activities: A novel target of lithium therapy. *Journal of Molecular Biology*, 315(4), pp.677–685.

Pavelka, M.S., 2007. Another brick in the wall. *Trends in Microbiology*, 15(4), pp.147–149.

Pereira et al., 2011. Eukaryote-Like Serine/Threonine Kinases and Phosphatases in Bacteria. *Microbiology and Molecular Biology Reviews*, 75(1), pp.192–212.

Sakula, A., 1983. Robert Koch : Centenary of the Discovery of the Tubercle Bacillus , 1882. , pp.127–131.

Santi, I. & McKinney, J.D., 2015. Chromosome organization and replisome dynamics in Mycobacterium smegmatis. *mBio*, 6(1), pp.1–14.

Singh, A. et al., 2006. Dissecting virulence pathways of Mycobacterium tuberculosis through protein-protein association. *Proceedings of the National Academy of Sciences of the United States of America*, 103(30), pp.11346–11351.

Singh, B. et al., 2013. Asymmetric growth and division in Mycobacterium spp .: compensatory mechanisms for non-medial septa. , pp.64–76.

Singh, V. et al., 2016. Identification of Aminopyrimidine-Sulfonamides as Potent Modulators of Wag31-mediated Cell Elongation in Mycobacteria *Molecular* microbiology, 103(1)1, pp. 13-25.

Smith, I., 2003. Mycobacterium tuberculosis pathogenesis and molecular determinants of virulence. *Clinical Microbiology Reviews*, 16(3), pp.463–496.

Sung, M.T. et al., 2009. Crystal structure of the membrane-bound bifunctional transglycosylase PBP1b from Escherichia coli. *Proceedings of the National Academy of Sciences of the United States of America*, 106(22), pp.8824–8829.

Truglio, J.J. et al., 2006. Structural basis for DNA recognition and processing by UvrB. *Nature Structural and Molecular Biology*, 13(4), pp.360–364.

Turapov, O. et al., 2018. Two Faces of CwlM, an Essential PknB Substrate, in Mycobacterium tuberculosis. *Cell Reports*, 25(1), pp.57–67.

Veyron-Churlet, R. & Locht, C., 2019. In vivo methods to study protein–protein interactions as key players in Mycobacterium Tuberculosis virulence. *Pathogens*, 8(4).

WHO., 2019. Global Tuberclosis Report 2019.

WHO, 2015. Global Tuberculosis Report. *Blood*, pp.1–98.

Wiemels, R.E. et al., 2017. An intracellular peptidyl-prolycis/trans isomerase is required for folding and activity of the *Staphylococcus aureus* secreted virulence factor muclease. *Journal of bacteriology* , 199(1), pp.1–15.